



**Hydraulics Research**  
Wallingford

PREDICTING SHORT TERM PROFILE  
RESPONSE FOR SHINGLE BEACHES

K A Powell

Report SR 219  
February 1990

**Registered Office: Hydraulics Research Limited,  
Wallingford, Oxfordshire OX10 8BA.  
Telephone: 0491 35381. Telex: 848552**

This report describes work carried out by members of the Coastal Engineering Group of Hydraulics Research under Contract No CSA 1034 funded by the Ministry of Agriculture, Fisheries and Food, nominated officer Mr A Allison. At the time of reporting this project, Hydraulics Research's nominated project officer was Dr S W Huntington.

This report is published on behalf of the Ministry of Agriculture, Fisheries and Food, but any opinions expressed are those of the authors only, and not necessarily those of the ministry.

© Crown Copyright 1990

Published by permission of the Controller of Her Majesty's Stationery Office.

# Predicting short term profile response for shingle beaches

Report No SR 219

February 1990

## ABSTRACT

Recent years have seen a dramatic improvement in the prediction of inshore wave climates. Whilst this has brought obvious benefits to the design of many types of coastal structure, for beaches it has served only to emphasise the lack of a coherent design methodology. In recognition of this, a comprehensive series of physical model tests has been undertaken in order to examine more closely the behaviour of shingle beaches.

The tests were carried out in a random wave flume, at a nominal scale of 1:17, and covered a range of both beach material characteristics (size and grading) and wave conditions. The material used to represent the model beaches was a graded anthracite, scaled to reproduce both the correct beach permeability, and threshold and direction of sediment motion.

During the study measurements were taken of beach profiles, wave run-up exceedance levels and wave reflection coefficients. Additional tests, coupled with the analysis of results from previous site specific studies, allowed the model results to be extended to a wider range of conditions, including beaches with depth limited foreshores, and beaches overlying impermeable sloping sea walls.

Methods for predicting wave run-up distributions, wave reflection coefficients and beach profile response have been derived. The development of a parametric profile model allows the quantification of shingle beach profile changes due to onshore/offshore sediment transport. Using the model, beach profiles can be predicted, and subsequently located against the initial profile through an area balance routine. The model also permits the derivation of confidence limits on the predicted profile.

Where possible all model results have been validated against field data, much of which was collected specifically for the purpose. The results of this validation are encouraging, suggesting that the techniques developed will prove to be valuable tools in the design and management of shingle beaches.



## Notation

A	Empirical coefficient - Weibull probability distribution.
$A_{1,2,3}$	Empirical coefficient - schematised beach profile curves.
$a_o$	Average upper beach slope - SWL to crest.
B	Empirical coefficient - Weibull probability distribution.
$B_D$	Beach thickness limited value of coefficient B - Weibull probability distribution.
$C_{ij}$	Cross co-variance of i and j.
$D_B$	Effective beach thickness measured perpendicular to initial beach slope.
$D_w$	Depth of water at toe of beach.
$D_{50}$	Median sediment size.
$D_{10,85}$	Sediment size corresponding to tenth percentile etc.
$f_m$	Mean spectral frequency.
$f_p$	Peak spectral frequency.
g	Acceleration due to gravity.
$H_o$	Nominal deepwater wave height.
$H_s$	Significant wave height.
$H_{sb}$	Depth limited significant wave height.
$h_b$	Schematised wave base elevation relative to SWL.
$h_c$	Schematised beach crest elevation relative to SWL.
$h_t$	Schematised beach step elevation relative to SWL.
Ir	Iribarren Number.
$K_D$	Wave energy dissipation coefficient.
$K_R$	Wave energy reflection coefficient.
$L_m$	Mean wavelength.
$L_{ms}$	Depth limited mean wavelength.
$L_o$	Nominal deepwater wavelength.
m	Average foreshore gradient.
N	Number of waves.
$n_{1,2,3}$	Empirical coefficients - schematised beach profile curves.
$P(i)$	Probability of exceedance.
$p_b$	Schematised wave base position relative to shoreline.
$p_c$	Schematised beach crest position relative to shoreline.
$p_r$	Schematised run-up limit relative to shoreline.
$p_t$	Schematised beach step position relative to SWL.

$R_{c_d}$	Depth limited foreshore correction for schematised beach profile parameters.
$R_{c_{n_1}}$	Restricted beach thickness correction factor for $n_1$ .
$R_{c_{p_c}}$	Restricted beach thickness correction factor for $p_c$ .
$R_i$	Nominal wave run-up level.
$R_s$	Significant wave run-up level.
$R_2$	2% wave run-up level.
$r$	Correlation coefficient.
$S_D$	Dissipated spectral energy.
$S_I$	Incident spectral energy.
$S_R$	Reflected spectral energy.
$S_u$	Wave set-up at shoreline.
$T_m$	Mean wave period.
$T_p$	Peak wave period.
$\bar{U}$	Coefficient of uniformity, $D_{85}/D_{15}$ .
$V(i)$	Parameter variance.
$\alpha$	Angle of slope to horizontal.
$\Delta$	Relative density of sediment, $(\rho_s - \rho_f)/\rho_f$ .
$\sigma$	Standard deviation.
$\rho_f$	Specific gravity of fluid.
$\rho_s$	Specific gravity of sediment.
$\phi$	Angle of wave attack.
$\nu$	Kinematic viscosity.

## CONTENTS

	Page
1 INTRODUCTION	1
1.1 General	1
1.2 Beach profile models	3
1.3 Scope and purpose of research	4
1.4 Outline of report	6
2 PHYSICAL MODEL TESTS	7
2.1 Test facility	7
2.2 Design of model beaches	8
2.3 Test programme and procedures	10
2.4 Data acquisition	11
2.4.1 Beach profiles	11
2.4.2 Wave run-up distributions	12
2.4.3 Wave energy dissipation coefficients	13
3 FACTORS GOVERNING BEACH PROFILE RESPONSE	15
3.1 General	15
3.2 Influence of wave height and period	15
3.3 Influence of wave duration	16
3.4 Influence of effective beach thickness	17
3.5 Influence of beach material size and grading	18
3.6 Additional factors	19
3.6.1 Foreshore level	19
3.6.2 Initial beach slope	20
3.6.3 Water level	22
3.6.4 Spectral shape	23
3.6.5 Angle of wave attack	23
3.7 Conclusions	24
4 DEVELOPMENT OF ANALYTICAL PROFILE MODEL	25
4.1 General	25
4.2 Profile schematization	26
4.3 Functional relationships for profile descriptors	27
4.4 Confidence limits on profile prediction	31
4.5 Locating predicted beach profiles	33
4.6 Treatment of wave duration	34
4.7 Correction for effective beach thickness	38
4.8 Correction for depth limited foreshores	41
4.9 Comparison of measured and predicted profiles	44
4.9.1 Initial validation	45
4.9.2 Additional test conditions	46
4.10 Limitations of parametric model	46
4.11 Application of parametric model	48

CONTENTS (CONT'D)

	Page	
5	WAVE ENERGY DISSIPATION ON SHINGLE BEACHES	49
	5.1 Introduction	49
	5.2 Results and discussion	50
6	WAVE RUN-UP DISTRIBUTIONS	52
	6.1 Introduction	52
	6.2 Run-up probability distributions	53
	6.3 Wave set-up	57
	6.4 Wave run-up distribution and effective beach thickness	58
	6.5 Comparison of wave run-up on shingle beaches and smooth planar slopes	60
7	COMPARISON BETWEEN FIELD AND MODEL DATA	61
8	CONCLUSIONS AND RECOMMENDATIONS FOR FURTHER RESEARCH	64
	8.1 Conclusions	64
	8.2 Recommendations for further research	70
9	ACKNOWLEDGEMENTS	71
10	REFERENCES	72

TABLES

2.1	Summary of shingle beach tests
4.1	Summary of functional relationships for beach profile descriptors
4.2	Parameter variances for confidence limits
4.3	Cross co-variances for confidence limits
4.4	Correction factors for depth limited foreshores
5.1	Wave energy dissipation coefficients
6.1	Wave run-up results

FIGURES

1.1	Location of major shingle features in UK
1.2	Idealised beach profile types
2.1	Model sediment grading curves
2.2	Prototype sediment grading curves
2.3	Layout and dimensions of model beach
3.1	Influence of wave height on profile development
3.2	Influence of wave period on profile development
3.3a	Influence of wave duration on profile development
3.3b	Influence of wave duration on profile development
3.4a	Influence of effective beach depth on profile development
3.4b	Influence of effective beach depth on profile development
3.5a	Influence of beach material size on profile development

FIGURES (CONT'D)

- 3.5b Influence of beach material size on profile development
- 3.6a Influence of beach material grading on profile development
- 3.6b Influence of beach material grading on profile development
- 3.7 Beach profiles formed over a depth limited foreshore
- 4.1 Schematised beach profile
- 4.2 Position of maximum wave run-up
- 4.3 Crest position
- 4.4 Crest elevation
- 4.5 Step position ( $H_s/L_m < 0.03$ )
- 4.6 Step position ( $H_s/L_m \geq 0.03$ )
- 4.7 Step elevation ( $H_s/L_m < 0.03$ )
- 4.8 Step elevation ( $H_s/L_m \geq 0.03$ )
- 4.9 Wave base position
- 4.10 Wave base
- 4.11 Curve A<sub>1</sub>
- 4.12 Curve n<sub>1</sub>
- 4.13 Curve A<sub>2</sub>
- 4.14 Curve n<sub>2</sub>
- 4.15 Curve A<sub>3</sub>
- 4.16 Curve n<sub>3</sub>
- 4.17 Confidence limits on predicted profile - wave steepness 0.05
- 4.18 Confidence limits on predicted profile - wave steepness 0.01
- 4.19 Typical wave duration trend -  $p_r/H_s$
- 4.20 Typical wave duration trend -  $h_c/H_s$
- 4.21 Typical wave duration trend -  $p_c D_{50}/H_s L_m$
- 4.22 Typical wave duration trend -  $h_t/H_s$
- 4.23 Typical wave duration trend -  $p_t/D_{50}$
- 4.24 Typical wave duration trend -  $h_b/L_m$
- 4.25 Typical wave duration trend -  $p_b/D_{50}$
- 4.26 Typical wave duration trend - n<sub>1</sub>
- 4.27 Typical wave duration trend - n<sub>2</sub>
- 4.28 Typical wave duration trend - n<sub>3</sub>
- 4.29 Schematic representation of wave duration and profile similarity dependence
- 4.30 Wave duration limited profile - Test No 16, 500 waves
- 4.31 Effective beach thickness correction factor for crest position
- 4.32 Comparison, measured and predicted profiles - Test 6
- 4.33 Comparison, measured and predicted profiles - Test 52
- 4.34 Comparison, measured and predicted profiles - depth limited foreshore
- 4.35 Comparison, measured and predicted profiles - depth limited foreshore
- 4.36 Comparison, measured and predicted profiles - limited beach thickness
- 4.37 Comparison, measured and predicted profiles - wave steepness 0.06
- 4.38 Comparison, measured and predicted profiles - wave steepness 0.01

## FIGURES (CONT'D)

- 5.1 Typical incident and reflected wave spectra
- 5.2 Typical wave energy dissipation curves - JONSWAP spectra
- 5.3 Correlation between mean wave frequency and frequency of maximum wave energy dissipation
- 5.4 Variation of characteristic energy dissipation coefficient with incident wave steepness
- 6.1 Typical wave run-up distributions
- 6.2 Variation in Weibull coefficient B
- 6.3 Measured verses back-calculated run-up exceedance levels
- 6.4 Comparison of field measurement and predicted run-up exceedance levels
- 6.5 Wave run-up exceedance levels - cumulative probability distribution
- 6.6 Wave run-up exceedance levels - wave steepness dependency
- 6.7 Correlation between measured wave set-up and mean sea steepness
- 6.8 Beach depth correction factor for Weibull probability distribution coefficient B
- 6.9 Comparison of smooth slope and shingle beach run-up
- 7.1 Location of field measurement sites
- 7.2 Beach crest elevation - comparison of predicted and field data
- 7.3 Beach crest position - comparison of predicted and field data

## APPENDICES

1. Review of previous studies
2. Selection of model sediment
3. Summary of prediction equations
4. Details of Field Surveys
5. Derivation of confidence limits for predicted profiles

# 1 INTRODUCTION

## 1.1 General

Recent years have seen a dramatic improvement in the prediction of inshore wave climates. Whilst this has brought obvious benefits to the design of many types of coastal structure, for beaches it has served only to emphasise the lack of a coherent design methodology. There is now an increasing need for researchers to concentrate on the prediction of beach behaviour, in response to changes in wave climate, if the management of natural coastal resources is to be optimised, and if the advances in wave prediction are to be fully utilised.

Around the UK coastline shingle, or gravel, beaches are a common sight. They may have many different forms ranging from the cusped forelands of Dungeness and Orfordness (Fig 1.1) down to the characteristic shingle deposits frequently found at the rear of coves and pocket beaches, such as those on the Lleyn peninsula. The composition of the beach may also vary: some consisting almost entirely of shingle, whilst others have a high sand content, either within the interstices of the shingle or on the lower foreshore. However, despite this diversity of form, all shingle beaches are essentially subject to the same processes and exhibit the same responses.

Historically two types of beach profile are recognised (Fig 1.2), that is

1. A step, or swell, profile formed by waves of low steepness and associated with beach accretion
2. A bar, or storm, profile formed by waves of high steepness and associated with beach erosion.

The identification of these two profiles has arisen largely through regular wave model testing. Under random waves, and in tidal environments, the situation is very much more complicated. Indeed for shingle beaches in particular it is doubtful whether bar type profiles can ever fully form. This arises partly because of the rapid response of a shingle beach to changes in the wave conditions - a speed of response which may even include reacting to individual waves in a train. Whilst this can result in a very variable profile it also ensures that a shingle beach is one of the most effective natural sea defences, capable of dissipating in excess of 90% of all incident wave energy.

Shingle beaches are therefore efficient and practical forms of coast protection with a high amenity and aesthetic value. However a shingle beach, in common with any other type of beach, can suffer erosion and a subsequent landward retreat of the shoreline. This may be particularly pronounced if the updrift supply of material is reduced, as unfortunately is often the case on groyned and 'stabilised' coasts. Consequently over a period of time a beach which was originally of satisfactory dimensions may be reduced to such an extent that it no longer constitutes an acceptable 'line of defence' under severe wave conditions.

Anticipating this state is clearly important if shingle beaches are to be managed efficiently, and landward structures are not to be damaged by wave action. The tools available to those responsible for beach management are however somewhat limited. Beach plan shape development can usually be satisfactorily predicted using numerical models: however these typically provide information on the displacement of only a few contours and then not often above the still water level. Shingle beach profile development models

also exist and are discussed in Appendix 1. Again, however, they have their limitations, arising chiefly from their derivation in physical model tests which either used regular waves, or which did not allow for the correct reproduction of the response of the model sediment. None of these models are regularly employed by UK engineers, and it is clear therefore that there is a requirement for development of improved beach profile models to aid in the design and efficient management of our natural coastal resources.

## 1.2 Beach profile models

Generally beach profile models fall into two categories:

1. Morphodynamic models
2. Parametric models

Morphodynamic models essentially attempt to describe the inshore velocity and suspended sediment concentration fields in 2D time and space. The instantaneous sediment transport is then found by integrating over the instantaneous depth, with bed changes subsequently being inferred from the time average value of the transport. Although great advances are being made in our understanding of the important physical processes, a lack of knowledge of both the velocity and concentration fields, and a consequent inability to accurately describe them in mathematical terms, still necessitates the use of a simplified transport description in these models.

Parametric models, on the other hand, generally ignore the underlying physical processes and attempt to relate directly the development of various features on the beach to the incident wave conditions and beach

material characteristics. As such they are generally simpler and easier to apply than morphodynamic models.

Most shingle beach profile models are of the parametric type. This is perhaps not surprising considering that the surface of a shingle beach, by exhibiting a number of readily identifiable features (Fig 1.2), is particularly amenable to a parametric description. Additionally the parametric model requires little or no understanding of the underlying hydrodynamics, which is an area of considerable uncertainty with shingle beaches. Consequently parametric modelling is at present the most suitable tool for describing shingle beaches, and is therefore the method adopted in this study.

### 1.3 Scope and purpose of research

It is the intention of this study to provide a more detailed understanding of the behaviour of shingle beaches from which improved parametric beach profile prediction models may be developed. Generally there are two main stages in the development of this type of beach profile model:

1. The prediction of the profile given specific wave and beach data.
2. Locating the predicted profile relative to an initial datum (often the still water level shoreline of an existing mean beach profile).

Usually the second of these stages involves balancing areas under the predicted and initial profile (assuming conservation of mass within the profile). As such it is totally dependent upon the accuracy of the profile prediction obtained in Stage 1. This in

turn depends to a large extent on the quality of the data used to derive the basic model formulations.

Ideally the model should be developed using data obtained from an intensive field measurement programme. However this introduces many practical problems, not least that of taking measurements from a complicated interacting system containing many variables, virtually none of which can be controlled. An alternative approach is to collect the data from a laboratory model. This may produce problems with scale effects and create a rather simplistic representation of the wave/beach interaction. Nevertheless it does allow certain aspects of beach behaviour to be investigated in a systematic manner, so that the general behaviour may be established. Generally the laboratory-based approach provides the better data base for the derivation of predictive models, and is thus the method employed for this study.

As with any study of this nature there are inevitably restrictions upon the application of the results. In this context it should be emphasised that the results of this study apply only to shingle beaches and, at present, only to waves approaching at normal incidence. It is however worth noting that additional research to address the problems of oblique wave attack is underway. Similarly it is envisaged that future studies will be set up to investigate the behaviour of sand and mixed sand/shingle beaches.

Finally it should be noted that the dimensions used throughout this report are in equivalent full scale terms. Conversion to actual test conditions can be made by dividing by the model scale of 1:17 unless otherwise stated.

#### 1.4 Outline of report

The design of the model tests is outlined in Chapter 2. This includes details of the test facility and data acquisition techniques, for wave run-up, wave energy dissipation and beach profiles, as well as details relating to the selection of the model sediments. Qualitative analysis of the results is contained in Chapter 3 where the most influential of the wave and beach parameters are identified. These parameters are then used in the derivation of functional relationships for various profile descriptors in Chapter 4. The confidence in the resulting relationships is discussed and a comparison is made of measured and predicted beach profiles. The limitations, and possible applications, of a profile prediction model based on these relationships are also considered.

In addition to the beach profile data, results were also collected relating to the wave energy dissipation characteristics of the model beaches, and to the wave run-up distributions in the swash zone. This data is presented and discussed in Chapters 5 and 6 respectively.

As with any model derived from laboratory testing it is important that the profile prediction model should be validated against field data. As already noted collecting useful data from the field is a complicated and usually costly procedure. Nevertheless attempts have been made to collect validatory data and these are described in Appendix 4. Comparison of the field data and model predictions is made in Chapter 7. Chapter 8 then draws together the conclusions arising from the study and makes recommendations for further research.

Finally a brief review of previous studies is given in Appendix 1; Appendix 2 details the selection of the model sediments; Appendix 3 summarises the profile prediction equations used in the predictive model, and Appendix 5 outlines the theory behind the derivation of the profile confidence limits.

## 2 PHYSICAL MODEL TESTS

### 2.1 Test facility

The model tests for this study were conducted in a random wave flume at Hydraulics Research, Wallingford. The flume used has a length of 42m, a width of 1.5m, and a depth of 1.4m. The operating water depth is within the range 0.7 to 0.9m.

The paddle is a buoyant wedge driven by a double-acting hydraulic ram. It incorporates a wave absorbing system to prevent wave energy being re-reflected from its front face. This system monitors water levels directly in front of the paddle using two sets of probes mounted on the paddle face; the signal from these probes is then compared with the input signal to the paddle via a feedback loop. When required the input signal can be modified to compensate for any additional energy (reflected waves) detected at the paddle without altering the characteristics of the wave train being produced. Removable baffles fitted to the front face of the paddle prevent cross waves from building up in the flume and ensure smooth operation of the absorption system.

The random wave control signal is supplied by a micro-computer based wave spectrum synthesiser developed at Hydraulics Research (Ref 1). A hierarchical system of PDP mini-computers is used to

perform on-line analysis of all suitable analogue measurement signals using either statistical or spectral analysis programs. The principles behind these measurement and analysis methods have been discussed by Dedow, Thompson and Fryer (Ref 2).

## 2.2 Design of model beaches

Prior to construction of the model beaches a brief study was undertaken to determine the range of typical shingle sizes and gradings on UK beaches. The results of this study are summarised below for a number of sites.

Site	Material size			Grading $D_{85}/D_{15}$
	$D_{10}$ (mm)	$D_{50}$ (mm)	$D_{100}$ (mm)	
Seaford	6.1	13.7	38.0	2.73
Whitstable	7.6	12.6	50.0	2.41
Chesil (Portland)	23.8	30.0	-	-
Chesil (W. Bexington)	8.5	10.0	13.0	1.34
Littlehampton	7.3	13.0	42.0	2.33
Hayling Island	7.0	16.0	64.0	4.00

Based on the results of this study four combinations of shingle size and grading were selected for reproduction in the model tests. These were intended to cover the range of materials identified above.

When modelling any beach sediment the three main requirements are to reproduce the beach permeability, the threshold of sediment mobility, and the relative onshore/offshore movement. However, although there are three requirements to be satisfied the model sediment particles have only two main characteristics, that is their size and specific gravity. It is therefore very unlikely that all three modelling requirements can be achieved simultaneously. Indeed some compromise is almost always necessary in the

selection of the theoretical characteristics for the model material. These complications in the modelling of beach sediments are further compounded by the fact that there is only a very limited range of specific gravities amongst the readily available material. Frequently, therefore, the selection of the model sediment is governed as much by availability as by theoretical considerations.

For this particular study the magnitude of the desired wave conditions, coupled with the limitations of the test facility, suggested a nominal model scale of about 1:17. At this scale the theoretical calculations (outlined in Appendix 2) indicated that a crushed anthracite would satisfy most of the modelling requirements and hence provide a satisfactory representation of natural beach shingle. The grading curves for the four beach mixes finally selected are given in Figure 2.1, in model terms, and in Figure 2.2 in equivalent full scale terms. The main sediment parameters are summarised below in full scale terms for each of the model mixes.

Mix	$D_{10}$ (mm)	$D_{50}$ (mm)	$D_{90}$ (mm)	$\bar{U}$ $D_{85}/D_{15}$
1	6.9	10.0	22.9	2.6
2	7.3	10.4	19.1	2.2
3	17.3	30.0	46.1	2.2
4	11.6	24.0	38.7	2.6

The layout of the model beach adopted for the tests is shown in Figure 2.3. For reasons of economy the model beach material was laid in a 325mm (model) thick layer on top of a bulk fill comprising pea shingle and coal dust. Overall slope of the beach face was 1:7. In order to minimize transitional effects between the anthracite and the bulk fill, the relative proportions of shingle and coal dust, used in the fill, were selected to provide a fill permeability similar to

that of the anthracite beach. This resulted in a fillmaterial containing 6 parts shingle to one part coal dust.

### 2.3 Test programme and procedures

In total 131 detailed tests were carried out using the shingle beach model. Of these, 62 were for the full 325mm depth of beach material while the remaining 69 were for beaches of restricted thickness. All tests employed waves of the Jonswap spectral type, with an operating static water depth of 0.8m (model). Up to 29 wave spectra were employed together with the 4 different material sizes and gradings already mentioned. The full list of test conditions is given in Table 2.1.

In general each test was run for 3000 waves (based on  $3000T_m$ ) where upon the beach profile had achieved a near-stable state. The exceptions to this were some of the 'restricted-thickness' beach tests which were run for only 1000 waves. Restricted-thickness beach tests were undertaken because it was felt that the concept of a near homogeneous beach of similar permeability throughout its structure was a somewhat artificial one. In practice most shingle beaches have a compact core of relatively low permeability. Consequently the basic model used in the tests is only really applicable to the surface layers of a natural beach, where the shingle is constantly re-worked by wave action. The restriction on the thickness of beach material in the model tests was introduced by incorporating impermeable layers of plastic sheeting at pre-determined depths within the anthracite layer. The sheets were placed parallel to the front face of the beach and at depths of 100, 140, 180 and 200mm (model) relative to the beach face.

All tests of 3000 waves duration generally followed the same format. Prior to the commencement of a set of tests the beach material was compacted for 3 hours using the largest waves calibrated for the study (see Table 2.1, Test number 2). The beach slope was then re-moulded to its initial 1:7 profile. Testing was based on the various wave steepness groupings (0.06, 0.05 etc), starting with the least severe waves in each grouping and gradually building up to the worst wave conditions. In this way sets of profiles were built up on top of each other. Following completion of a set of tests the beach was re-moulded to its initial profile and the sequence started again for the next wave steepness grouping.

## 2.4 Data acquisition

Generally three sets of measurements were made for each test. For the 3000 wave duration tests these measurements included beach profiles, wave run-up exceedence distributions and wave energy dissipation coefficients. For the 1000 wave duration tests only beach profiles were recorded.

### 2.4.1 Beach profiles

Monitoring of the model beach was carried out using a bed profile plotter to record chainage and level readings at any location along the beach. The profiler has a vertically mounted probe attached to a potentiometer which records vertical displacement, and hence the beach level. A second potentiometer records the position (chainage) of the probe as it is moved along a horizontal beam suspended above the beach. The series of X-Y coordinates produced are then converted to equivalent full scale values and stored on a Kemitron data logger for subsequent analysis and plotting.

Other than for tests specifically set up to assess the duration of beach formation, profiles were generally collected at  $500T_m$  intervals. Only one profile was collected at each stage, that being down the centre of the flume. This was felt to be acceptable given the consistency of beach form across the flume and the fact that edge effects were fairly minimal.

#### 2.4.2 Wave run-up distributions

Attempts to record wave run-up distributions in laboratory beach models usually meet with two main problems.

1. The mobility of the beach - which tends to restrict the use of instrumentation on the beach face itself.
2. The presence of edge effects along the side walls of the flume - which can affect visual recordings taken at beach level.

To overcome these problems a simple method was developed for measuring wave run-up distributions along the centre line of the flume. This involved blacking out the half of the flume furthest from the observer whilst lighting the front half from above. The image of an illuminated marker board located outside the flume, and referenced to still water level, was then reflected into the flume and projected on to the centre line boundary, between the light and dark sections of the flume. The marker board was drawn up with twelve numbered bands in such a way that its image appeared correctly orientated. With a little practise an observer was able to record the total number, and hence proportion, of wave run-ups exceeding specified levels on the image of the marker board. Initial proving of the method demonstrated a

high degree of repeatability, which appeared to be independent of the observers involved.

Generally five wave run-up recordings, of  $300T_m$  duration, were taken for each test, with each recording being separated by a  $200T_m$  interval. All observations were recorded to cassette tape for subsequent analysis.

#### 2.4.3 Wave energy dissipation coefficients

The measurement and analysis of wave energy dissipation coefficients is perhaps best described in terms of sine waves. A certain proportion of the energy of a sine wave incident on a slope will be reflected as a sine wave of the same period but of a lower height. If it is assumed that all energy incident upon the slope is either reflected or dissipated then,

$$S_D = S_I - S_R$$

where  $S_D$  is the energy dissipated and  $S_I$  and  $S_R$  are, respectively, incident and reflected energy.

Assuming that irregular waves can be regarded as the sum of sine waves of different frequencies, the reflection, and hence dissipation, coefficients,  $K_R$  and  $K_D$ , can be calculated for each frequency considered in the incident wave spectrum.

Alternatively a 'characteristic' value of  $K_D$  or  $K_R$  can be obtained by integrating for the areas under the reflected and incident spectra. The reflection and dissipation coefficients  $K_R$  and  $K_D$  can then be defined in terms of the reflected and incident energy densities,  $S_R$  and  $S_I$  respectively:

$$K_R = (S_R/S_I)^{1/2} \quad K_D = (1 - S_R/S_I)^{1/2}$$

hence,

$$K_D = (1 - K_R^2)^{1/2}$$

In this study wave measurements were made using 3 wave probes. The incident and reflected wave spectra cannot be measured directly but are calculated in an analysis program devised by Gilbert and Thompson (Ref 3), based on the method of Kajima (Ref 4).

The analysis method calculates values of  $K_R$  over a wide range of frequencies, but the method is only valid over a restricted band width related to the probe spacing. For the current study, the use of the three wave probes effectively provided three different probe spacings thus allowing a wide range of frequencies to be covered.

Because beaches are constantly adjusting their form in response to the incident wave conditions, it seems likely that the proportions of wave energy reflected or dissipated may also vary as the beach gradually evolves. To test this hypothesis three sets of measurements were made for each experimental run, after first allowing the beach an initial development period of  $500T_m$ .

### 3 FACTORS GOVERNING BEACH PROFILE RESPONSE

#### 3.1 General

The development of shingle beach profiles under wave action may be influenced by a number of variables including:

- Wave height
- Wave period
- Wave duration
- Beach material size
- Beach material grading
- Effective depth of beach material
- Foreshore level
- Water level
- Angle of wave attack
- Spectral shape
- Initial beach profile (slope)

Of these, the first six have been assessed directly during the current test series. The effect of a depth limited foreshore, and hence depth limited wave climate can be obtained both by comparing results from this study with those of a previous study, and from recently published work (Ref 9). The influence of the remaining four variables can be determined from the literature (Refs 5, 6 and 7).

#### 3.2 Influence of wave height and period

Figures 3.1 and 3.2 demonstrate the effect of wave height ( $H_s$ ) and wave period ( $T_m$ ) on the beach profiles. As can be seen variations in both parameters have a substantial effect upon the resulting profiles.

The influence of the wave height parameter manifests itself mainly in the upper portion of the profile. Here, the surf zone width increases markedly in response to an increasing wave height, and hence increasing levels of wave energy. This is compatible with Hughes and Chiu's (Ref 8) supposition that the extra surf zone volume necessary to dissipate an increased incident wave energy is obtained by a lengthening of the surf zone rather than by a change in profile.

The effect of variations in the wave period is apparent more in the vertical dimensions of the profile than in the horizontal displacements. Thus, as the wave period increases so does the beach crest elevation and, as a consequence, the volume of material above the still water line. This is matched by a corresponding increase in the erosion of the beach profile below the step position, and hence a seaward displacement of the lower limit of profile deformation.

### 3.3 Influence of wave duration

Figures 3.3a and 3.3b demonstrate the effect of wave duration on beach profile development for mean sea state steepnesses of 0.06 and 0.01 respectively. In both cases the development of the profile is very rapid in the early stages of wave attack, to the extent that approximately 80% of the 'total' (3000 waves) volumetric change occurs during the first 500 waves. Generally all sections of the profile evolve at similar rates and this ensures that the main features of a particular profile quickly become apparent. Subsequent wave action therefore serves only to hone the final profile shape.

### 3.4 Influence of effective beach thickness

The effect of restricting the natural development of flow fields within the beach structure by incorporating an impermeable membrane parallel to the initial beach slope is shown in Figures 3.4a and 3.4b for wave steepnesses of 0.02 and 0.06 respectively. This situation may be considered representative of natural beaches overlying sloping sea walls or containing compacted cores of finer (lower permeability) material. As such it is discussed further in section 2.3.

Figures 3.4a and 3.4b each consist of 4 profiles representing  $D_B/D_{50}$  values of 29.4, 41.2, 52.9 and  $>95$ . In each case  $D_B$  is the effective thickness of beach material measured relative to the initial slope and  $D_{50}$  is the median diameter of the sediment particles. The profiles corresponding to  $D_B/D_{50} > 95$  are taken from the main body of tests with a full thickness of beach material. All values of  $D_B/D_{50} < 29.4$  generally lead to exposure of the impermeable membrane and subsequent de-stabilisation of the beach slope. This is compatible with field results reported by Longuet-Higgins and Parkin (Ref 20) who found that a layer of roofing felt buried 75mm deep in a shingle beach provoked erosion of the overlying beach. In this case the beach material was between 2.5 and 25mm in diameter, yielding a possible effective thickness range of  $3 < D_B/D_{50} < 30$ .

The results of the model tests clearly show that the influence of  $D_B/D_{50}$  on the beach profiles is largely confined to the horizontal profile displacements, at least within the tested range, and is most pronounced above the still water level. The general trends across different wave conditions are however somewhat

confusing and appear to show a partial wave steepness dependency. This is discussed further in section 4.7.

### 3.5 Influence of beach material size and grading

The relative importance of sediment characteristics, such as size ( $D_{50}$ ) and grading ( $D_{85}/D_{15}$ ), in determining beach profile response to a particular set of wave conditions is illustrated in Figures 3.5a to 3.6b. Each figure contains two profiles formed under the same wave conditions. The profiles in Figures 3.5a and 3.5b demonstrate the effect of material size on beach development, while those in Figures 3.6a and 3.6b examine the influence of grading.

From the examples given it may be concluded that beach material size is the more important of the two parameters with respect to profile change. However there is a suggestion that the degree of this importance is partly dependent upon the characteristic steepness of the incident wave field. Thus the greatest deviations between two 'corresponding' profiles are seen to occur under the steeper wave conditions (Fig 3.5b).

On the basis of Figures 3.6a and 3.6b there is little or no variation in beach profile response due to sediment grading other than an apparent reduction in the crest elevation as the beach grading narrows. This effect appears to be consistent throughout the test results, and in accordance with data reported elsewhere (Ref 9). However, with only two beach gradings employed during the current tests a reliable trend cannot be established at present.

### 3.6 Additional factors

There are a number of additional factors which may be important to the development of shingle beach profiles. Whilst not considered in the present study their effect may be ascertained by reference to previous work.

#### 3.6.1 Foreshore level

Throughout this study the toe of the beach was located in deepwater ( $0.22 < H_s/D_w < 0.035$ , where  $D_w$  is depth of water at beach toe). Although adopted to simplify test procedures, this is a situation representative of relatively few natural shingle beaches (Chesil, Dungeness etc). Indeed the majority of shingle beaches are usually fronted by a sand foreshore located in relatively shallow water.

To examine whether foreshore elevation would play a significant part in the development of the beach profile recourse was made to the published literature and also to a series of tests conducted some years earlier at HR.

As part of his study, aimed primarily at dynamically stable rock beaches, van der Meer (Ref 9) considered the case of a raised foreshore in front of the beach. He carried out a number of tests covering the range  $0.56 < H_s/D_w < 0.74$ , and found that the effect of a reduced foreshore depth manifested itself in a shortening of the beach profile below still water level. Above the still water level there was no apparent effect on the profile.

A wider range of  $H_s/D_w$  values may be considered by comparing results from the current investigation with those of an earlier, unpublished, study carried out at

HR. In this earlier study tests were conducted in a wave flume using an anthracite beach scaled to represent shingle with a  $D_{50}$  of approximately 10mm. The foreshore depth at the toe of the beach was taken as 1.25m. Wave conditions were compatible with those of the present study and yielded a range of  $H_s/D_w$  values from 0.8 to 2.5. Typical results from the earlier work are shown in Figure 3.7 from which it can be seen that profiles formed above a depth limited foreshore do not exhibit a distinctive step feature below the still water line. This is perhaps not surprising given that the step normally forms at the position of, and in response to, wave breaking. However, on a depth limited foreshore this breaking occurs seaward of the beach structure and hence the conditions responsible for step formation on a beach are removed.

Further comparison of profiles formed in the present study with those formed under similar conditions in the earlier tests suggests that with the elevated foreshore there is also a reduction in profile dimensions above the shoreline. Although this contradicts van der Meer's results it is perhaps not surprising given that crest dimensions are largely determined by wave run-up, which will itself be limited by the increased energy losses associated with wave action in depth limited conditions.

### 3.6.2 Initial beach slope

The importance of the initial beach slope in determining the type of profile formed has been debated for many years. Dalrymple and Thompson (Ref 10) found that initial slopes from 1:5 to 1:10 had no effect on the beach profile for 0.4mm sand. Similarly, Nicholson (Ref 11) with 2mm sand and initial slopes from 1:5 to 1:20, and van Hijum

(Ref 12) with material from 1.8mm to 16.5mm and slopes of 1:5 and 1:10, both reached the same conclusion. Rector (Ref 13) using sands from 0.21mm to 3.44mm on slopes of 1:15 to 1:30 found that the initial gradients had no effect on the final profiles other than determining whether the upper beach was formed by erosion or accretion. Van der Meer (Ref 9) working with much coarser material, and random waves, also found that the major part of the profile was unaffected by the choice of initial slope. Again however the direction of material transport and hence the mode of profile formation varied with slope.

Conversely, Chesnutt (Ref 14) found that beach profiles formed in 0.2mm sand were affected by the initial profile slope when the latter was changed from 1:10 to 1:20, and Sunamura and Horikawa (Ref 15) observed that initial slopes of 1:10, 1:20 and 1:30 influenced the final profile shape formed in 0.2mm and 0.7mm sands. This led Gourlay (Ref 16) to conclude that the initial slope did not affect the shape of the beach profile when the former was steep, but could have an effect if the initial slope was very gentle.

King (Ref 17) observed that the initial gradient modified the critical wave steepness which effectively divides breaking and non-breaking sea states; critical steepness being higher for steeper beaches than shallow beaches. However, any increase in beach slope will produce a slight change in the type of characteristic breaking wave even if the wave steepness remains constant. In the extreme case, this change will be from spilling through plunging and collapsing to surging. Thus a wave steepness that is critical on a steep slope (collapsing/plunging waves) might well result in spilling waves on a shallow slope where the critical value is in fact much lower. The variation in profile shapes obtained by different

investigations, on different slopes, may therefore be partly explained by Kings' observation, particularly if the wave steepness is close to the critical value.

Thus it may be concluded that whilst the initial beach slope does not necessarily affect the form of the active length of beach profile it does affect its mode of formation.

### 3.6.3 Water level

Although tides play a significant part in the development of natural beach profiles comparatively little laboratory research has been carried out under such conditions. Indeed, even in field studies of beach profiles the effect of tidal action is often neglected.

Of the work that has been carried out, that of Watts and Dearduff (Ref 5) is perhaps the most comprehensive. They compared profiles formed under a variety of tidal ranges and durations and concluded that the introduction of tides, regardless of range or duration, did not materially affect the shape or slopes of the resulting beach profiles. The only exception occurred when the changes in wave steepness, induced by the varying water depth in the wave channel, spanned the critical value for the transformation from accretion to erosion profiles.

Kemp (Ref 18) observed that natural shingle beaches reacted far more rapidly to tidal changes than did sand beaches, the profiles appearing to move up and down the beach with the tide. This effect was also noted by van Hijum and Pilarczyk (Ref 19) under laboratory conditions. Van der Meer (Ref 9) examined tidal variation and the influence of storm surges on beaches of coarse material under random waves. He

noted that the beach profile responded immediately to changes in water level but that the profile shape at the end of each tide was generally unaffected. Again the profile was observed to move up and down the beach face with water level. Similar findings were also reported by Powell (Ref 6) for shingle beaches under regular wave attack. It may therefore be concluded that gradually varying water levels do not affect the shape or slope of beach profiles. They will however determine the location of the profile on the beach face.

#### 3.6.4 Spectral shape

In order to assess the influence of spectral type on the development of beach profiles van der Meer (Ref 7) compared profiles formed under a very narrow spectrum with those formed under a much wider Pierson Moskowitz spectrum. On the basis of these tests he concluded that spectral shape had only minor influence on the beach profiles provided that the average zero-crossing period,  $T_m$  (and not the peak spectral period  $T_p$ ) was used to compare the profile. It would therefore appear that although the present series of model tests have concentrated on wave spectra of the JONSWAP type, the results have a much wider applicability.

#### 3.6.5 Angle of wave attack

The influence of the angle of wave attack on the development of gravel beach profiles has been examined by van Hijum and Pilarczyk (Ref 19) for both regular and random waves. Three dimensional model tests were carried out utilising approach angles,  $\phi$ , of  $0^\circ$ ,  $20^\circ$  and  $45^\circ$  for the regular waves, and  $0^\circ$  and  $30^\circ$  for the random waves. From the results of these tests it was concluded that the dimensions of beach profiles formed

under oblique wave attack were less than those formed under normally incident waves, by a factor equivalent to  $(\cos \phi)^{\frac{1}{2}}$ .

Van der Meer (Ref 9) subsequently re-analysed van Hijum and Pilarczyk's random wave results and concluded that whilst there was indeed a general reduction in the dimensions of beach profiles formed under oblique wave action, this reduction was more closely described by a factor of  $\cos \phi$ . Moreover he found that the position of the beach crest relative to the shoreline was unaffected by the angle of wave attack.

Without further data it is difficult to draw firm conclusions regarding the influence of the angle of wave attack on the development of beach profiles. However it does appear that oblique wave action restricts the full development of at least part of the profile.

### 3.7 Conclusions

Following qualitative analysis of beach profile response to a number of potential governing variables it may be concluded that the following are of immediate importance to the development of shingle beach profiles:

- wave height,  $H_s$
- wave period,  $T_m$
- wave duration
- beach material size,  $D_{50}$
- angle of wave attack,  $\phi$

Additionally the following variables are influential in determining at least part of the profile:

- effective thickness of beach material,  $D_B$
- foreshore level,  $D_w$

Of these variables the angle of wave attack has not been examined further in this study but is clearly of some consequence and worth pursuing in more detail. The effect of beach sediment grading may also be of some importance, particularly to the crest elevation. Further data should therefore be collected to allow a full evaluation to be undertaken.

#### 4 DEVELOPMENT OF ANALYTICAL PROFILE MODEL

##### 4.1 General

As stated in the introduction to this report the successful development of a beach profile model requires two things:

1. A means of predicting the profile shape, and
2. A means of locating that profile against an initial datum.

Both of these aspects are addressed in this chapter. In addition there is an increasing need for a probabilistic rather than deterministic approach to the design of coastal structures. Adoption of this type of approach necessitates a means of evaluating the probabilities of exceedance of specific profile configurations and landward displacements. This in turn requires an understanding of the confidence limits that can be set on the profile prediction. The calculation of such confidence intervals is also covered in this chapter.

## 4.2 Profile schematization

The profile schematization adopted for the present model is essentially a combination of those employed in three previous shingle beach profile models, namely van Hijum and Pilarczyk (Ref 19), Powell (Ref 6) and van der Meer (Ref 9). These models are discussed in more detail in Appendix 1.

Whereas in previous models the beach profile has usually been described by two hyperbolic curves the present model employs three curves: between the prescribed limits of:-

- a) Beach crest and still water level shoreline.
- b) Still water level shoreline and top edge of step.
- c) Top edge of step and lower limit of profile deformation, ie wave base.

The resultant schematisation is shown in Figure 4.1 and characterised, relative to the still water level and shoreline axes, by

- $p_r$  - the position of the maximum run-up (-ve)
- $h_c$  - the elevation of the beach crest (+ve)
- $p_c$  - the position of the beach crest (-ve)
- $h_t$  - the elevation of the beach step (-ve)
- $p_t$  - the position of the beach step (+ve)
- $h_b$  - the elevation of the wave base (-ve)
- $p_b$  - the position of the wave base (+ve)

The co-ordinates for the first curve (crest to still water level) are denoted by  $x_1$ ,  $y_1$ , and those for the second and third curves by  $x_2$ ,  $y_2$  and  $x_3$ ,  $y_3$  respectively.

With the profile schematisation decided, it is then a matter of determining functional relationships for each of the parameters listed above.

#### 4.3 Functional relationships for profile descriptors

From Chapter 3 it can be concluded that the variables most influential in the profile development under normal wave attack are  $H_s$ ,  $T_m$ ,  $D_{50}$ , wave duration,  $D_w$  and  $D_B$ . Leaving aside, for the moment, the active depth of beach material parameter,  $D_B$ , the wave duration,  $N$ , and the toe water depth,  $D_w$ , dimensional analysis based on the remaining variables yields three dimensionless parameter groupings:

- a)  $H_s/D_{50}$  - ratio of wave height to sediment size
- b)  $H_s/L_m$  - wave steepness
- c)  $H_s T_m g^{1/2}/D_{50}^{3/2}$  - effectively a ratio of wave power to sediment size and equivalent to van der Meer's dimensionless parameter  $H_o T_o$  (Ref A9, App 1).

Since each of the profile descriptors listed in Section 4.2 can be non-dimensionalised by either  $H_s$ ,  $L_m$  or  $D_{50}$ , a general functional relationship linking the profile descriptors and determining variables can be written as,

$$\frac{\text{profile descriptor}}{H_s, L_m, D_{50}} = f(H_s/D_{50}, H_s/L_m, H_s T_m g^{1/2}/D_{50}^{3/2}) \quad (4.1)$$

For each profile descriptor the actual form of equation 4.1 was determined using data from tests

carried out with the full thickness of beach material (Tests 1-62). Since parameter variations were found to be largely independent of wave duration, for durations in excess of 500 waves, a mean parameter value was used for each test. The resulting functional relationships, obtained using regression analysis, are summarised in Table 4.1 and plotted in Figures 4.2 to 4.10. Each figure contains the derived regression line, and 90% confidence limits, as well as the mean parameter values.

It is interesting to note from Table 4.1 that the results for both  $p_t$  and  $h_t$  indicate that the minimum value of the parameters occurs at a wave steepness of about 0.03. As this limit also applies to a number of other parameters it seems reasonable to assume that this is the steepness at which the waves effectively change from breaking to non-breaking ie the steepness coincident with maximum energy entering the surf zone.

Previous attempts to derive beach profile models have usually used equations of the form  $y = Ax^n$  to describe the hyperbolic curves of both sand and shingle beaches. However use of this type of equation can lead to complications, particularly when the value of  $n$  is not constant, where upon  $A$  becomes a coefficient of variable dimension ( $A$  has units of metres<sup>1-n</sup>) and thus extremely difficult to represent in a dimensionless form.

To avoid this un-necessary complication the profile equations have been re-written in the non-dimensional form:

$$1. \quad \frac{y}{h_c} = -A_1 \left( \frac{x}{p_c} \right)^{n_1} \quad (4.11)$$

$$2. \quad \frac{y}{h_t} = -A_2 \left( \frac{x}{p_t} \right)^{n_2} \quad (4.12)$$

$$3. \quad \frac{y - h_t}{(h_b - h_t)} = -A_3 \left( \frac{x - p_t}{p_b - p_t} \right)^{n_3} \quad (4.13)$$

Regression analysis of data from Tests 1 to 62 then allows the following values to be assigned to the A and n coefficients (Figures 4.11 to 4.16).

Curve 1:

$$a) \quad \bar{A}_1 = -1.045 \quad ; \quad \sigma = 0.14$$

b) For  $H_s/L_m < 0.03$

$$n_1 = 0.84 + 23.93 (H_s/L_m) \quad ; \quad r = 0.87$$

For  $H_s/L_m \geq 0.03$

$$n_1 = 1.56 \quad , \quad \sigma = 0.21$$

Curve 2:

$$a) \quad \bar{A}_2 = -1.005 \quad , \quad \sigma = 0.21$$

$$b) \quad n_2 = 0.84 - 16.49 (H_s/L_m) + 290.16 (H_s/L_m)^2$$

$$r = 0.50$$

Note that the poor correlation for  $n_2$  reflects the extreme variability of the beach at, or about, the step. This is the section of the profile that is most responsive to the waves. Note also that both  $n_1$  and  $n_2$  tend to 0.84 as  $H_s/L_m$  tends to zero ie the two separate curves tend toward one continuous curve.

Curve 3:

a)  $A_3 = -1.109$  ,  $\sigma = 0.15$

b)  $n_3 = 1.005$  ,  $\sigma = 0.10$

In order to prevent cumulative errors occurring within the predicted profile it is desirable to force each curve through its prescribed limits ( $h_c$ ,  $p_c$  etc). From the results the simplest and most accurate method of achieving this would be to put  $A_1$ ,  $A_2$  and  $A_3$  equal to -1.0.

Although this approximation is perfectly acceptable for most of the profiles it will introduce a slight error in curve 3 (step to wave base) for waves of steepness less than 0.02. This error arises because of a minor dependency of  $A_3$  on  $H_s/L_m$  (Fig 4.15) which results in all values of  $A_3$  being higher than the mean value when  $H_s/L_m < 0.02$ . This effect can be compensated for by setting  $A_3 = -1.0$  and recalculating  $n_3$  using regression analysis. This yields:

$$\text{For } H_s/L_m < 0.03$$

$$n_3 = 0.45 \quad , \quad \sigma = 0.05$$

and

$$\text{For } H_s/L_m \geq 0.03$$

$$n_3 = 18.3 (H_s/L_m) - 0.1$$

The resulting trend is plotted in Figure 4.16.

In summary, the equations for predicting beach curves may be written as:-

1. Crest to still water level.

$$\frac{y}{h_c} = \left(\frac{x}{p_c}\right)^{n_1} \quad (4.14)$$

$$\begin{aligned} \text{where } n_1 &= 0.84 + 23.93 H_s/L_m & \text{for } H_s/L_m < 0.03 \\ \text{and } n_1 &= 1.56 & \text{for } H_s/L_m \geq 0.03 \end{aligned} \quad (4.15)$$

2. Still water level to step.

$$\frac{y}{h_t} = \left(\frac{x}{p_t}\right)^{n_2} \quad (4.16)$$

$$\text{where } n_2 = 0.84 - 16.49 H_s/L_m + 290.16 (H_s/L_m)^2 \quad (4.17)$$

3. Step to wave base.

$$\frac{y - h_t}{h_b - h_t} = \left(\frac{x - p_t}{p_b - p_t}\right)^{n_3} \quad (4.18)$$

$$\begin{aligned} \text{where } n_3 &= 0.45 & \text{for } H_s/L_m < 0.03 \\ \text{and } n_3 &= 18.6 (H_s/L_m) - 0.1 & \text{for } H_s/L_m \geq 0.03 \end{aligned} \quad (4.19)$$

All the equations necessary for predicting a beach profile are listed again in Appendix 3.

#### 4.4 Confidence limits on profile prediction

From the foregoing regression analysis it is possible to establish the variation, measured within the tests, in X and Y at any point along the predicted beach profile. With this variation obtained, confidence limits on the predicted profile can be determined.

The derivation of the confidence limits is outlined in Appendix 5, from which the following equations may be obtained:

1) Curve 0:

$$V(X_0) = (1-t)^2 V(p_c) + t^2 V(p_r) + 2.34t(1-t) \quad (4.20)$$

$$V(Y_0) = (1-t)^2 V(h_c) + a_0 t^2 V(p_r) + 0.49 a_0 t(1-t) \quad (4.21)$$

2) Curve 1:

$$V(X_1) = t^2 V(p_c) \quad (4.22)$$

$$V(Y_1) = t^{2n_1} V(h_c) + (y_1 \log t)^2 V(n_1) \quad (4.23)$$

3) Curve 2:

$$V(X_2) = t^2 V(p_t) \quad (4.24)$$

$$V(Y_2) = t^{2n_2} V(h_t) + 0.037 (y_2 \log t)^2 + 0.062 t^{n_2} y_2 \log t \quad (4.25)$$

4) Curve 3:

$$V(X_3) = (1-t)^2 V(p_t) + \frac{t^2}{a_3} V(h_b) \quad (4.26)$$

$$\begin{aligned} V(Y_3) = & (1-t^{n_3})^2 V(h_t) + t^{2n_3} V(h_b) + [(y_3 - h_t) \log t]^2 V(n_3) \\ & - 0.44t^{n_3} (1-t^{n_3}) + (y_3 - h_t) \log t (0.036t^{n_3} - 0.014) \end{aligned} \quad (4.27)$$

Here  $V(i)$  is the variance of parameter  $i$ , and  $t$  varies from 0 to 1 as  $X$  and  $Y$  vary from 0 to  $X_{\max}$ ,  $Y_{\max}$ .

Values of the parameter variances for use in equations 4.20 to 4.27 are given in Table 4.2. These allow the variance in X and Y for the four component curves of the profile to be calculated, from which the standard deviations  $V^{1/2}(X_i, Y_i)$  can be determined. These, when multiplied by the specified test statistic, Z, provide the required confidence limits.

Figures 4.17 and 4.18 illustrate equations 4.20 to 4.27 as applied to two typical mean profiles. The assumption has been made that there is no variance within the profile beyond its predicted limits, therefore the 90% confidence limits shown in the figures are assumed to converge back onto the profile at  $(p_r - \Delta x, h_r + \Delta y)$  and  $(p_b + \Delta x, h_b - \Delta y)$ .

#### 4.5 Locating predicted beach profiles

The position of the predicted mean beach profile relative to an initial (pre-existing) profile can be established by assuming initially that material moves only in an onshore-offshore direction, or that the differential longshore transport across a section is zero. Comparing the areas under the two curves relative to a common datum, and shifting the predicted curve along the SWL axis until the areas equate, then provides the location of the predicted profile.

If differential longshore transport across the section is significant, then a preliminary estimate of the position of the predicted curve can still be made provided a reasonable value can be assigned to the area loss due to longshore transport. This additional area loss is then simply added in to the area balance. Research currently underway at HR is attempting to improve upon this method by establishing the precise

cross-shore distribution of the longshore transport. This should identify those sections of the profile which are most susceptible to discontinuities in the longshore transport.

#### 4.6 Treatment of wave duration

Previous results obtained both in this study (Section 3.3) and by other investigators (Ref 7) have confirmed the importance of the duration of wave activity to the form of the final beach profile. Therefore the question is not whether the duration of wave activity should be included in the profile prediction methodology but rather how its inclusion should be effected. To answer this question a number of tests were run with more frequent profiling of the beach than usual. Analysis of the results yielded a number of important points.

1. Not all the profile prediction parameters exhibited a pronounced wave duration dependency. Figure 4.24 shows a typical result for the profile parameter  $h_b$ . The significant lack of any duration related trend is also reflected in the results for the profile parameters  $p_b$ ,  $n_1$ ,  $n_2$  and  $n_3$  (Figs 4.25 to 4.28). That there should be little in the way of duration effects within  $h_b$  and  $p_b$  is not surprising given that they represent the lower limit of the profile, where nett accretion or erosion of the beach material should, by definition, be negligible. No duration limited corrections need therefore to be applied to either  $h_b$ ,  $p_b$ ,  $n_1$ ,  $n_2$  or  $n_3$
2. Among the parameters most strongly affected by wave duration are  $p_r$ ,  $p_c$  and  $h_c$  whilst  $p_t$  and  $h_t$  show some dependency albeit largely masked by the scatter associated with these parameters.

Typical duration trends for  $p_r$ ,  $h_c$ ,  $p_c$ ,  $h_t$  and  $p_t$  are given in Figures 4.19-4.23 from which it can be seen that most of the parameters reach reasonably stable values within about 500 waves. Any subsequent duration related increase, in excess of the initial 500 wave period, is usually within the confidence limits on the original prediction equations. Consequently any correction for a wave duration limited profile need only be applied if the number of waves incident on the beach is less than 500.

3. The duration of wave activity required for the beach to achieve a particular form was found to be heavily influenced by the relative similarity between the final beach form and the initial 'starting' profile. Thus if the initial profile closely resembles the final beach profile, less waves will be required to mould that profile than if starting from, say, a plane slope. This process is schematically represented in Figure 4.29, from which it can be seen that the time saved in forming profile  $p_1$  from initial profile  $p_{o1}$  (see inset sketch) rather than from the plane slope  $p_o$  is  $(N_o - N_{o1})$ ; where  $N$  is the number of waves required to achieve a stable parameter value (in this case  $h_c$ ) and  $h_{co}$ ,  $h_{co1}$  and  $h_{c1}$  are elevations corresponding to the beach crest for profiles  $P_o$ ,  $P_{o1}$  and  $P_1$  respectively.

This result serves to emphasize the importance of making allowance for the relative similarity, or dissimilarity, between the initial and final beach profiles when introducing wave duration effects. It also greatly complicates the direct inclusion of a wave duration parameter within the profile prediction equations since, by implication, one would require

knowledge of the position of the initial beach profile relative to the final beach profile, prior to calculating the final profile.

To avoid this problem the method adopted in this report for assessing wave duration limited profiles (ie less than 500 waves) does not rely upon the inclusion of a wave duration parameter within the prediction equations but rather applies a correction to the predicted profile. This correction is applied after the predicted profile has been located relative to the initial profile (Section 4.5) and therefore takes into account any similarity between the two beach forms.

The steps required in the calculation of a duration limited profile using this approach are as follows.

1. Plot the mean beach profile using the prediction equations given in Section 4.3 and Table 4.1.
2. Position the predicted beach profile against the initial beach profile using the area balance method outlined in Section 4.5.
3. At positions  $p_c$  and  $p_t$  measure the vertical extent of any accretion/erosion from the initial profile,  $h_c - h_{c_o}$ ,  $h_t - h_{t_o}$ , and reduce in proportion to the number of waves,  $N$ , using

$$h_{c_N} = (h_c - h_{c_o}) \left(\frac{N}{500}\right)^{0.12} + h_{c_o} \quad (4.28)$$

and

$$h_{t_N} = (h_t - h_{t_o}) \left(\frac{N}{500}\right) + h_{t_o} \quad (4.29)$$

where  $h_{cN}$ ,  $h_{tN}$  are the values of parameters  $h_c$  and  $h_t$  after  $N$  waves ( $N < 500$ )  
 $h_{c0}$ ,  $h_{t0}$  are the vertical displacements of the initial profile from the still water level at positions  $p_c$  and  $p_t$  on the final mean beach profile.

The power term, 0.12, in equation 4.28 was determined using regression analysis on the duration trends for parameter  $h_c$  over the range  $0 < N \leq 500$ . For parameter  $h_t$  the trend over this range was considered to be linear.

4. Reduce the values of the  $p_c$  and  $p_t$  for the predicted profile in accordance with,

$$\left(\frac{p_{cN}}{p_c}\right) n_1 = \frac{h_{cN}}{h_c} \quad (4.30)$$

and

$$\left(\frac{p_{tN}}{p_t}\right) n_2 = \frac{h_{tN}}{h_t} \quad (4.31)$$

where  $p_{cN}$ ,  $p_{tN}$  are the duration limited values of the predicted parameters  $p_c$  and  $p_t$  ( $N < 500$ )  
and  $n_1$ ,  $n_2$  are the curve parameters given in Section 4.3.

5. Replot profile using values of  $h_{cN}$ ,  $p_{cN}$ ,  $h_{tN}$  and  $p_{tN}$  together with the original values of  $h_b$ ,  $p_b$ ,  $n_1$ ,  $n_2$  and  $n_3$ . At the upper limit of the profile maintain the slope previously established between

$h_c$  and  $p_r$  (ie reduce  $p_r$  proportionately).

6. Re-locate the duration limited profile using the area balance method of Section 4.5.

A typical duration limited profile predicted using this method is shown in Figure 4.30. The comparison between the predicted and measured profile is reasonable and may therefore be taken as an initial validation of the method outlined above.

Finally it should be noted that in nature the evolution of a beach profile is a continuing process both in time and over a range of wave conditions. Furthermore a particular wave condition builds up over a period of time, rather than being switched on instantaneously as in a laboratory model. Therefore it is unlikely that a beach will be drastically out of phase with its incident wave conditions, and thus the evolution of a quasi-equilibrium profile will depend less on the duration of wave action and rather more upon the duration of a particular water level. It is therefore recommended that the assessment of a typical wave duration for use in the profile prediction methodology should be based upon the duration of representative water levels rather than upon that of an arbitrary number of waves.

#### 4.7 Correction for effective beach thickness

Section 3.4 showed that the presence of a relatively impermeable layer (either an underlying revetment or core of finer material) within the beach could have a marked effect on the horizontal displacement of the profile. These effects were most pronounced at the beach crest, and in particular in the profile parameter  $p_c$  and the curve parameter  $n_1$ . Smaller,

less obvious effects could also be discerned at the transition (step) and profile toe.

Subsequent analysis of the data indicated that the effect of an underlying boundary on the resultant beach profile could be categorised according to the ratio of the effective beach thickness,  $D_B$ , to the median material size,  $D_{50}$ . Thus,

: For  $D_B/D_{50} \geq 100$  , the beach profile is largely unaffected.

: For  $30 \leq D_B/D_{50} < 100$  , the profile is distorted but the effects are confined mainly to the horizontal displacements and in particular to the parameter  $p_c$ .

: For  $D_B/D_{50} < 30$  , the thickness of beach is usually insufficient to retain material over the profile, and the beach structure breaks down.

In the critical mid range ( $30 \leq D_B/D_{50} < 100$ ) analysis of the data from all 69 tests carried out with the inclusion of an impermeable boundary within the beach, showed no significant trends for  $p_t$  and  $p_b$  within the general data scatter. In most cases however the profiles at these points were still located within the confidence limits as given in Section 4.4.

At the beach crest  $p_c$  was found to increase with decreasing  $D_B/D_{50}$ , although the rate of increase was dependent upon the wave steepness. As a consequence

the influence of  $D_B/D_{50}$  was most pronounced for breaking waves and less so for non-breaking waves. Interestingly no direct dependence on a wave energy parameter was found.

Regression analysis on the data allows a correction factor  $R_{c_{pc}}$  to be derived, where

$$R_{c_{pc}} = P_c (D_B/D_{50}) / P_c (D_B/D_{50} \geq 100) \quad (4.32)$$

and  $R_{c_{pc}}$  is confirmed as a function of both  $D_B/D_{50}$  and  $H_s/L_m$  by the final equation.

$$R_{c_{pc}} = 6646 H_s/L_m \cdot (D_B/D_{50})^{-1.68} + 0.88 \quad (4.33)$$

This equation is plotted in Figure 4.31 with the curves limited so that  $R_{c_{pc}} \geq 1.0$ .

The shape of the beach profile between the shoreline and crest, as defined by  $n_1$ , was also found to vary within the critical  $D_B/D_{50}$  range. This variation appears to be a complex function of beach thickness, sediment size and wave characteristics. However, within the available data set it is not possible to determine the precise form of the relationship.

In summary the profiles predicted by the equations outlined in Section 4.3 and Table 4.1 can be corrected to allow for a limited thickness of beach material by applying the correction factor  $R_{c_{pc}}$  (equation 4.33) to the predicted  $p_c$  value. This correction is only required when the effective depth of beach material  $D_B$  lies between  $30 D_{50}$  and  $100 D_{50}$ .

#### 4.8 Correction for depth limited foreshores

In the current study the toe of the model beach extended directly into deep water. This set-up was, however, adopted for practical reasons and is representative of only a few UK beaches (Chesil, Dungeness, Seaford). The majority of shingle beaches have a toe located on a sand foreshore, in conditions that are usually depth limited at some state of the tide.

As the water depth in front of a beach decreases the largest waves in a train become depth limited and begin to break offshore of the beach. In doing so, much of their energy is expended, reducing their subsequent impact on the beach. As the depth of water reduces still further an increasing proportion of the waves break offshore. Eventually so much energy is dissipated seaward of the beach that its response to the incident wave conditions is significantly affected. If we assume that wave heights offshore of a beach follow a Rayleigh distribution, then depth limiting can be assumed to occur when  $H_s/D_w \geq 0.55$ .

Section 3.6.1 established from a comparison of earlier test results for depth limited beaches with those from the current study, that over the toe water depth to wave height range,  $2.5 > H_s/D_w > 0.8$ , many of the profile parameters were substantially reduced. Further analysis suggests that the reduction is largely dependent upon the ratio  $H_s/D_w$ .

To gain a clearer understanding of the dependency between the profile parameters and  $H_s/D_w$ , values taken from depth limited profiles have been compared with those predicted using the equations derived in section 4.3. A depth limited correction factor,  $R_{c_d}$ , for each

of the profile parameters has then been established, where

$$R_{c_d} = \text{Par}_{\text{measured}} / \text{Par}_{\text{predicted}} \quad (4.34)$$

In an attempt to relate the deep water beach equations derived in section 4.3 more directly to depth limited situations, wave conditions at the toe of the beach have been employed in the calculations. Where these conditions are depth limited, use has been made of a form of Goda's equation (Ref 25), modified for random waves, to predict the depth limited significant wave height,  $H_{s_b}$ .

$$H_{s_b} = 0.12 L_m [1.0 - \exp(-4.712 D_w (1.0 + 15m^{1.33})/L_m)] \quad (4.35)$$

Here  $m$  is the foreshore slope and  $L_m$  is the mean deepwater wave length. This latter parameter will differ from the depth limited wavelength at the toe of the beach,  $L_{ms}$ , which is given by,

$$L_{ms} = T_m (g D_w)^{1/2} \quad (4.36)$$

Predicted profile parameters, obtained using the wave conditions at the toe of the beach, depth limited or otherwise, were then compared with the measured values taken from the depth limited model beaches, to establish the correction factor,  $R_{c_d}$  (equation 4.34).

For most of the profile parameters the value of the correction factor was found to vary with the ratio  $H_s/D_w$ .

The use of depth limited wave conditions in the evaluation of the initial predicted parameter values

results in a substantial under estimate of the measured parameters. This may in part be due to a partial re-distribution of energy following wave breaking. However, as a consequence the reduction factors to be applied to the predicted values will always be greater than unity.

The correction factors derived for each of the profile parameters are summarised in Table 4.4, together with their limits of applicability. For practical reasons no correction factor has been derived for the wave base elevation,  $h_b$ . In practice it is suggested that this parameter is interpolated from the initial beach profile using the corrected value of  $p_b$ . Note also that no correction is necessary for the curve parameters  $n_1$ ,  $n_2$  and  $n_3$ .

Further analysis of equations 4.37 to 4.43 (Table 4.4) reveals two interesting points. Firstly, while the elevation parameters,  $h_c$  and  $h_t$ , show the expected shallow water effect for values of  $H_s/D_w > 0.55$ , the positional parameters  $p_r$ ,  $p_c$  and  $p_b$  suggest that this effect is felt for values of  $H_s/D_w$  as low as 0.3. This may indicate that the horizontal dimensions of a shingle beach profile are determined by the largest waves in a train, whilst the vertical dimensions depend rather more on the mean wave climate.

Secondly the wave base position,  $p_b$ , displays a disjointed dependency on  $H_s/D_w$ . As  $H_s$  increases from 0.3 to  $0.8D_w$  the lower limit of the profile rapidly retreats landward. However as  $H_s$  increases still further there is an abrupt change in the behaviour of the wave base with the result that it begins to migrate seawards again, albeit at a much slower rate than its previous retreat. This sudden change in behaviour may, however, be more of a response to

processes occurring further up the profile than to any variation in the incident wave conditions.

In summary therefore, the profiles predicted by the equations outlined in section 4.3 and Table 4.1 can be corrected to allow for a depth limited foreshore by,

1. using the wave conditions calculated at the toe of the beach (equations 4.35 and 4.36) to derive the predicted parameters values, and
2. then applying the correction factors of equations 4.37 to 4.43 (Table 4.4) to those predicted values.

Analysis of the results suggest that corrections to the positional profile parameters  $p_r$ ,  $p_c$  and  $p_b$  may be required when  $H_s > 0.3D_w$ . Corrections to  $h_c$  and  $h_t$  are not however likely to be required until  $H_s > 0.55D_w$ , which is the criterion usually given for wave breaking.

#### 4.9 Comparison of measured and predicted profiles

Sections 4.3 to 4.8 have outlined a series of equations by which the profile response of shingle beaches to short term wave attack may be determined. In this section predicted profiles derived from these equations are compared with those measured during the actual model tests. As such this represents the first phase in the validation of the proposed profile prediction technique - that is validation of the analysis method. Following this initial comparison, predicted profiles are compared with a separate set of test conditions, not used in the original derivation of the profile equations. This extension of the prediction technique to 'new' data provides the second

phase of the validation. The final phase is then the testing of the model results and prediction techniques against field data. This validation of the theory behind the physical modelling of shingle beaches is covered separately in Chapter 7.

#### 4.9.1 Initial validation

In the initial validation, tests have been chosen at random from the range of conditions studied in the model. From these tests, five typical examples have been selected and reproduced as Figures 4.32 to 4.36. The comparisons covered by these figures are as follows:

1. Figure 4.32 - Test 6 (see Table 2.1), full thickness beach, toe extending into deep water.
2. Figure 4.33 - Test 52, as above.
3. Figure 4.34 - full thickness beach, toe in shallow water. Measured profile taken from concurrent site specific study.
4. Figure 4.35 - as above, measured profile taken from earlier site specific study.
5. Figure 4.36 - Test 69, effective beach thickness limited, deep water toe.

As can be seen the comparisons between measured and predicted profiles are generally very good. This is particularly true at the beach crest, which, since it generally defines the size of beach required to maintain an adequate sea defence, tends to be the area of most interest to coastal engineers. There is some

discrepancy between the profiles in the general vicinity of the transition (step). However, as this is the area of the beach which displays the greatest natural variability, lying as it does within the wave breaking zone, this is to be expected. Overall, therefore, the results suggest a satisfactory validation of the chosen analysis method.

#### 4.9.2 Additional test conditions

Figures 4.37 and 4.38 extend the profile prediction method to conditions not previously encountered in the research programme. In both cases profiles were built up on arbitrarily formed beaches, using, in the case of Figure 4.37, storm waves characterised by a mean sea steepness of 0.06, and for Figure 4.38, swell waves with a mean sea steepness of 0.01. As can be seen the comparison between measured and predicted profiles is again very good - a situation which augurs well for the subsequent extension of the prediction methodology to natural beaches.

#### 4.10 Limitations of parametric model

The methodology outlined in the preceding sections may be used to check that existing, or proposed, shingle beaches will continue to provide adequate protection to the land that they front, under a range of wave conditions. However, due to the model's empirical derivation, it has a number of limitations which must be recognised and borne in mind in any subsequent application. These are discussed below in more detail.

##### 1. Range of application

It would be unwise to attempt to use the equations for situations outside the range of conditions for which

they were derived. Essentially, their use should be confined to homogeneous shingle beaches with a median particle diameter,  $D_{50}$ , of between 10mm and 50mm. Similarly, wave conditions should be limited to those with a mean sea steepness,  $H_s/L_m$ , of 0.005 to 0.06. Incident waves should also be approaching near normal to the beach, although research to extend the parametric model to oblique wave attack is currently underway.

## 2. Wave duration

As outlined in section 4.6 wave duration can be an important factor in determining beach profile variations particularly if less than 500 waves are considered. It is however extremely difficult to accurately quantify wave duration effects since they are very much dependent upon the similarity, or lack of it, between the initial and final beach profiles. Although a method to account for duration limited profile changes has been proposed in section 4.6, much more work is required before it can be confidently applied. At present therefore it is suggested that the model is confined to the analysis of profile changes occurring over durations in excess of 500 waves. If the model is to be used to represent profile response over a tidal cycle, each step in the cycle must similarly be in excess of 500 waves.

## 3. Longshore transport

Due to its origin in two dimensional model tests, the parametric profile model deals only with onshore-offshore sediment transport. Neglecting longshore transport is not, however, a problem provided that it does not result in a nett loss, or gain, of material in the profile (ie longshore transport into the section must equal that leaving,

and vice versa). In nature, however, differential longshore transport effects can result in additional erosion or accretion of the beach over and above that due to onshore-offshore transport. Where this occurs the parametric profile model can still be used, provided an estimate of the volumetric loss or gain due to longshore transport, and its cross shore distribution, can be obtained. Work currently in hand should provide the necessary understanding of the cross-shore distribution of the longshore transport on shingle beaches. However, until the results of this investigation are available it is probably sufficient to assume that the loss, or gain, of beach volume due to longshore transport is evenly spread over the profile. Allowance for the longshore transport effect can then be made while equating areas under the profiles (section 4.5).

#### 4.11 Application of parametric model

It is envisaged that the beach profile prediction model outlined in the preceding sections will have two main uses:

1. In optimising maintenance programmes for beaches - typically by allowing a 'critical beach volume' to be identified for a particular site, below which the beach cannot be permitted to drop if it is to continue to perform satisfactorily in a coast protection role. Clearly this critical volume will also be dependent upon the perceived needs for that stretch of beach. Thus a beach serving both an amenity and coast protection function may be allocated a higher critical volume than a similar structure serving only in a coast protection role.

2. In improving and optimising the design of shingle beach renourishment schemes.

A typical application of the model is outlined below:

- Step 1. Calculate mean profile using deepwater wave conditions and median sediment diameter in equations 4.2-4.10 (Table 4.1) and 4.14-4.19.
- Step 2. Apply corrections for depth limited foreshore (equations 4.34 and 4.37-4.43) or limited beach thickness (equations 4.32 and 4.33), if required.
- Step 3. Locate predicted profile relative to initial profile using area balance method. Allow for differential longshore sediment transport if required.
- Step 4. If necessary, apply proposed wave duration correction and re-locate profile.
- Step 5. Establish confidence limits on predicted profile using equations 4.20 to 4.27.

Subsequent validation against field data suggests that, used in this way, and within its limits, the model will provide a good estimate of potential profile changes for shingle beaches.

## 5 WAVE ENERGY DISSIPATION ON SHINGLE BEACHES

### 5.1 Introduction

The effectiveness of a shingle beach in dissipating wave energy is an important measure of its usefulness

as a coast protection structure. This is particularly true of beaches used as energy absorbing structures in enclosed waters (ie marinas etc) where high levels of reflected energy can have undesirable consequences for small vessels.

During the course of the present study measurements were made of wave reflection, and hence wave energy dissipation, for a variety of wave and beach conditions. A detailed account of the measurement procedures adopted is given in Section 2.4.3. This chapter will therefore concentrate on presenting and analysing the data obtained.

## 5.2 Results and discussion

Generally three sets of reflection measurements were collected for each test, after first allowing a period of  $500 T_m$  for the main features of the beach to evolve. The reflection measurements were taken between 500–1000, 1500–2000 and 2500–3000  $T_m$  from the commencement of the test. On-line analysis of the results produced details of the incident and reflected wave spectra together with values for the reflection coefficients, both for discrete frequency bands within the spectrum and for the wave spectrum as a whole. Typical spectra obtained from the tests are plotted in Figure 5.1, from which it can be seen that the levels of energy reflected from the beach are minimal compared to those in the incident wave field.

The variation of the wave energy dissipation coefficient,  $K_D$ , across each of the wave spectra plotted in Figure 5.1, is shown in Figure 5.2. Here the values of  $K_D$  have been obtained from the reflection coefficients,  $K_R$ , for each frequency band within the spectrum, by means of the transformation:

$$K_D = (1 - K_R^2)^{1/2} \quad (5.1)$$

The resulting curves, with their characteristic parabolic shape, are a combination of data from the three sets of reflection measurements for each test. Within these measurements no duration related trends could be established, suggesting that the energy dissipating capabilities of the beach are largely established by  $500 T_m$  (cf section 4.6). Generally the curves suggest that in excess of 90% of the wave energy may be dissipated by the shingle beach. The frequency at which the maximum dissipation occurs was found to be most strongly correlated with the mean spectral frequency,  $f_m$ , rather than the peak frequency,  $f_p$ . This correlation is shown in Figure 5.3.

Although the curves given by Figure 5.2 are of interest they are not of immediate use to the practising engineer. Therefore the analysis of the results was extended so as to obtain a single 'characteristic' value of  $K_D$  for each of the wave spectra/beach conditions tested. This value was derived through integration of the areas under the incident and reflected spectra coupled with the transformation to  $K_D$  given by equation 5.1. Values of the characteristic dissipation coefficient are tabulated in Table 5.1 for each set of measurements, together with a mean value for each test. The table confirms the previous conclusion that duration trends within the development of the beach profile do not significantly affect its energy dissipation capabilities.

From Table 5.1 it is clear that the dissipation coefficient,  $K_D$ , is not constant but is related rather to the incident sea steepness,  $H_s/L_m$ . This

relationship is depicted in Figure 5.4 for all the mean  $K_D$  values listed in Table 5.1. The resulting trend shows that the proportion of wave energy dissipated by a shingle beach is reasonably constant, at around 99%, for all values of sea steepness greater than 0.02 (ie breaking wave conditions). For sea steepnesses less than 0.02 the effectiveness of the beach in dissipating wave energy begins to reduce but still remains relatively high. It is interesting to note that Figure 5.4 shows the material size,  $D_{50}$ , and the effective beach depth,  $D_B/D_{50}$ , to be of little consequence to the overall  $K_D$  trend. This may suggest that wave energy is primarily dissipated in the processes of wave breaking, and overcoming frictional losses in flow over and within the surface layers of the beach. Thus flow within the body of the beach (ie the propagation of internal waves) adds little to the overall dissipation of wave energy.

In conclusion it would appear that Figure 5.4 can be used to estimate the energy dissipation coefficient,  $K_D$ , for a wide range of shingle structures under normally incident wave action. This value can then be combined with equation 5.1 to yield the wave energy reflection coefficient,  $K_R$ . For storm waves a shingle beach will typically dissipate 99% of the incident wave energy. For swell waves the proportion of energy dissipated is slightly less.

## 6 WAVE RUN-UP DISTRIBUTIONS

### 6.1 Introduction

Since a detailed account of the measurement of the wave run-up distributions on the model beaches is given in Section 2.4.2, this chapter will concentrate only on the analysis of the data and the results obtained.

Generally five wave run-up recordings, of  $300 T_m$  duration, were taken for each test, with each recording being separated by a  $200 T_m$  interval. Prior to any measurements being taken the profile was allowed to evolve naturally for a period of  $500 T_m$ . This was generally long enough for the major profile features to develop, and subsequent analysis of the results showed no evidence of any duration dependent trends.

On completion of a test the records were processed to provide, firstly, the cumulative number of wave run-ups exceeding a specified level per record; and then, secondly, the combined exceedance probability of wave run-up for those levels, for all five sets of data. The resulting probability distribution was then used in the subsequent analysis.

## 6.2 Run-up probability distributions

Typical wave run-up distributions recorded during the model tests are given in Figure 6.1. These measured distributions have been tested against theoretical Weibull and Rayleigh distributions of the form:

$$\text{Weibull : } P(R) = \exp(-B(R-C)^A) \quad (6.1)$$

$$\text{Rayleigh : } P(R) = A \exp(-\frac{BR^2}{2}) \quad (6.2)$$

where A and B are curve fitting coefficients

C is a lower limiting value of R

R is a specified level relative to still water level

and P(R) is the probability of a wave run-up event exceeding R

In this particular instance the lower limiting value C in the Weibull distribution has been taken as zero. The run-up has therefore been measured relative to still water level rather than to an arbitrary mean water level which would necessarily include a component due to wave set-up.

Generally the differences between the two distributions were small when compared to the measured data. However the Weibull distribution usually returned slightly better correlation coefficients and hence provide a better fit to the data, particularly over the lower end of the range. The Weibull distribution was therefore taken as providing the best description of wave run-up on the model beaches. This is confirmed by Figure 6.1 where the theoretical Weibull distributions show excellent agreement with the model data.

Values of the curve fitting coefficients A and B (equation 6.1) obtained for the Weibull distributions are tabulated in Table 6.1 for all wave conditions tested. The corresponding correlation coefficients are also given. From the table it may be seen that there is a considerable variation in the value of coefficient B, which appears related to the incident wave climate. In particular B appears to be a function of both wave height,  $H_s$ , and mean sea steepness,  $H_s/L_m$ . The precise form of this relationship is given in Figure 6.2, from which regression analysis yields:

$$B = 0.3 [H_s \exp(-30.0 H_s/L_m)]^{-1.6} \quad (6.3)$$

with a correlation coefficient,  $r = 0.96$ .

As may be seen, B is therefore proportional to  $H_s/L_m$  but inversely proportional to  $H_s$ . Thus for a constant

value of A, increasing B (ie increasing sea steepness or decreasing wave height) reduces the probability of the wave run-up exceeding a specified level. This trend is confirmed by previous results (Fig 4.4).

In contrast to coefficient B, the values of coefficient A given in Table 6.1 appear to be reasonably constant, and largely independent of wave climate. This allows a mean value of 2.2 (standard deviation,  $\sigma = 0.22$ ) to be assigned to A. Combining this value with equations 6.1 and 6.3 yields an expression for determining the probable distribution of wave run-up on a shingle beach, relative to still water level,

$$\text{ie } P(R) = \exp(-BR^2 \cdot 2) \quad (6.4)$$

where the value of B is given by equation 6.3.

It is interesting to note that although equation 6.4 does not include an allowance for variations in beach sediment size, this was not found to be a serious handicap. This is perhaps not surprising given the findings of Section 4.3 which show the vertical elevation of the beach crest to be independent of beach material size. Indeed throughout the test series no dependency between wave run-up and the beach material characteristics could be observed.

The applicability of equation 6.4 to the test results is confirmed by Figure 6.3 where measured and calculated run-up levels are compared for three exceedance probabilities, namely  $P(R) = 0.5, 0.1$  and  $0.02$ . The 90% confidence limits on the calculated values are given by  $R_c \pm 0.085 \bar{R}_c$ , where  $\bar{R}_c$  is the calculated run-up exceedance level. Figure 6.4 offers further proof of the ability of equation 6.4 to

predict the probabilistic distribution of wave run-up on beaches. Here data gathered during field measurement exercises at Chesil Beach and Hurst Castle spit (Appendix 4 and Figure 7.1) is compared with the predictions of equation 6.4 for values of  $P(R) = 0.5$  and  $0.02$ . Again the agreement between the predicted and measured values is good.

### 6.2.1 Wave run-up and beach crest elevation

Observations made during the course of the test programme suggested that, even when fully developed, the beach crest would be overtopped by a small percentage of the wave run-ups. Analysis of the data, based on the assumption that it fitted a Weibull distribution, allowed this percentage to be estimated for each test condition. The resulting exceedance probabilities, calculated for a crest height at 3000 waves, are listed in Table 6.1. From here it can be seen that generally less than 3% of the wave run-ups overtop the beach crest, with the mean probability of overtopping  $\overline{P(R > h_c)} = 0.015 \pm 0.011$ . No systematic variations, based on wave conditions, are apparent within the results.

The derivation of a probability factor for overtopping of the beach crest allows equation 6.4 to be re-written in a form which negates the need to explicitly determine the Weibull coefficient  $B$ . For a given wave condition Figure 6.2 shows  $B$  to be a function of only  $H_s$  and  $H_s/L_m$ . Therefore if equation 6.4 is re-written as

$$\frac{P(R \geq R_i)}{P(R \geq h_c)} = \frac{\exp(-B R_i^{2.2})}{\exp(-B h_c^{2.2})} \quad (6.5)$$

and  $P(r \geq h_c) = 0.015$ , then

$$R_i = h_c \left[ - \frac{\ln P(R \geq R_i)}{4.2} \right]^{0.455} \quad (6.6)$$

where  $R_i$  is any beach elevation measured relative to the still water level. This equation, which can be applied to all shingle beach profiles, is plotted in Figure 6.5 as a cumulative probability distribution. It allows the probability of normally incident wave run-up crests exceeding any given point on the beach profile to be determined, regardless of the incident wave conditions.

If equation 6.6 is divided through by  $H_s$  the resultant expression,

$$\frac{R_i}{H_s} = \frac{h_c}{H_s} \left[ - \frac{\ln P(R \geq R_i)}{4.2} \right]^{0.455} \quad (6.7)$$

combined with equation 4.4, allows wave run-up exceedance levels to be related directly to incident wave steepness. This relationship is shown in Figure 6.6 for values of  $P(R)$  equal to 0.5, 0.1, 0.05, 0.02 and 0.005. The exceedance level corresponding to the mean elevation of the beach crest,  $P(R) = 0.015$ , is also given.

### 6.3 Wave set-up

As a wave propagates into shallow water, forced changes in the radiation stress result initially in a set-down of the mean water level below the still water level. Following breaking this process is reversed leading to an elevation, or set-up, of the mean water level above the still water level in the surf zone. This phenomenon has been theoretically proven, and widely observed on natural beaches; it is also present in most laboratory beach studies.

The typical run-up distributions given in Figure 6.1 clearly show the presence of wave set-up - the abrupt step in the probability distribution on the right hand side of the graph - and therefore allow an estimate to be made of the likely magnitude of this effect under a variety of wave conditions. Values of the wave set-up,  $S_u$ , recorded at the shoreline are tabulated in Table 6.1, and plotted in a dimensionless format against mean sea steepness in Figure 6.7. Generally the degree of wave set-up is between 10% and 30% of the significant wave height and is thus in accordance with field measurements. However it is clear from Figure 6.7 that there is a pronounced wave steepness dependency, with  $S_u/H_s$  generally higher under low steepness swell waves than under storm waves. Although there is considerable scatter within the results the trend can be defined by an equation of the form:

$$S_u/H_s = 0.31 - 0.35 H_s/L_m \quad (6.8)$$

with a correlation coefficient,  $r = 0.85$ .

This equation can be used to evaluate set-up under normally incident waves on shingle beaches. However, it should be noted that throughout this study all measurements have been directly related to still water level, therefore the set-up component is implicitly included.

#### 6.4 Wave run-up distribution and effective beach thickness

In addition to the main body of wave run-up measurements, data was also collected during a number of the tests with a restricted thickness of beach material. Although, as previously discussed

(Section 4.7), the beach thickness limitation does not noticeably affect the beach crest elevation, it does have a marked influence on  $p_c$  and hence on the run-up distributions. This influence manifests itself in the values of the two curve fitting coefficients, A and B, in the Weibull distribution. For the range of effective beach thicknesses,  $D_B/D_{50}$ , tested (ie 29.4, 41.2 and 52.9) there is a constant reduction in the value of coefficient A of the order of 30%; giving a new beach thickness limited value for A of 1.56 ( $\sigma = 0.08$ ). For coefficient B the correction required is rather more complicated, depending both upon the effective beach thickness,  $D_B$ , and the incident wave conditions as characterised by wavelength,  $L_m$ . The resulting relationship is given in Figure 6.8 in terms of the dimensionless beach thickness parameter  $D_B/L_m$  and a correction factor for coefficient B, defined as,

$$\text{Correction factor, } R_B = B_D/B \quad (6.9)$$

where  $B_D$  is the beach thickness limited value of coefficient B in the Weibull distribution

From the graph it can be seen that for values of  $D_B/L_m \geq 0.1$  no correction to coefficient B is required. However for values of  $D_B/L_m < 0.1$  a correction factor is required indicating that within this range the value of B for thickness limited beaches is significantly increased. From regression analysis an expression can be derived for the correction factor,  $R_B$ , whereby,

$$R_B = 0.25 (D_B/L_m)^{-0.6} \quad (6.10)$$

for  $D_B/L_m < 0.1$

and  $R_B = 1.0$

for  $D_B/L_m \geq 0.1$

The correlation coefficient of 0.87 for equation 6.10 confirms the fit to the data.

### 6.5 Comparison of wave run-up on shingle beaches and smooth planar slopes

Figure 6.9 compares wave run-up on the laboratory shingle beaches, as characterised by crest elevation,  $h_c$ , with the 2% exceedance run-up level for smooth plane slopes. This 2% level is derived using the following expressions (Refs 21 and 22):

$$\begin{aligned} 1. \quad R_s/H_s &= I_r && ; \text{ for } 0 < I_r < 2.5 \\ & && R_s/H_s = 2.5 - (I_r - 2.5)/3.0; \text{ for } 2.5 < I_r < 4.0 \\ 2. \quad R_2 &= 1.4 R_s && (6.11) \end{aligned}$$

where  $I_r$  is the Iribarren number  $\tan\alpha/(H_s/L_m)^{1/2}$

$\alpha$  is the slope angle

$R_s$  is the significant wave run-up level

and  $R_2$  is the 2% wave run-up level

The results confirm the traditional view that shingle beaches have 'effective' gradients of between 1:5 and 1:10 above the shoreline. Moreover an observed tendency for these gradients to flatten out under storm waves (Ref 23) is also borne out by the results, with the run-up curve for shingle tending more closely to that for the 1:10 smooth slope at the higher sea steepnesses. However at the same time the results must raise doubts as to the reliability of the past

practice of calculating wave run-up on smooth slopes, and then reducing it using factors to account for permeability/roughness effects, to obtain a value for shingle beaches (Ref 24). Clearly the present research suggests that no reduction factors should be applied when using this method.

## 7 COMPARISON BETWEEN FIELD AND MODEL DATA

As discussed in Section 4.9, there are a number of stages in the validation of empirical models such as that developed in this report. The final, and perhaps most important stage, is the validation against field data. This, if successful, confirms the correctness of the theory behind beach physical models, and generates confidence in the application of results from those models to natural situations.

In an initial validation of the profile prediction model developed in this study, field data was either collected directly or drawn from available sources. Details of the field data collected are given in Appendix 4, but briefly there were four main sources of useful data (see Fig 7.1):

1. A short field measurement exercise undertaken by staff from HR at West Bexington, Chesil Beach.
2. Data collected under contract by staff from Southampton University, at Hordle Cliff and Hurst Castle spit.
3. Data collected by HR staff for an earlier study at Rustington near Littlehampton.
4. A small amount of calibration data collected for an earlier study at Seaford, Sussex.

Unfortunately none of this data provided simultaneous wave measurements and full beach profiles, although corresponding wave, and wave run-up, recordings were available from West Bexington and Southampton. The results from Rustington have to be treated with caution as there were no tidal records collected and the profiles were only taken at fortnightly intervals. Thus, although a complete set of wave records is available, it is difficult to relate profile changes to a particular wave condition. In practice, the only useful information to be gained from this site relates to variation in beach crest elevation - the difference between successive profiles being assumed to be due to the wave/water level combination producing the greatest wave run-up in the intervening fortnight.

As a consequence of these deficiencies in the field data the comparison between field and model results has to be limited to a comparison of the beach crest parameters  $h_c$  and  $p_c$ , and the wave run-up exceedance levels. A detailed comparison of wave run-up exceedance levels, between the model results and the data collected at Chesil Beach and Hurst Castle spit, has been undertaken in Section 6.2. This found excellent agreement between measured and predicted values (Fig 6.4) across a range of run-up exceedance levels. Since there must be a very strong dependency between the wave run-up distribution over a beach profile and the general form of that profile, a good correspondence between run-up distributions implies a good agreement in profile shape above the still water line. As such this may be taken as a validation of the model predictions for Curve 1, from the crest to still water level.

Measured values of the beach crest parameters  $h_c$  and  $p_c$  are compared with the predicted trends in

Figures 7.2 and 7.3. As can be seen the agreement is generally good. It is noticeable, however, that in Figure 7.2 much of the Southampton data lies outside the valid range of the model results. In doing so it suggests that the predicted  $h_c$  trend will under-estimate crest elevation at lower wave steepnesses ( $<0.005$ ). A revised trend over this range is included in Figure 7.2, and given by,

$$h_c/H_s = 6.0 - 566.7 (H_s/L_m) \quad (7.1)$$

It may subsequently be prudent however to produce a revised prediction curve for the model results for  $h_c$ , which will allow direct extrapolation to lower wave steepnesses.

The scatter apparent in the results for Rustington in Figure 7.2 probably arises as a result of the lack of accurate water level records. Both  $h_c$  and  $p_c$  are measured from the waterline, and therefore errors in both will occur if the location of the water line is uncertain. These errors will be most pronounced for  $p_c$ , since a difference of a few centimetres in water level will result in a much greater difference in the position of the shoreline, particularly given the relatively flat nature of beach profiles in this region. As a result data from the Rustington surveys has not been included in Figure 7.3, where measured  $p_c$  values are compared with the predicted trend.

The comparisons between model and field data so far undertaken are generally encouraging and suggest that the parametric model is capable of predicting natural shingle beach profiles, at least above the water line. There is, however, an urgent need for further calibration data, comprising concurrent wave, water level and beach profile data. The difficulties involved in collecting this data, particularly as the

profile data should ideally be recorded throughout the tidal cycle, should not, however, be underestimated.

## 8 CONCLUSIONS AND RECOMMENDATIONS FOR FURTHER RESEARCH

### 8.1 Conclusions

A comprehensive series of physical model tests has been undertaken to explore the behaviour of shingle beaches under normally incident random waves. The tests considered the effect of wave height, wave period, beach sediment size and grading, and effective beach thickness on the resultant profiles. Use was made of data from earlier studies to extend the results to beaches located in relatively shallow water. The results have allowed the development of a parametric profile model, for predicting shingle beach profile changes resulting from onshore/offshore sediment transport, as well as yielding methods for predicting wave run-up distributions and wave reflection coefficients.

The major conclusions of this research are summarised below;

1. Beach profile changes are primarily governed by,
  - wave height,  $H_s$
  - wave period,  $T_m$
  - wave duration
  - beach material size,  $D_{50}$
  - angle of wave attack,  $\phi$

Additionally the effective thickness of beach material,  $D_B$ , and the foreshore level,  $D_w$ , are

influential in determining at least part of the profile.

2. The initial beach profile does not affect the form of the final profile, though it does determine its duration and mode of formation.
3. The grading of the beach material may influence crest elevation, with a narrower grading corresponding to a lower crest. There is however insufficient data available at present to confirm this trend.
4. Shingle beach profiles evolve rapidly, so that within 500 waves over 80% of the total volumetric change has occurred. Generally all sections of the profile evolve at similar rates and this ensures that the main features of a profile quickly become apparent. Subsequent wave action therefore serves only to hone the final profile shape.

The rate of development of a profile is however highly dependent on the relative similarity, or dissimilarity, that exists between it and the initial beach profile. The more closely the final profile resembles the initial beach form, the more rapidly the profile will evolve. Consequently, the direct inclusion of a wave duration effect within any beach profile prediction methodology is very difficult, requiring details of the final profile prior to calculating it. Ideally then, the effect of wave duration should be included as a correction factor on the final predicted profile.

5. Gradually varying water levels do not affect the shape or slope of beach profiles. They do

however determine the location of the profile on the beach face.

6. Shingle beach profiles schematised on the basis of Figure 4.1 can be satisfactorily described in terms of the dimensionless parameters  $H_S/D_{50}$ ,  $H_S/L_m$  and  $H_S T_m g^{1/2}/D_{50}^{3/2}$  by equations 4.2 to 4.10 and 4.14 to 4.19. Confidence limits on the predicted profiles can be established by reference to equations 4.20 to 4.27.
7. Analysis of the profile parameter trends suggests that waves incident on shingle beaches effectively change from breaking to non-breaking at a mean sea steepness of approximately 0.03. This is the steepness coincident with the maximum energy entering the surf zone.
8. The beach is most responsive to wave action within the wave breaking zone (ie at the transition from curve 2 to curve 3 - Fig 4.1). Consequently this is the area of greatest variability within the beach profile.
9. The presence of an underlying impermeable structure, or relatively impermeable core, within a shingle beach can have marked effect on the development of the emergent portion of the beach if the ratio of effective beach thickness,  $D_B$ , to median material size,  $D_{50}$  is less than 100. Provided  $D_B/D_{50} \geq 30$ , this effect is mainly confined to the parameter  $p_c$  and can be predicted using equations 4.32 and 4.33. For values of  $D_B/D_{50} < 30$ , the thickness of beach is usually insufficient to retain material over the profile, and the beach structure breaks down.

10. Allowance for shallow water effects in the prediction of shingle beach profiles may need to be made, at least for the positional parameters  $p_r$ ,  $p_c$  and  $p_b$ , when the ratio of offshore significant wave height,  $H_s$ , to toe water depth,  $D_w$ , exceeds 0.3. For the elevation parameters  $h_c$  and  $h_t$  a shallow water correction is not required until  $H_s/D_w > 0.55$ , which is the usual criterion for wave breaking. In order to correct for depth limited conditions at the beach toe it is first necessary to use the wave conditions derived at the toe of the beach (equations 4.35 and 4.36) to calculate the predicted parameter values, and then to correct these parameters using equations 4.37 to 4.43.
11. Results obtained from the analysis of shallow water effects indicate that the horizontal dimensions of a shingle beach profile are determined by the largest waves in a train, whilst the vertical dimensions depend rather more on the mean wave climate.
12. For mean sea steepnesses greater than 0.02 a shingle beach typically dissipates around 99% of the incident wave energy. This percentage drops however for mean sea steepnesses less than 0.02, indicating that the beach is slightly less effective under swell waves than under storm waves. For waves of normal incidence Figure 5.4 allows wave energy dissipation coefficients to be predicted as a function of mean sea steepness.
13. Within the scope of the study no dependency between wave energy dissipation and beach material size, or effective beach thickness, could be found.

14. Maximum energy dissipation occurs at the mean spectral frequency rather than the peak frequency.
15. Wave duration trends were not apparent within either the wave energy dissipation results or the wave run-up distribution. This again suggests that the most important profile features largely evolve within the first 500 waves.
16. A Weibull distribution was found to provide the best description of the wave run-up on shingle beaches. The exact form of this distribution is given by equations 6.3 and 6.4.
17. Even when fully developed the beach crest is still overtopped by a small proportion of the wave run-ups. Analysis of the test results suggests that this mean probability of overtopping  $\overline{P(R > h_c)} = 0.015 \pm 0.011$ . Within the test results the overtopping appeared to be independent of wave climate.
18. The distribution of wave run-up crests over the emergent beach profile was found to be positively skewed. This is in accordance within previous results for run-up on rough, porous planar slopes (Ref 22).
19. Within the scope of the test results no dependency between wave run-up and beach material size could be determined. Wave run-up was however found to be dependent upon the effective thickness of beach material. The form of this dependency is outlined in Section 6.4.

20. A comparison between wave run-up on shingle beaches and smooth planar slopes confirms the traditional view that shingle beaches have an effective gradient of between 1:5 and 1:10, above the shoreline, and that the beach gradient tends to flatten out under storm waves. The results raise doubts, however, as to the reliability of the past practice of calculating run-up on smooth slopes, and then reducing it using factors to account for permeability/roughness effects, to obtain a value for shingle beaches. The present research suggests that no reduction factors should be used when applying this method.
21. Wave set-up effects were observed in the model tests. The set-up recorded at the shoreline was found to be between 10% and 30% of the incident wave height and thus in accordance with field measurements. It was clear from the results however that there was a pronounced dependency on wave steepness, with greater set-up recorded under swell waves than under storm waves. The form of this dependency is given by equation 6.8.
22. Initial validation of the model predictions against field data yielded encouraging results, suggesting that above the shoreline, at least, the physical model provides a good representation of natural beaches. Further field data, particularly relating to the submerged portion of the profile, is however required in order to confirm these initial findings.
23. Beach profile prediction models derived on the basis of empirical random wave studies can only yield reliable results if the sediment response has been correctly reproduced in the model.

Amongst the factors needing to be accurately scaled in the model are the permeability of the beach, the threshold of sediment motion and the relative magnitudes of onshore/offshore sediment transport.

## 8.2 Recommendations for further research

This study has highlighted a number of areas which need to be explored more fully. Effects such as those due to oblique wave attack and the inclusion of longshore sediment transport within the profile prediction methodology, are currently under investigation in a related study. However there is also a need to look more closely at the influence of beach grading on the profile response of shingle beaches, and to consider more fully ways in which the duration of wave action may be incorporated within the profile prediction methodology.

It should also be recognised that the present research applies only to shingle beaches, and that there will be an increasing need in future years to develop similar techniques for sand and mixed sand-shingle beaches. Research to meet these needs should be put in hand as soon as possible.

Finally, there is an urgent need for detailed field data against which to calibrate the model results. To be of maximum use this data should include concurrent wave, water level and beach profile measurements taken under a range of conditions and on a variety of beaches. Consideration should be given to both setting up the necessary field measurement exercises and making maximum use of ongoing field studies. Only when sufficient data has been collected can the model

results be fully validated for beach design and management purposes.

## 9 ACKNOWLEDGEMENTS

This report describes work carried out by members of the Coastal Engineering Group at Hydraulics Research. The study was designed and supervised by Dr K A Powell who also carried out the analysis and reporting. Mr R E Sadler and Mr A R Channell assisted with the experimental work.

Field data from Chesil Beach and Rustington was collected by Mr A R Channell, while the wave data from Chesil was supplied by Mr M Blackley and Mr P Hardcastle from the Proudman Oceanographic Laboratory, Bidston. Staff from the Civil Engineering Department at Southampton University, and in particular Mr M Riley and Mr J Cross, undertook the field measurements at Hordle and Hurst Castle spit under a separate contract.

10 REFERENCES

1. Hydraulics Research. "BBC Wave Spectrum Synthesiser - Version 1(A)", Wallingford, Nov 1985.
2. Dedow H R A, Thompson D M and Fryer D K. "On the generation, measurement and analysis of random seas", Poona, Nov 1976, Hydraulics Research reprint L98.
3. Gilbert G and Thompson D M. "Reflections in random waves - the frequency response function method", HRS Report IT 173, Wallingford, March 1978.
4. Kajima R. "Estimation of an incident wave spectrum under the influence of reflection", Coastal Engineering in Japan, Vol 12, 1969.
5. Watts G M and Dearduff R F. "Laboratory study of effects of tidal action on wave formed beach profiles", BEB Tech memo No 52, 1954.
6. Powell K A. "The hydraulic behaviour of shingle beaches under regular waves of normal incidence", PhD Thesis, Univ of Southampton, Sept 1986.
7. Van der Meer J W and Pilarczyk K W. "Dynamic stability of rock slopes and gravel beaches", Proc 20th Int Conf Coastal Engineering, Taipei, 1986.
8. Hughes S A and Chiu T S. "Beach and dune erosion during severe storms", Coastal and Oceanographic Engrg Dept, Univ of Florida, Report No UFL/COEL/TR/043, 1981.

9. Van der Meer J W. "Rock slopes and gravel beaches under wave attack", Delft Hydraulics Communication No 396, 1988.
10. Dalrymple R A and Thompson W W. "Study of equilibrium beach profiles", Proc 15th Conf on Coastal Eng, 2, 1976.
11. Nicholson J. "A laboratory study of the relationship between waves and beach profiles", Inst Engrs Aust Conf on Hydraulics and Fluid Mechanics, 1968.
12. Van Hijum E. "Equilibrium profiles of coarse material under wave attack", Proc 14th Conf on Coastal Eng, 2, 1974.
13. Rector R L. "Laboratory study of the equilibrium profiles of beaches", US Army BEB Tech Memo 41, 1954.
14. Chesnutt C B. "Laboratory effects in coastal movable bed models", ASCE Proc Sym on Modelling Techniques, 2, 1975.
15. Sunamura T and Horikawa K. "Two dimensional beach transformation due to waves", Proc 14th Conf on Coastal Eng, 2, 1974.
16. Gourlay M R. "Beaches: Profiles, Processes and Permeability", Res Report No CE14, Dept of Civil Eng Univ of Queensland, Australia, 1980.
17. King C A M. "Beaches and Coasts", Edward Arnold Ltd, London, 1972.

18. Kemp P H. "A field study of wave action on natural beaches", 10th IAHR Congress, London, 1963.
19. Van Hijum E and Pilarczyk K W. "Equilibrium profile and longshore transport of coarse material under regular and irregular wave attack", Delft Hydraulics Lab, Publ No 274, 1982.
20. Longuet-Higgins M S and Parkin D W. "Sea waves and beach cusps", The Geographical Jour, Vol 128, pt 2, June 1962.
21. Allsop N W H, Franco L and Hawkes P J. "Wave run-up on steep slopes: a literature review", Hydraulics Research Report No SR 1, Wallingford, 1985.
22. Allsop N W H, Hawkes P J, Jackson F A and Franco L. "Wave run-up on steep slopes - model tests under random waves", Hydraulics Research Report No SR 2, Wallingford, 1985.
23. Hydraulics Research Station. "Hydraulic design of sea dikes", Publication No DE6, Wallingford, 1973.
24. Berkeley Thorn R and Roberts A G. "Sea defence and coast protection works", Pub Thomas Telford Ltd, 1981.
25. Goda Y. Irregular wave deformation in the surf zone. Coastal Engineering in Japan. Vol 18, 1975.

## TABLES



TABLE 2.1 Summary of shingle beach tests

Test No	Material Size $D_{50}$ (m)	Material Grading $D_{85}/D_{15}$	Beach Depth $D_B$ (m)	No of Waves	Wave Height $H_S$ (m)	Wave Period $T_m$ (s)	Actual Wave Steepness
1	0.0100	2.60	0.325	3000	2.976	5.76	0.058
2	0.0100	2.60	0.325	3000	2.998	5.69	0.060
3	0.0100	2.60	0.325	3000	2.599	5.28	0.060
4	0.0100	2.60	0.325	3000	2.402	5.04	0.060
5	0.0100	2.60	0.325	3000	2.055	4.67	0.060
6	0.0100	2.60	0.325	3000	2.690	5.90	0.050
7	0.0100	2.60	0.325	3000	2.373	5.56	0.049
8	0.0100	2.60	0.325	3000	1.982	5.03	0.050
9	0.0100	2.60	0.325	3000	1.808	4.84	0.049
10	0.0100	2.60	0.325	3000	1.457	4.29	0.050
11	0.0100	2.60	0.325	3000	2.313	6.16	0.039
12	0.0100	2.60	0.325	3000	2.066	5.77	0.040
13	0.0100	2.60	0.325	3000	1.746	5.24	0.040
14	0.0100	2.60	0.325	3000	1.524	4.99	0.039
15	0.0100	2.60	0.325	3000	1.452	4.77	0.040
16	0.0100	2.60	0.325	3000	0.870	3.76	0.039
17	0.0100	2.60	0.325	3000	1.947	6.54	0.029
18	0.0100	2.60	0.325	3000	1.642	6.03	0.029
19	0.0100	2.60	0.325	3000	1.310	5.41	0.029
20	0.0100	2.60	0.325	3000	1.154	4.96	0.030
21	0.0100	2.60	0.325	3000	0.500	3.35	0.029
22	0.0100	2.60	0.325	3000	1.784	7.35	0.021
23	0.0100	2.60	0.325	3000	1.290	6.49	0.020
24	0.0100	2.60	0.325	3000	1.037	5.70	0.020
25	0.0100	2.60	0.325	3000	0.749	4.96	0.020
26	0.0100	2.60	0.325	3000	1.286	9.08	0.010
27	0.0100	2.60	0.325	3000	1.126	8.51	0.010
28	0.0100	2.60	0.325	3000	1.007	7.95	0.010
29	0.0100	2.60	0.325	3000	0.947	11.18	0.005
30	0.0104	2.19	0.325	3000	2.998	5.69	0.060
31	0.0104	2.19	0.325	3000	2.599	5.28	0.060
32	0.0104	2.19	0.325	3000	2.055	4.67	0.060
33	0.0104	2.19	0.325	3000	2.690	5.90	0.050
34	0.0104	2.19	0.325	3000	1.982	5.03	0.050
35	0.0104	2.19	0.325	3000	1.457	4.29	0.050
36	0.0104	2.19	0.325	3000	2.313	6.16	0.039
37	0.0104	2.19	0.325	3000	2.066	5.77	0.040
38	0.0104	2.19	0.325	3000	1.524	4.99	0.039
39	0.0104	2.19	0.325	3000	0.870	3.76	0.039
40	0.0104	2.19	0.325	3000	1.642	6.03	0.029
41	0.0104	2.19	0.325	3000	1.154	4.96	0.030
42	0.0104	2.19	0.325	3000	1.037	5.70	0.020
43	0.0104	2.19	0.325	3000	1.126	8.51	0.010
44	0.0300	2.22	0.325	3000	2.998	5.69	0.060
45	0.0300	2.22	0.325	3000	2.599	5.28	0.060
46	0.0300	2.22	0.325	3000	2.055	4.67	0.060
47	0.0300	2.22	0.325	3000	2.313	6.16	0.039

TABLE 2.1 (Cont'd) Summary of shingle beach tests

48	0.0300	2.22	0.325	3000	2.066	5.77	0.040
49	0.0300	2.22	0.325	3000	1.524	4.99	0.039
50	0.0300	2.22	0.325	3000	0.870	3.76	0.039
51	0.0300	2.22	0.325	3000	1.784	7.35	0.021
52	0.0300	2.22	0.325	3000	1.037	5.70	0.020
53	0.0300	2.22	0.325	3000	1.126	8.51	0.010
54	0.0240	2.64	0.325	3000	2.998	5.69	0.060
55	0.0240	2.64	0.325	3000	2.599	5.28	0.060
56	0.0240	2.64	0.325	3000	2.055	4.67	0.060
57	0.0240	2.64	0.325	3000	2.313	6.16	0.039
58	0.0240	2.64	0.325	3000	2.066	5.77	0.040
59	0.0240	2.64	0.325	3000	1.524	4.99	0.039
60	0.0240	2.64	0.325	3000	0.870	3.76	0.039
61	0.0240	2.64	0.325	3000	1.784	7.35	0.021
62	0.0240	2.64	0.325	3000	1.037	5.70	0.020
63	0.0100	2.60	0.100	1000	2.976	5.76	0.058
64	0.0100	2.60	0.100	3000	2.998	5.69	0.060
65	0.0100	2.60	0.100	1000	2.599	5.28	0.060
66	0.0100	2.60	0.100	1000	2.402	5.04	0.060
67	0.0100	2.60	0.100	3000	2.055	4.67	0.060
68	0.0100	2.60	0.100	1000	2.313	6.16	0.039
69	0.0100	2.60	0.100	3000	2.066	5.77	0.040
70	0.0100	2.60	0.100	1000	1.746	5.24	0.040
71	0.0100	2.60	0.100	1000	1.524	4.99	0.039
72	0.0100	2.60	0.100	1000	1.452	4.77	0.040
73	0.0100	2.60	0.100	1000	0.870	3.76	0.039
74	0.0100	2.60	0.100	1000	1.784	7.35	0.021
75	0.0100	2.60	0.100	1000	1.290	6.49	0.020
76	0.0100	2.60	0.100	3000	1.037	5.70	0.020
77	0.0100	2.60	0.100	1000	0.749	4.96	0.020
78	0.0100	2.60	0.140	1000	2.976	5.76	0.058
79	0.0100	2.60	0.140	3000	2.998	5.69	0.060
80	0.0100	2.60	0.140	1000	2.599	5.28	0.060
81	0.0100	2.60	0.140	1000	2.402	5.04	0.060
82	0.0100	2.60	0.140	3000	2.055	4.67	0.060
83	0.0100	2.60	0.140	1000	2.313	6.16	0.039
84	0.0100	2.60	0.140	3000	2.066	5.77	0.040
85	0.0100	2.60	0.140	1000	1.746	5.24	0.040
86	0.0100	2.60	0.140	1000	1.524	4.99	0.039
87	0.0100	2.60	0.140	1000	1.452	4.77	0.040
88	0.0100	2.60	0.140	1000	0.870	3.76	0.039
89	0.0100	2.60	0.140	1000	1.784	7.35	0.021
90	0.0100	2.60	0.140	1000	1.290	6.49	0.020
91	0.0100	2.60	0.140	3000	1.037	5.70	0.020
92	0.0100	2.60	0.140	1000	0.749	4.96	0.020
93	0.0100	2.60	0.180	1000	2.976	5.76	0.058
94	0.0100	2.60	0.180	3000	2.998	5.69	0.060
95	0.0100	2.60	0.180	1000	2.599	5.28	0.060
96	0.0100	2.60	0.180	1000	2.402	5.04	0.060
97	0.0100	2.60	0.180	3000	2.055	4.67	0.060
98	0.0100	2.60	0.180	1000	2.313	6.16	0.039
99	0.0100	2.60	0.180	3000	2.066	5.77	0.040
100	0.0100	2.60	0.180	1000	1.746	5.24	0.040

TABLE 2.1 (Cont'd) Summary of shingle beach tests

101	0.0100	2.60	0.180	1000	1.524	4.99	0.039
102	0.0100	2.60	0.180	1000	1.452	4.77	0.040
103	0.0100	2.60	0.180	1000	0.870	3.76	0.039
104	0.0100	2.60	0.180	1000	1.784	7.35	0.021
105	0.0100	2.60	0.180	1000	1.290	6.49	0.020
106	0.0100	2.60	0.180	3000	1.037	5.70	0.020
107	0.0100	2.60	0.180	1000	0.749	4.96	0.020
108	0.0104	2.19	0.100	1000	2.998	5.69	0.060
109	0.0104	2.19	0.100	3000	2.055	4.67	0.060
110	0.0104	2.19	0.100	1000	2.066	5.77	0.040
111	0.0104	2.19	0.100	1000	1.037	5.70	0.020
112	0.0104	2.19	0.140	3000	2.998	5.69	0.060
113	0.0104	2.19	0.140	3000	2.055	4.67	0.060
114	0.0104	2.19	0.140	3000	2.066	5.77	0.040
115	0.0104	2.19	0.140	3000	1.037	5.70	0.020
116	0.0104	2.19	0.180	1000	2.998	5.69	0.060
117	0.0104	2.19	0.180	1000	2.055	4.67	0.060
118	0.0104	2.19	0.180	1000	2.066	5.77	0.040
119	0.0104	2.19	0.180	1000	1.037	5.70	0.020
120	0.0104	2.19	0.220	1000	2.998	5.69	0.060
121	0.0104	2.19	0.220	1000	2.055	4.67	0.060
122	0.0104	2.19	0.220	1000	2.066	5.77	0.040
123	0.0104	2.19	0.220	1000	1.037	5.70	0.020
124	0.0300	2.22	0.140	1000	2.998	5.69	0.060
125	0.0300	2.22	0.140	1000	2.055	4.67	0.060
126	0.0300	2.22	0.140	1000	2.066	5.77	0.040
127	0.0300	2.22	0.140	1000	1.037	5.70	0.020
128	0.0240	2.64	0.140	1000	2.998	5.69	0.060
129	0.0240	2.64	0.140	1000	2.055	4.67	0.060
130	0.0240	2.64	0.140	1000	2.066	5.77	0.040
131	0.0240	2.64	0.140	1000	1.037	5.70	0.020

TABLE 4.1 Summary of functional relationships for beach profile descriptors

Functional Relationship	Limit of Applicability	Correlation (r)	Standard deviation ( $\sigma$ )	Equation Number
1. $\rho_r/H_s = 6.38 + 3.25 \ln (H_s/L_m)$	$0.01 \leq H_s/L_m \leq 0.06$	0.94	0.68	(4.2)
2. $\rho_c D_{50}/H_s L_m = -0.23 (H_s T_m g^{1/2}/D_{50}^{3/2})^{-0.588}$	$0.01 \leq H_s/L_m \leq 0.06$	0.94	0.18	(4.3)
3. $h_c/H_s = 2.86 - 62.69 (H_s/L_m) + 443.29 (H_s/L_m)^2$	$0.01 \leq H_s/L_m \leq 0.06$	0.97	0.13	(4.4)
4. $\rho_t D_{50}/H_s L_m = 1.73 (H_s T_m g^{1/2}/D_{50}^{3/2})^{-0.81}$	$0.01 \leq H_s/L_m < 0.03$	0.94	0.22	(4.5)
5. $\rho_t/D_{50} = 55.26 + 41.24 (H_s^2/L_m D_{50}) + 4.90 (H_s^2/L_m D_{50})^2$	$0.03 \leq H_s/L_m \leq 0.06$	0.97	140.9	(4.6)
6. $h_t/H_s = -1.12 + 0.65 (H_s^2/L_m D_{50}) - 0.11 (H_s^2/L_m D_{50})^2$	$0.01 \leq H_s/L_m < 0.03$	0.90	0.11	(4.7)
7. $h_t/D_{50} = -10.41 - 0.025(H_s^2/D_{50}^{3/2} L_m^{1/2}) - 7.5 \times 10^{-5} (H_s^2/D_{50}^{3/2} L_m^{1/2})^2$	$0.03 \leq H_s/L_m \leq 0.06$	0.95	13.10	(4.8)
8. $\rho_b/D_{50} = 28.77 (H_s/D_{50})^{0.92}$	$0.01 \leq H_s/L_m \leq 0.06$	0.94	0.20	(4.9)
9. $h_b/L_m = -0.87 (H_s/L_m)^{0.64}$	$0.01 \leq H_s/L_m \leq 0.06$	0.89	0.18	(4.10)

TABLE 4.2 Parameter variances for confidence limits

Parameter	Bounds	Variance, $V(\alpha)$
$P_r$		$0.467 H_s^2$
$h_c$		$0.017 H_s$
$P_c$		$0.031 \overline{P_c^2}$
$h_t$	$(H_s/L_m \geq 0.03)$	$171.72 D_{50}^2$
$h_t$	$(H_s/L_m < 0.03)$	$0.012 H_s^2$
$P_t$	$(H_s/L_m \geq 0.03)$	$1.99 \times 10^4 D_{50}^2$
$P_t$	$(H_s/L_m < 0.03)$	$0.05 \overline{P_t^2}$
$h_b$		$0.032 \overline{h_b^2}$
$n_1$	$(H_s/L_m \geq 0.03)$	0.043
$n_1$	$(H_s/L_m < 0.03)$	0.011
$n_2$		0.037
$n_3$	$(H_s/L_m > 0.02)$	0.035
$n_3$	$(H_s/L_m \leq 0.02)$	0.002

TABLE 4.3 Cross co-variances for confidence limits

Dependency	Cross Co-variance $C_{i,j}$	Correlation $r$	Significant at 1% level
$C_{h_c, n_1}$	0.007	0.034	x
$C_{h_b, n_3}$	0.011	0.141	√
$C_{h_t, n_2}$	0.031	0.211	√
$C_{h_t, h_b}$	-0.219	0.476	√
$C_{h_t, n_3}$	-0.007	-0.214	√
$C_{P_c, P_r}$	1.169	0.248	√
$C_{P_t, h_b}$	-0.117	-0.046	x
$C_{P_r, h_c}$	0.245	0.172	√

TABLE 4.4 Correction Factors for Depth Limited Foreshores

Profile Descriptor	Correction Factor ( $R_{cd}$ )	Limit of Applicability	Equation No.
$P_r$	$1.08(H_s/D_w)+0.72$	$0.3 < H_s/D_w < 2.5$	(4.37)
$P_c$	$3.03(H_s/D_w)+0.12$	$0.3 < H_s/D_w < 2.5$	(4.38)
$h_c$	$(H_s/D_w) + 0.41$	$0.55 < H_s/D_w < 2.5$	(4.39)
$P_t$	$0.007(L_m/D_w)^{1.2} + 0.45$	$40 < L_m/D_w < 130$	(4.40)
$h_t$	1.0	$0.55 < H_s/D_w < 2.5$	(4.41)
$P_b$	$-1.14(H_s/D_w)+1.31$	$0.3 < H_s/D_w < 0.8$	(4.42)
$P_b$	$0.20(H_s/D_w)+0.28$	$0.8 \leq H_s/D_w < 2.5$	(4.43)

**TABLE 5.1 Wave energy dissipation coefficients**

Test No.	Characteristic Dissipation Coefficients, $K_D$			Mean Dissipation Coefficient, $\bar{K}_D$
	500-1000 waves	1500-2000 waves	2500-3000 waves	
1	0.996	0.995	0.995	0.995
2	0.995	0.995	0.995	0.995
3	0.992	0.993	0.993	0.993
4	0.995	0.995	0.994	0.995
5	0.995	0.995	0.995	0.995
6	0.994	0.993	0.994	0.994
7	0.995	0.995	0.996	0.995
8	0.994	0.993	0.994	0.994
9	0.995	0.995	0.995	0.995
10	0.994	0.993	0.994	0.994
11	0.993	0.994	0.995	0.994
12	0.995	0.995	0.995	0.995
13	0.995	0.995	0.995	0.995
14	0.994	0.995	0.995	0.994
15	0.996	0.995	0.996	0.996
16	0.995	0.993	0.996	0.995
17	0.995	0.996	0.996	0.996
18	0.995	0.995	0.996	0.995
19	0.996	0.996	0.995	0.996
20	0.993	0.992	0.993	0.992
21	0.992	0.993	0.992	0.993
22	0.992	0.992	0.993	0.993
23	0.993	0.993	0.993	0.993
24	0.994	0.994	0.994	0.994
25	0.992	0.991	0.992	0.992
26	0.966	0.977	0.979	0.974
27	0.977	0.979	0.979	0.979
28	0.969	0.978	0.979	0.975
29	0.895	0.911	0.902	0.903
54	0.995	0.995	0.995	0.995
55	0.993	0.990	0.989	0.991
56	0.994	0.996	0.996	0.996
57	0.996	0.996	0.995	0.995
58	0.995	0.995	0.996	0.996
59	0.995	0.995	0.995	0.995
60	0.996	0.996	0.995	0.996
61	0.995	0.994	0.995	0.995
62	0.993	0.993	0.993	0.993
64	0.995	0.996	0.996	0.996
67	0.995	0.993	0.996	0.995
69	0.996	0.997	0.996	0.996
76	0.992	0.992	0.993	0.992
94	0.996	0.996	0.995	0.996
97	0.994	0.994	0.993	0.993
99	0.994	0.995	0.994	0.994
106	0.994	0.993	0.993	0.993

**TABLE 6.1 Wave run-up results**

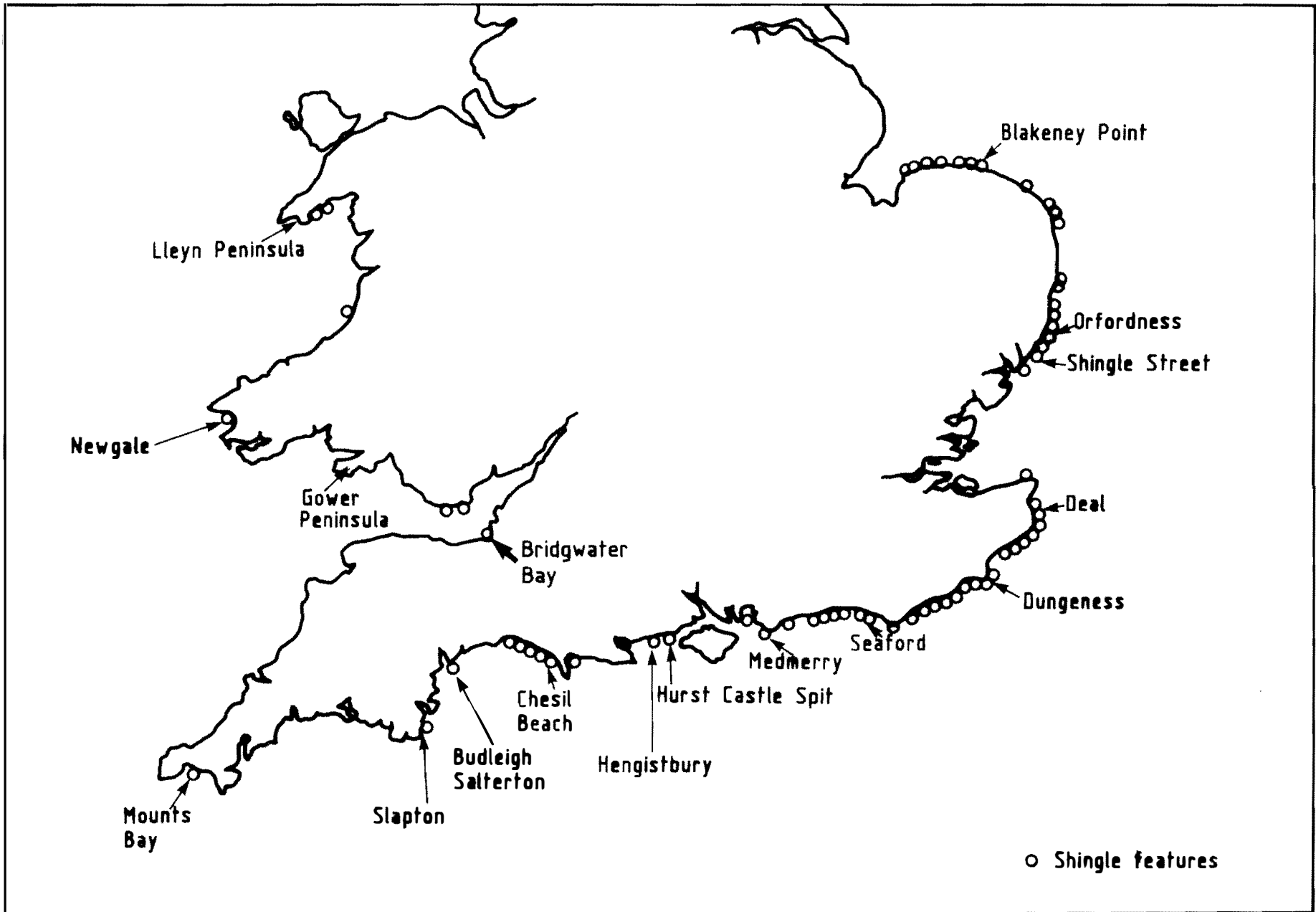
Test No.	Weibull curve fitting			Wave set-up	P(R > h <sub>c</sub> )
	A	B	r	S <sub>u</sub> (m)	
1	2.31	0.63	0.996	0.33	0.013
2	2.15	0.82	0.998	0.30	0.009
3	2.02	1.01	0.999	0.27	0.030
4	1.86	1.54	0.993	0.20	0.003
5	2.06	1.84	0.995	0.17	0.003
6	2.18	0.64	0.998	0.31	0.012
7	2.07	0.74	0.993	0.35	0.023
8	2.22	0.99	0.993	0.24	0.016
9	2.08	1.10	0.998	0.22	0.020
10	2.10	2.11	0.999	0.24	0.010
11	2.22	0.46	0.993	0.32	0.008
12	2.31	0.55	0.995	0.30	0.008
13	2.31	0.83	0.997	0.24	0.013
14	2.39	0.89	0.992	0.33	0.008
15	2.49	1.05	0.997	0.32	0.020
16	2.66	2.52	0.998	-	0.053
17	2.07	0.43	0.995	0.33	0.013
18	2.02	0.62	0.997	0.26	0.014
19	2.24	0.86	0.996	0.32	0.016
20	2.24	1.13	0.997	0.29	0.013
21	2.25	5.01	1.000	-	0.012
22	1.88	0.41	0.996	0.40	0.029
23	1.86	0.59	0.997	0.25	0.023
24	2.05	0.87	0.996	0.28	0.022
25	2.65	1.09	0.993	-	0.012
26	2.53	0.28	0.992	0.35	0.002
27	2.56	0.34	0.995	0.40	0.004
28	2.05	0.63	0.998	0.20	0.005
29	2.41	0.61	0.998	0.12	0.006



## FIGURES



Fig 1.1 Location of major shingle features in U.K.



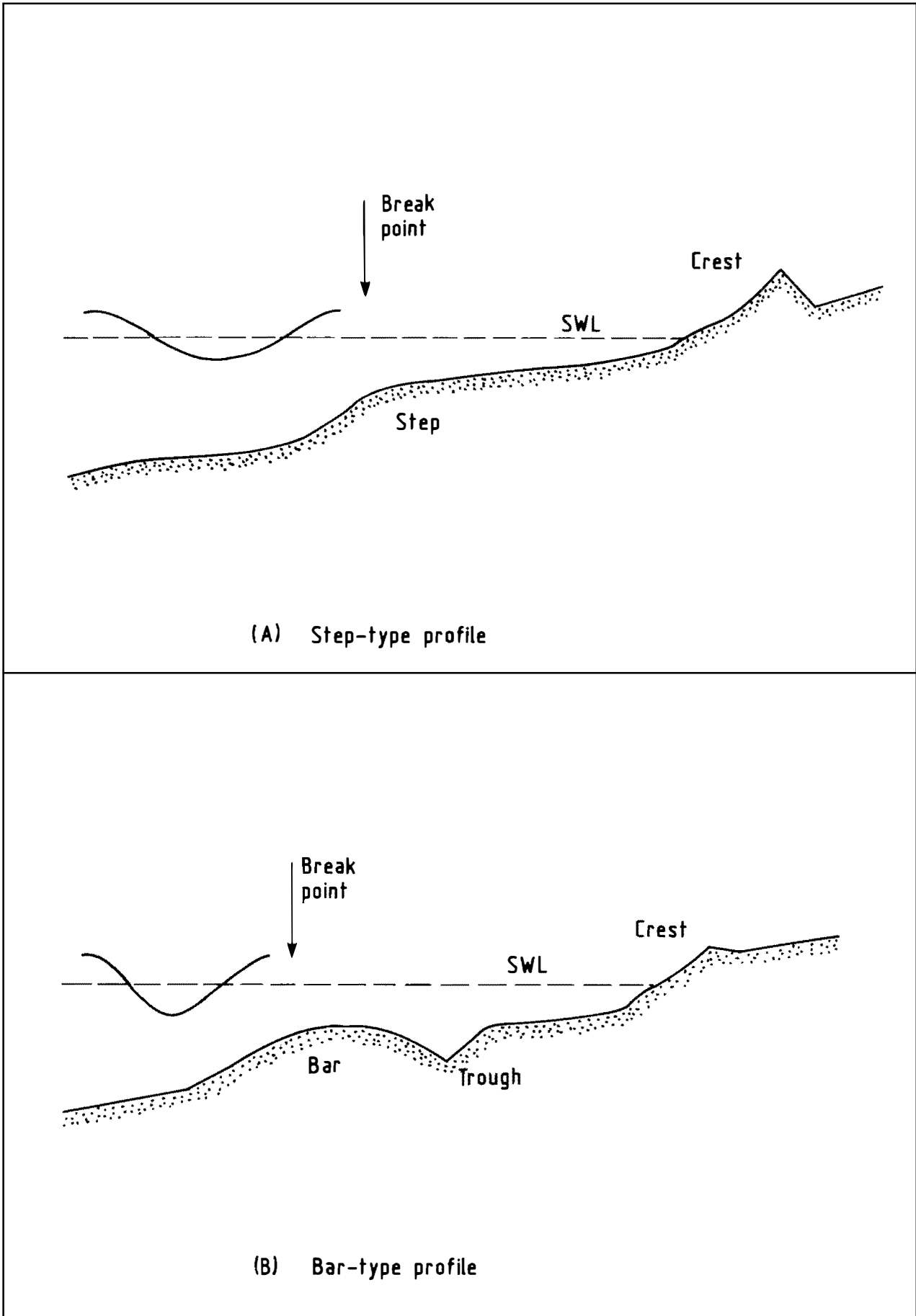


Fig 1.2 Idealised beach profile types

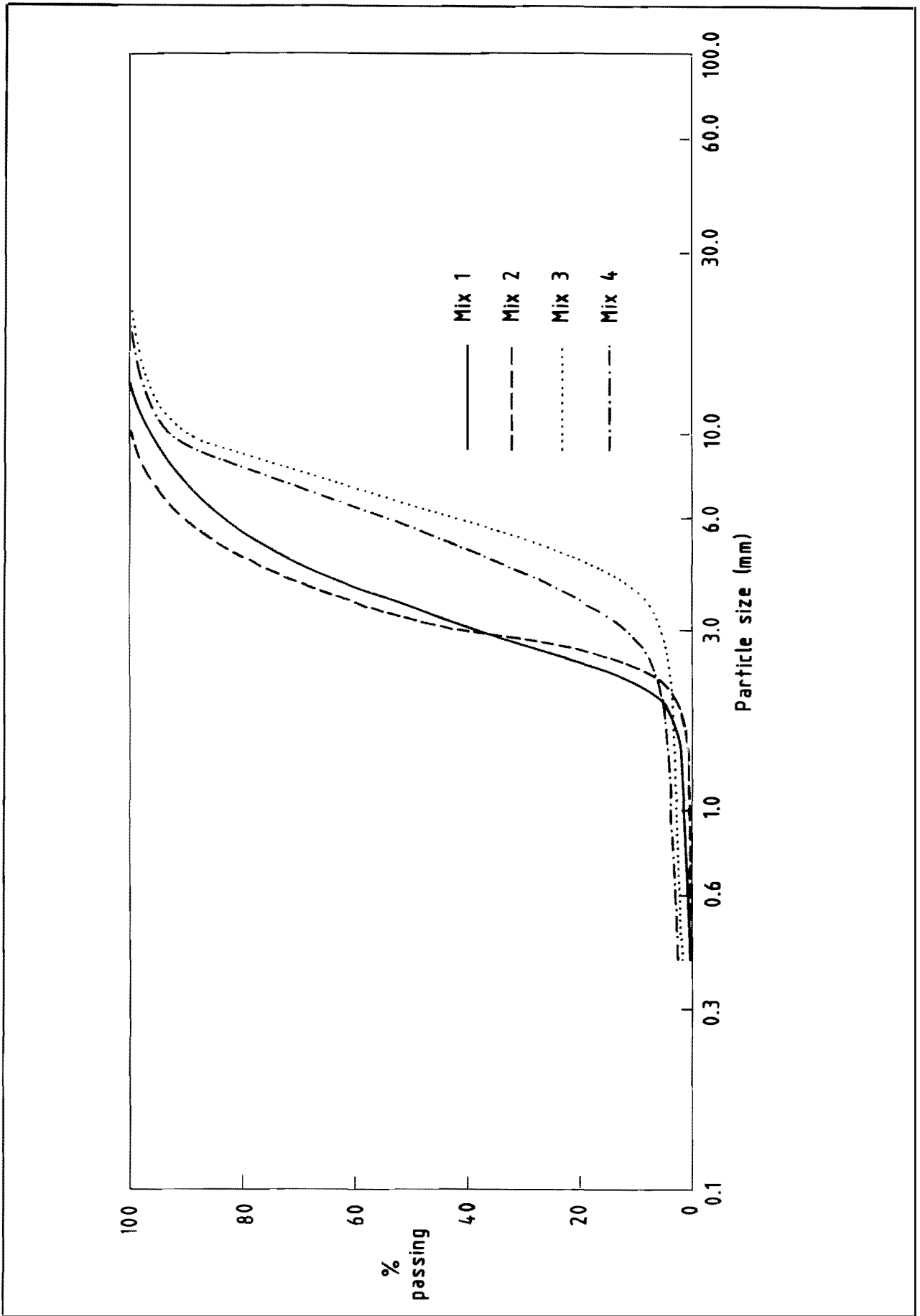


Fig 2.1 Model sediment grading curves

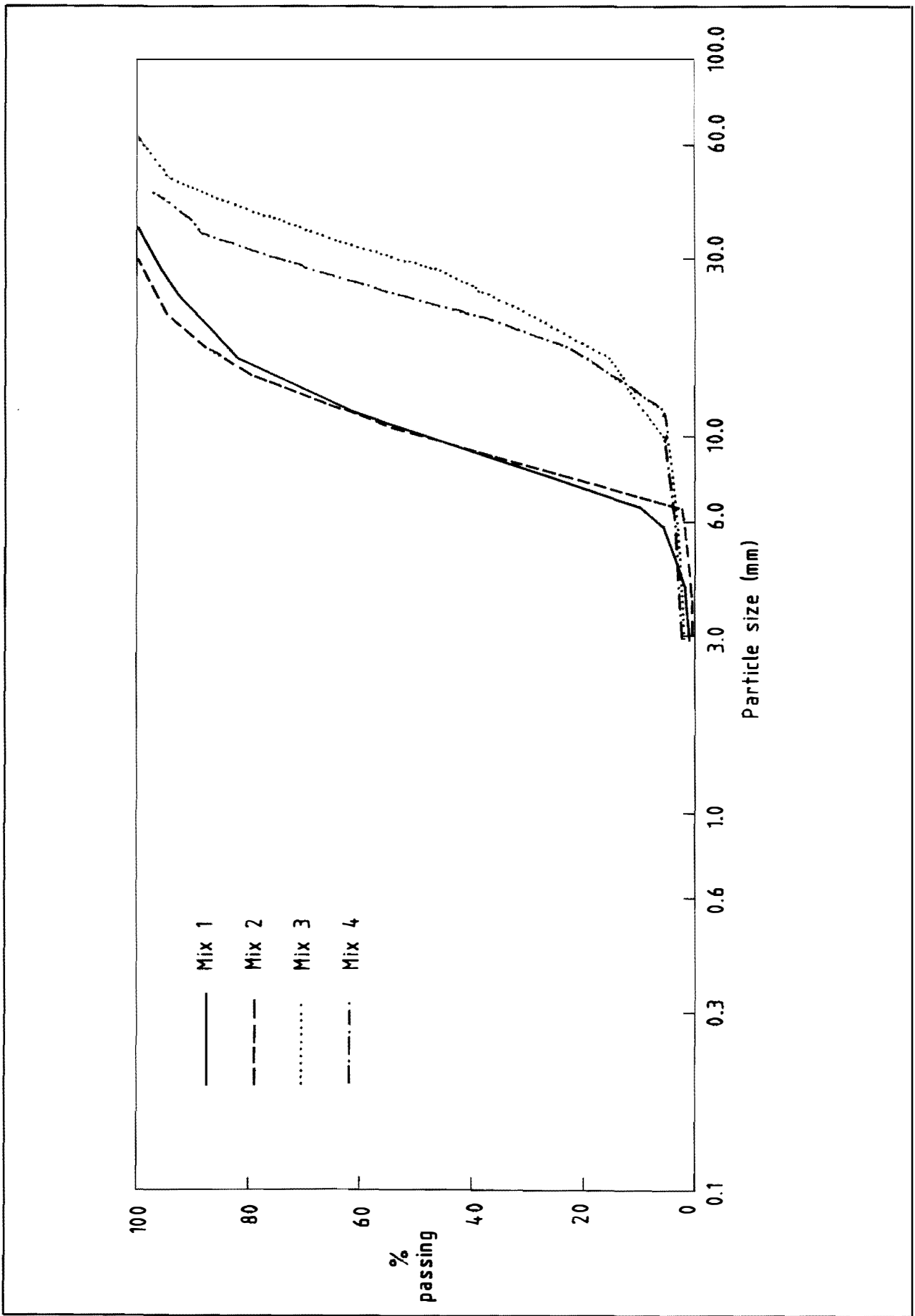


Fig 2.2 Prototype sediment grading curves

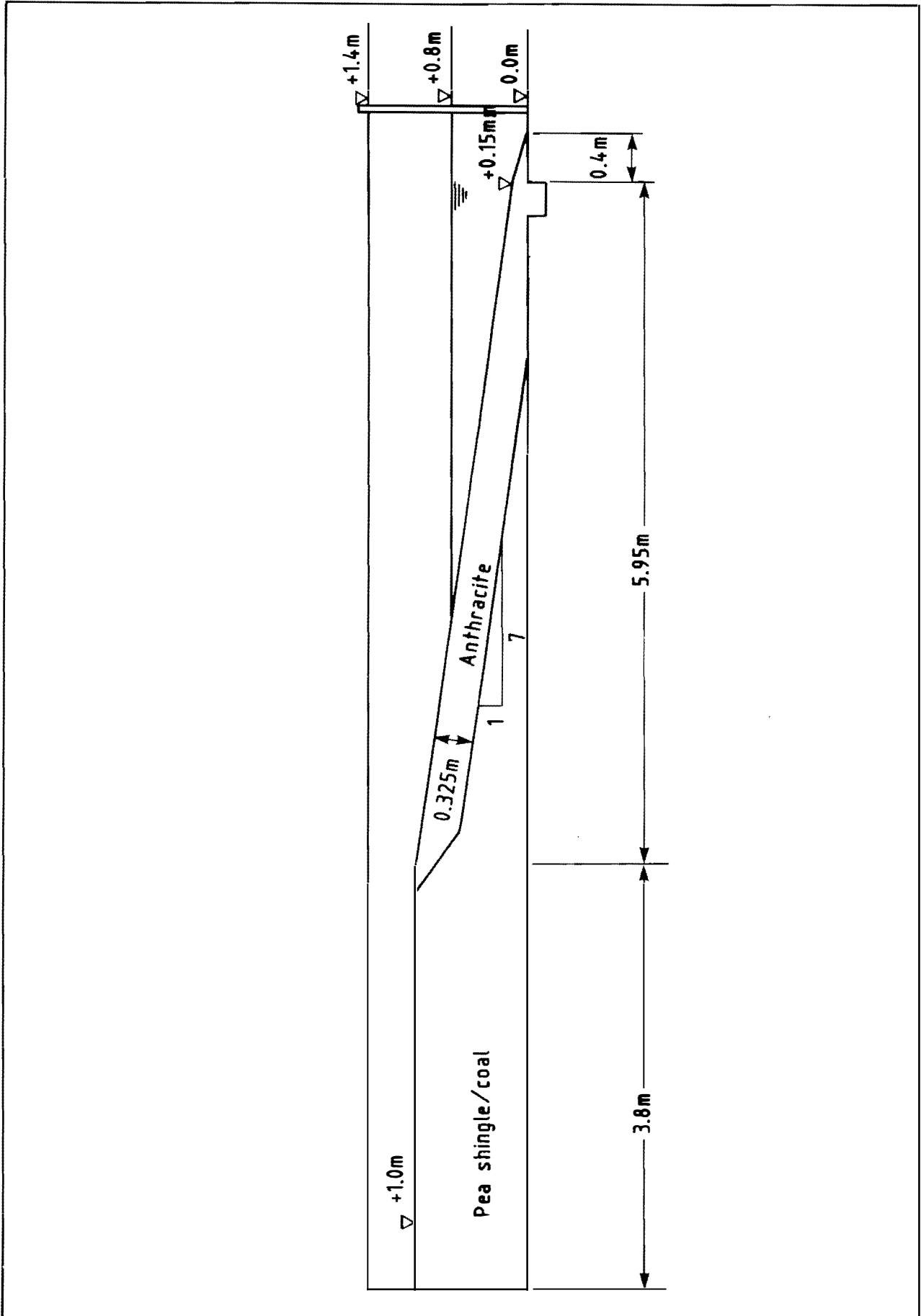


Fig 2.3 Layout and dimensions of model beach

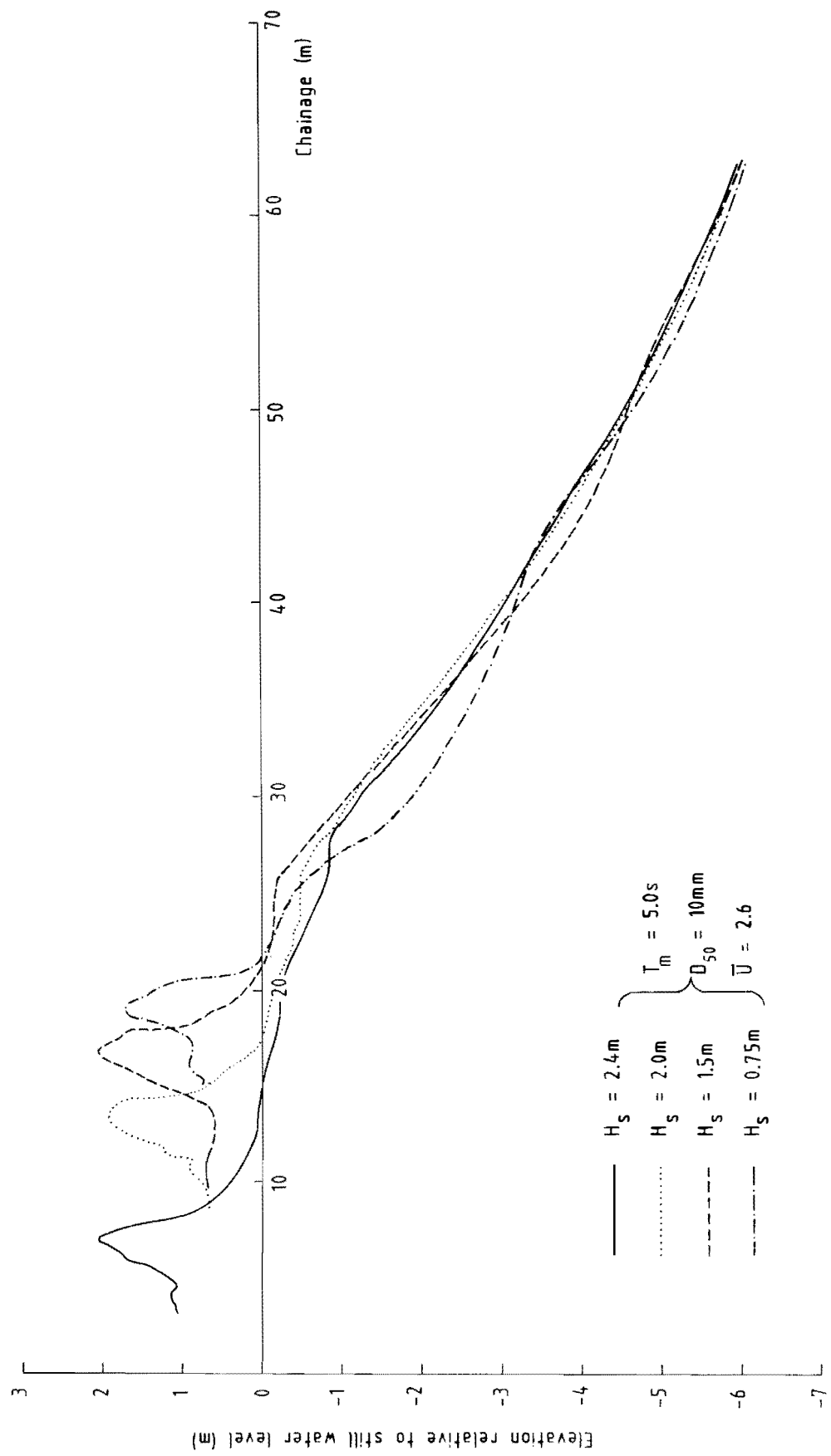


Fig 3.1 Influence of wave height on profile development

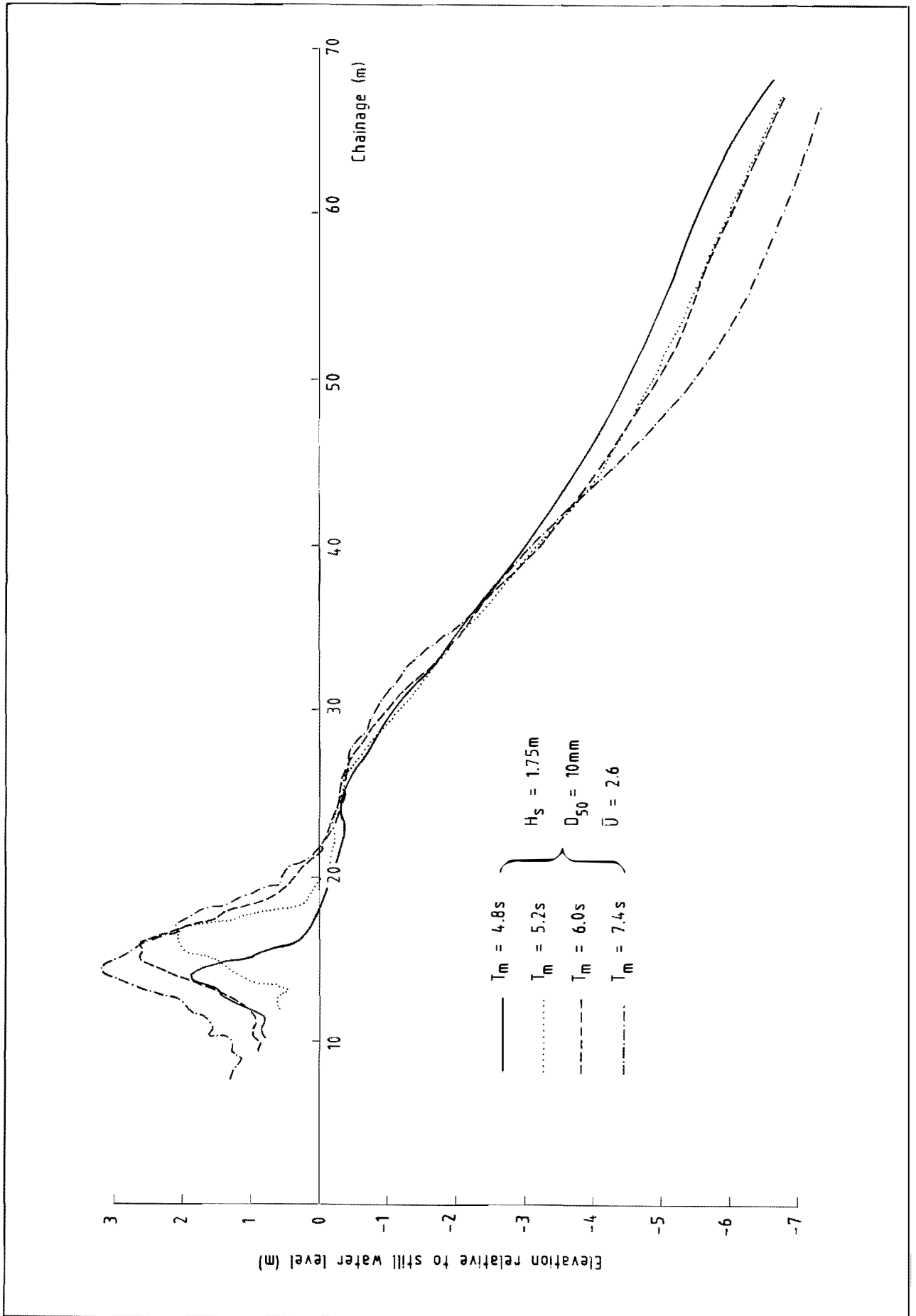


Fig 3.2 Influence of wave period on profile development

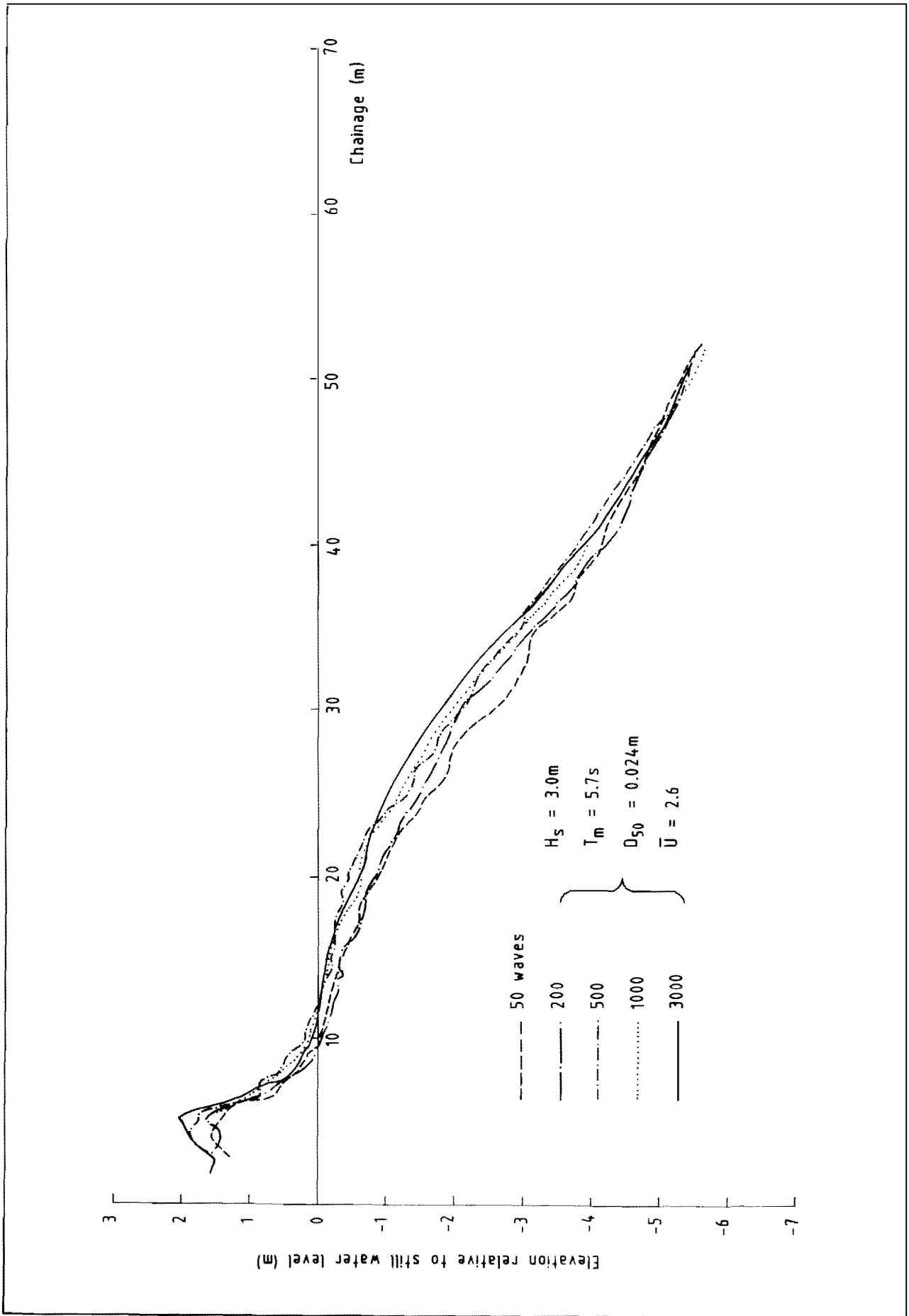


Fig 3.3a Influence of wave duration on profile development

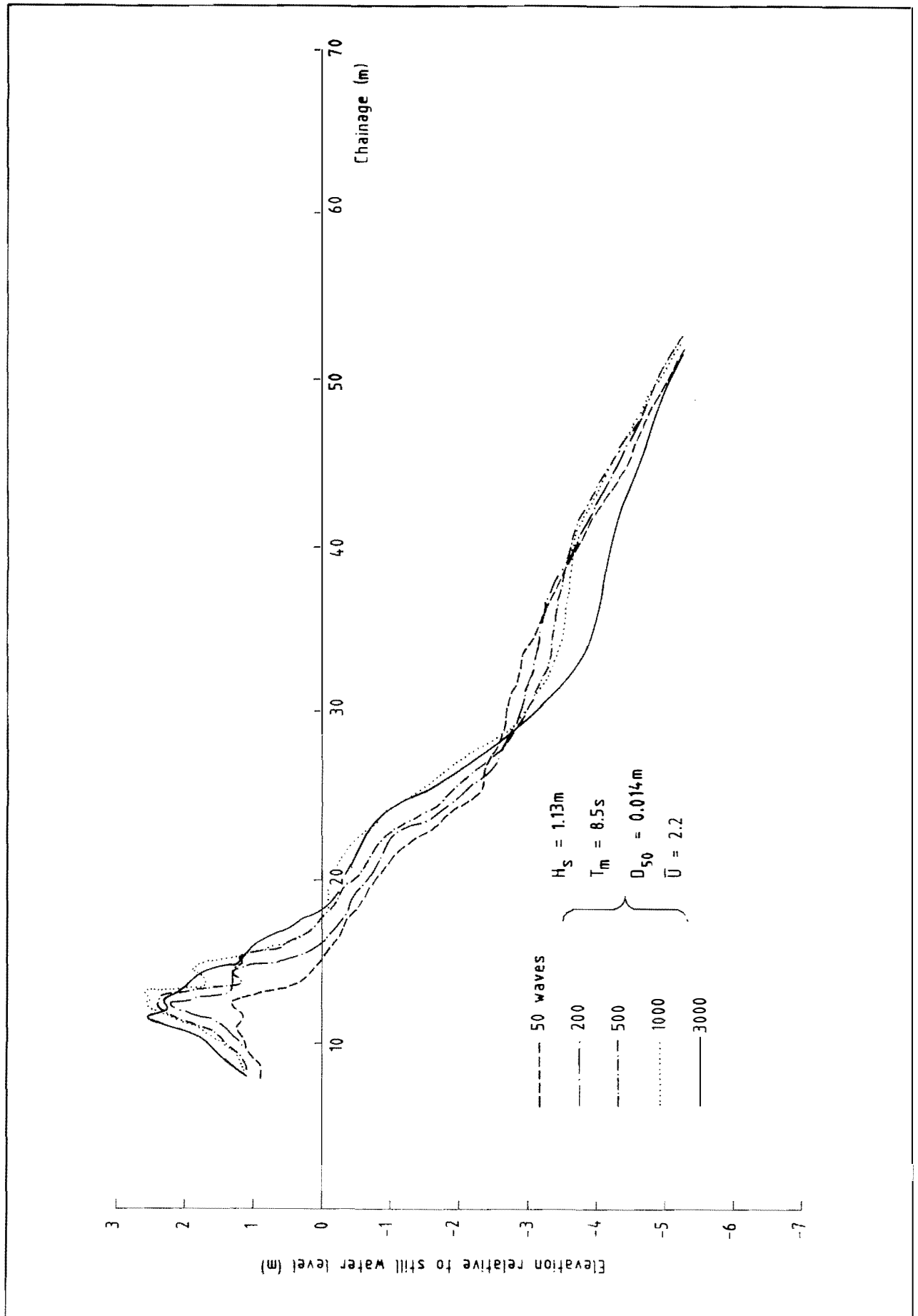


Fig 3.3b Influence of wave duration on profile development

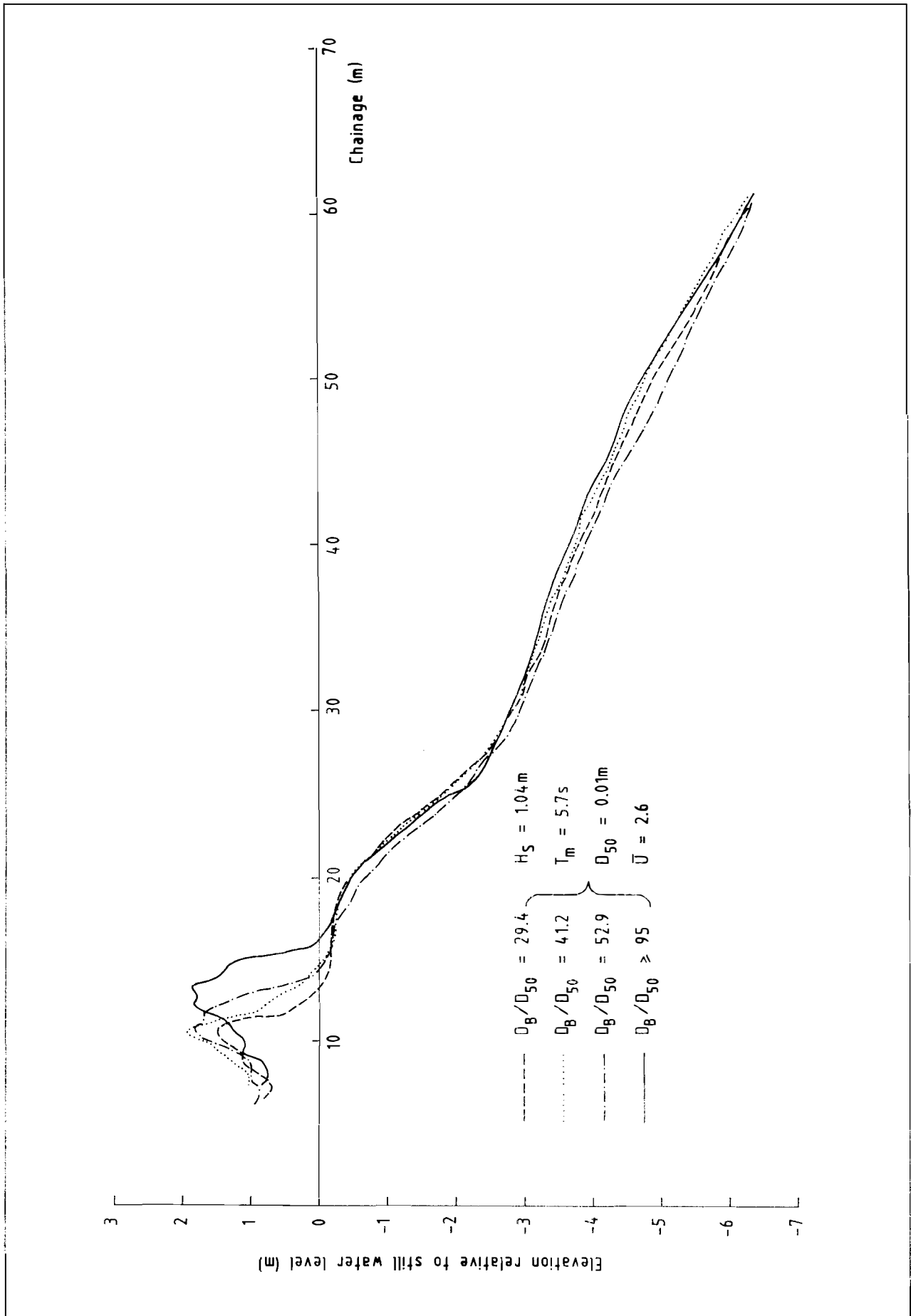


Fig 3.4a Influence of effective beach depth on profile development

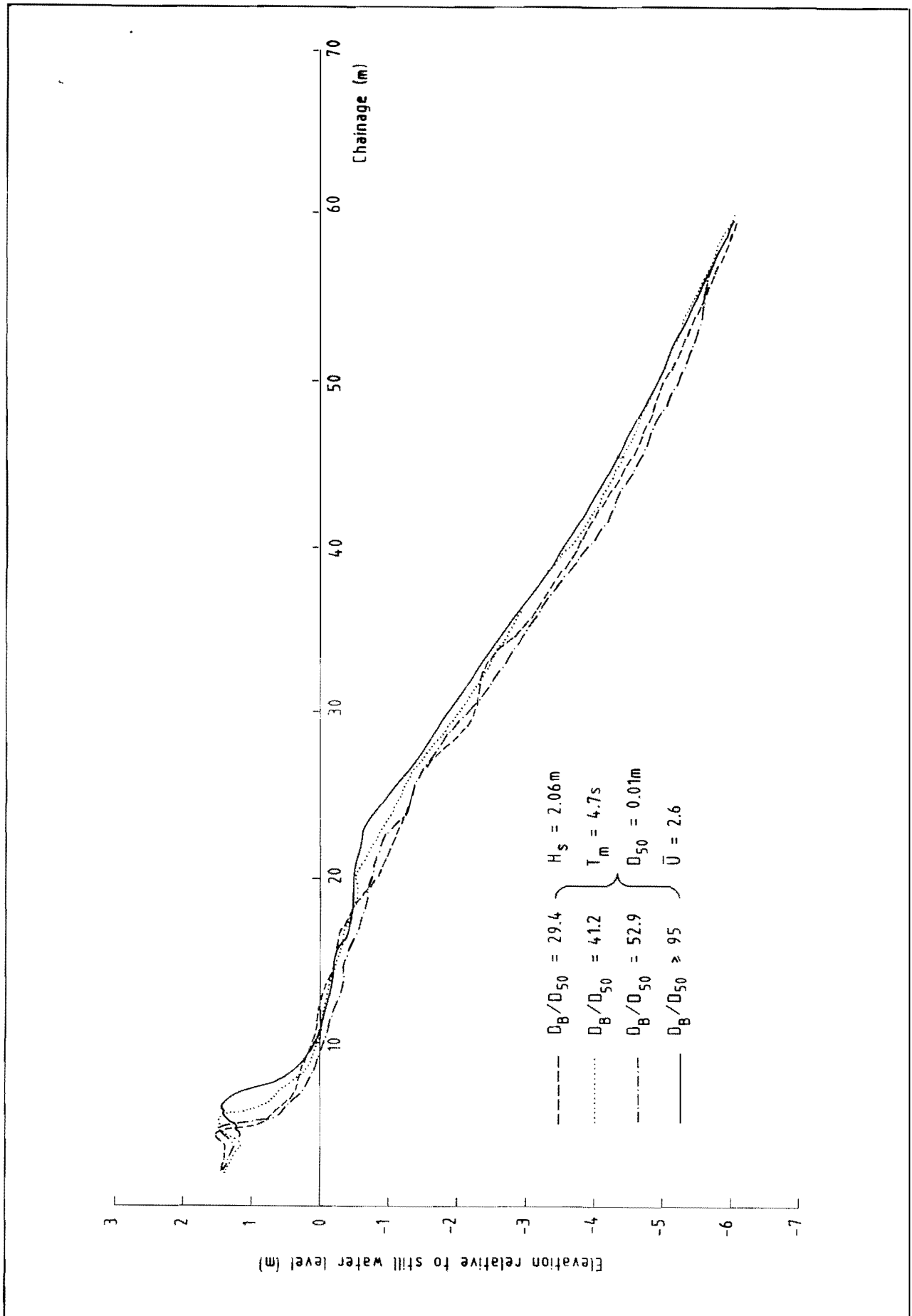


Fig 3.4b Influence of effective beach depth on profile development

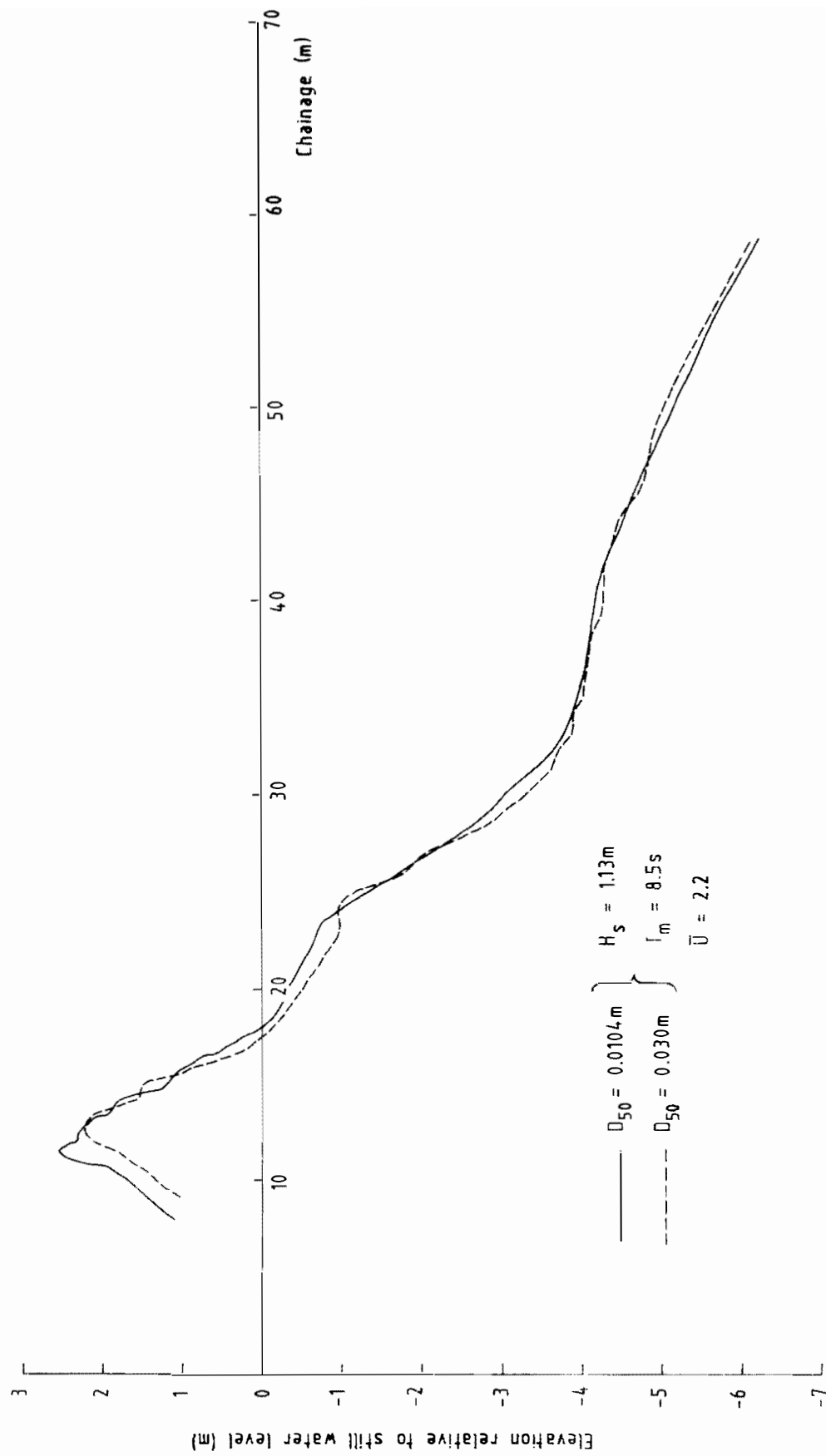


Fig 3.5a Influence of beach material size on profile development

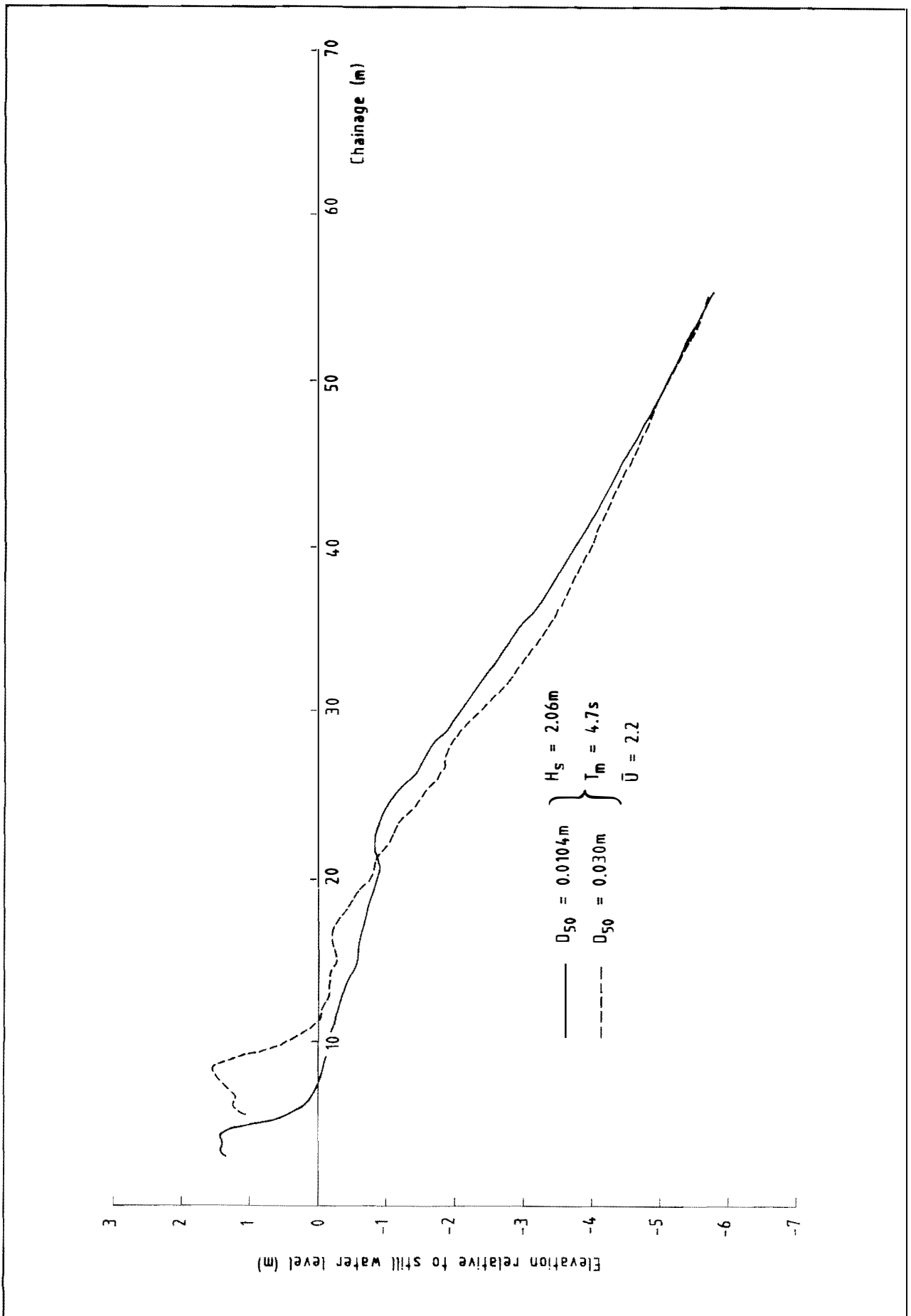


Fig 3.5b Influence of beach material size on profile development

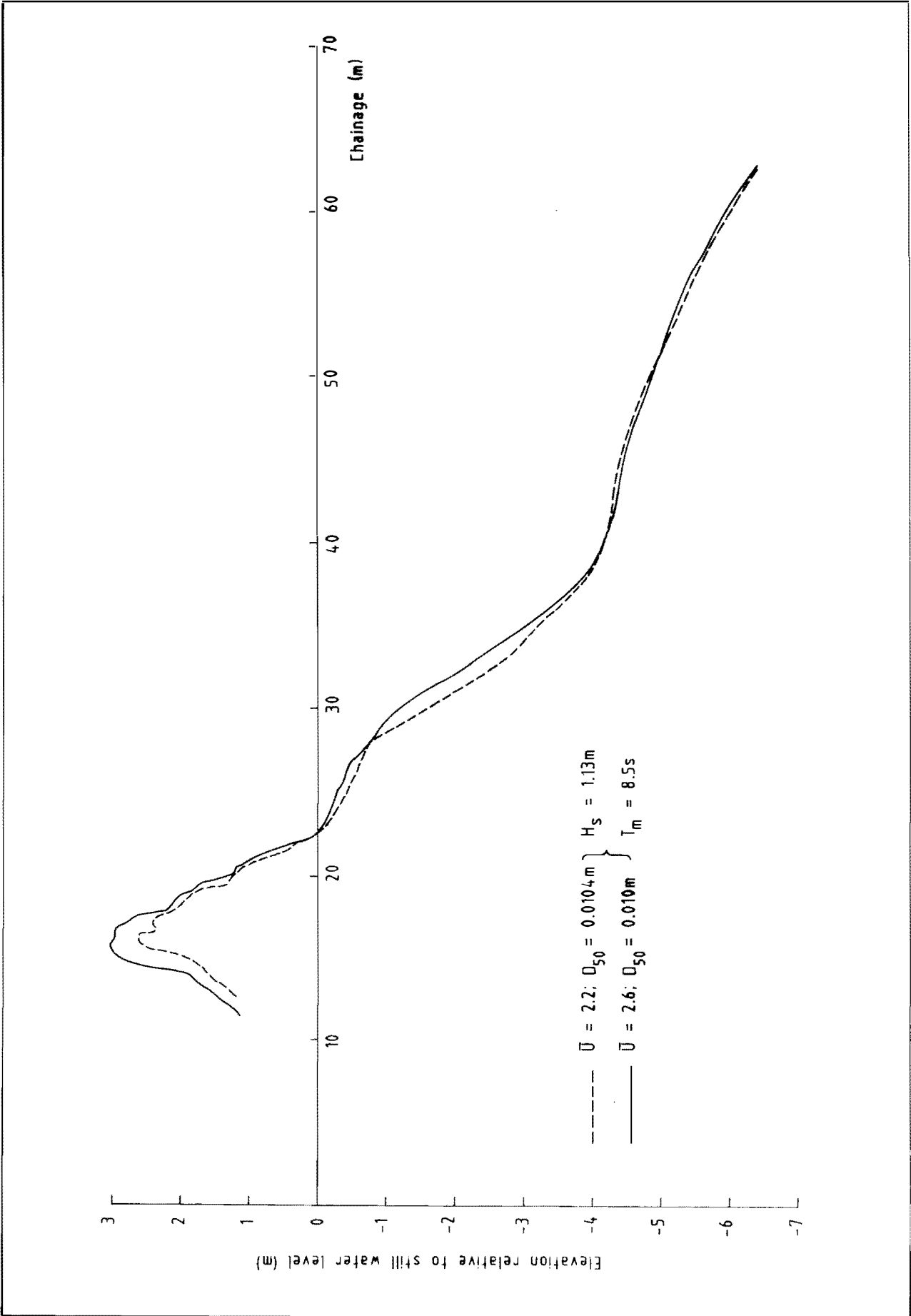


Fig 3.6a Influence of beach material grading on profile development

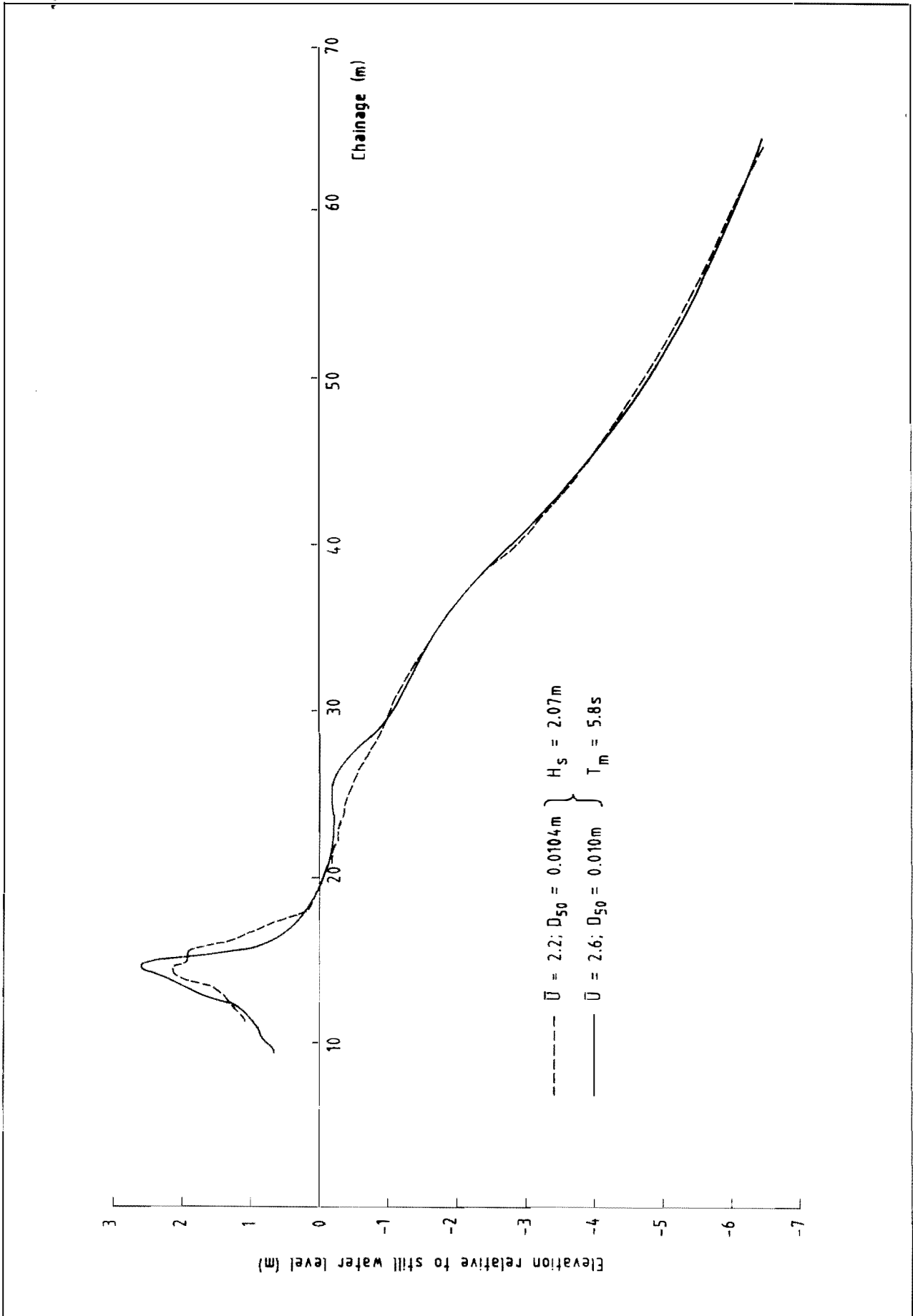


Fig 3.6b Influence of beach material grading on profile development

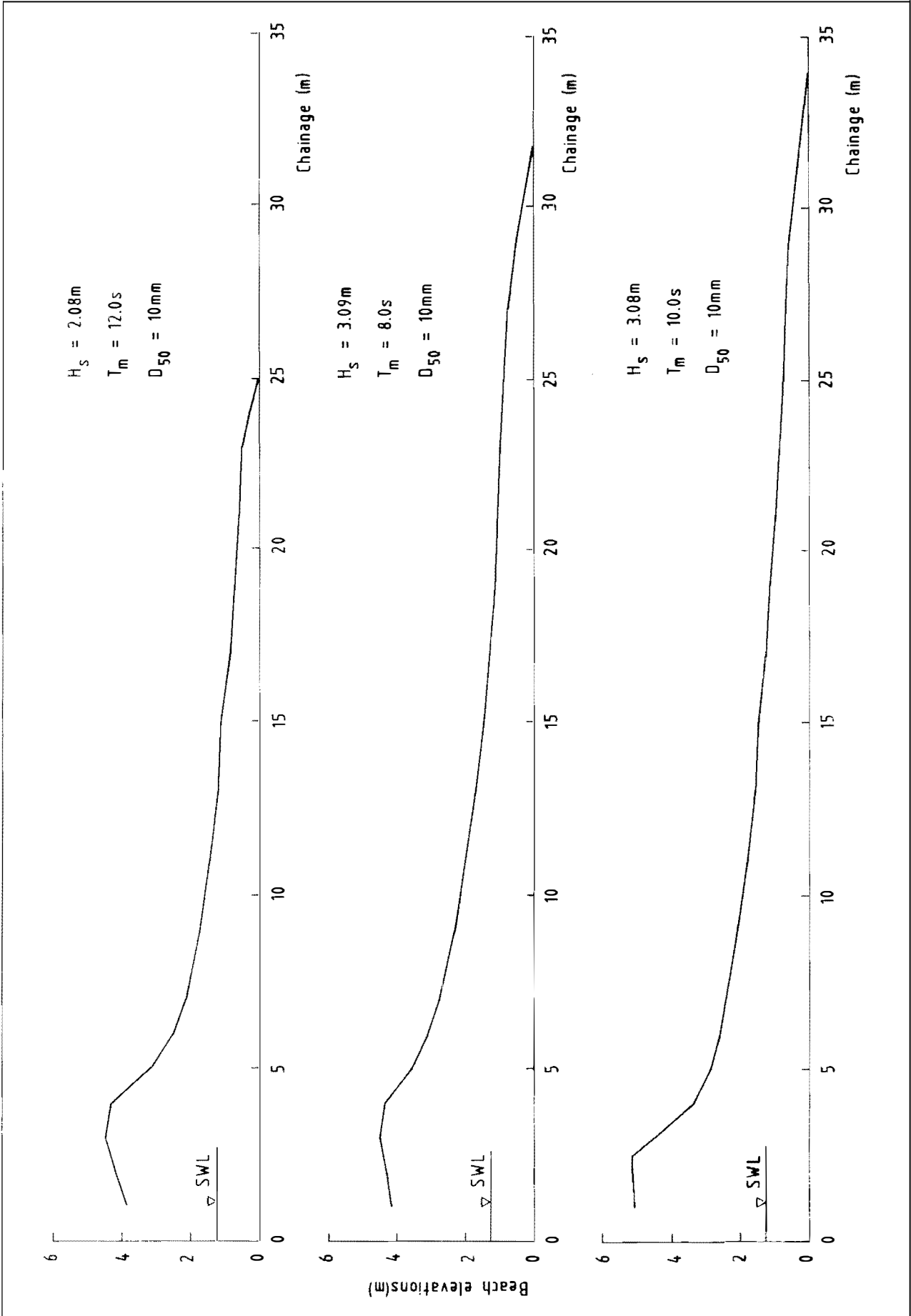


Fig 3.7 Beach profiles formed over a depth limited foreshore

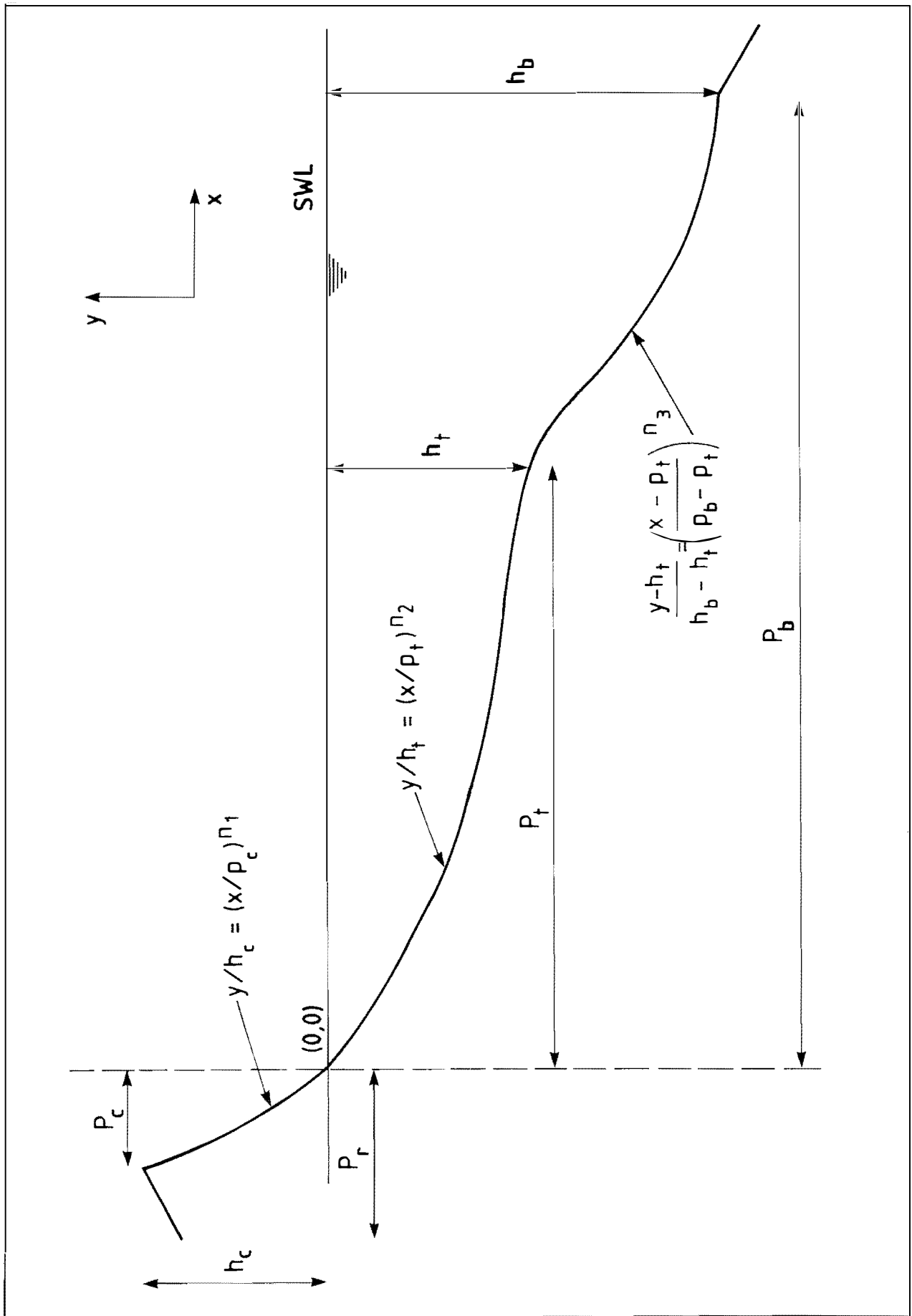


Fig 4.1 Schematised beach profile



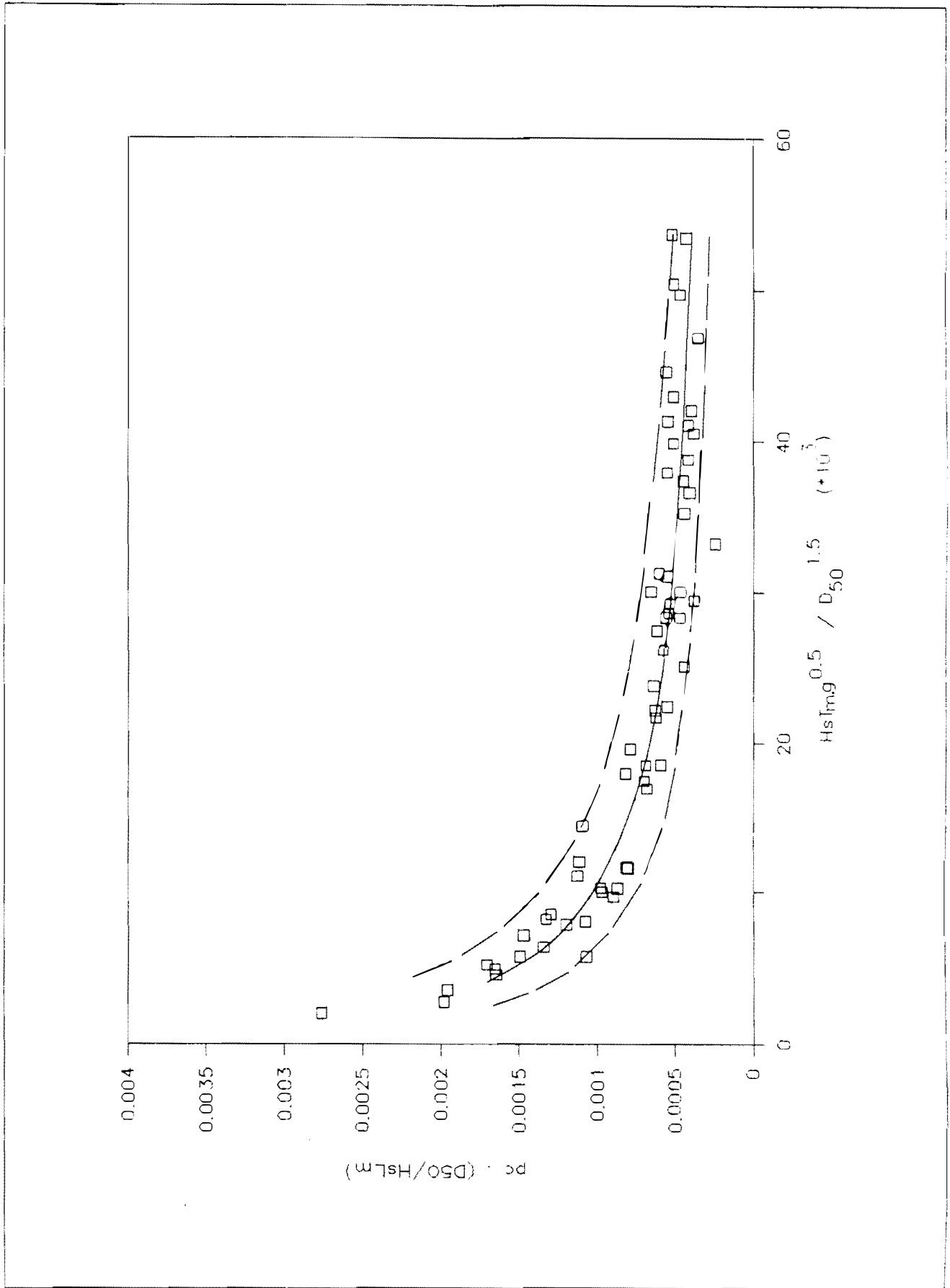


Fig 4.3 Crest position.

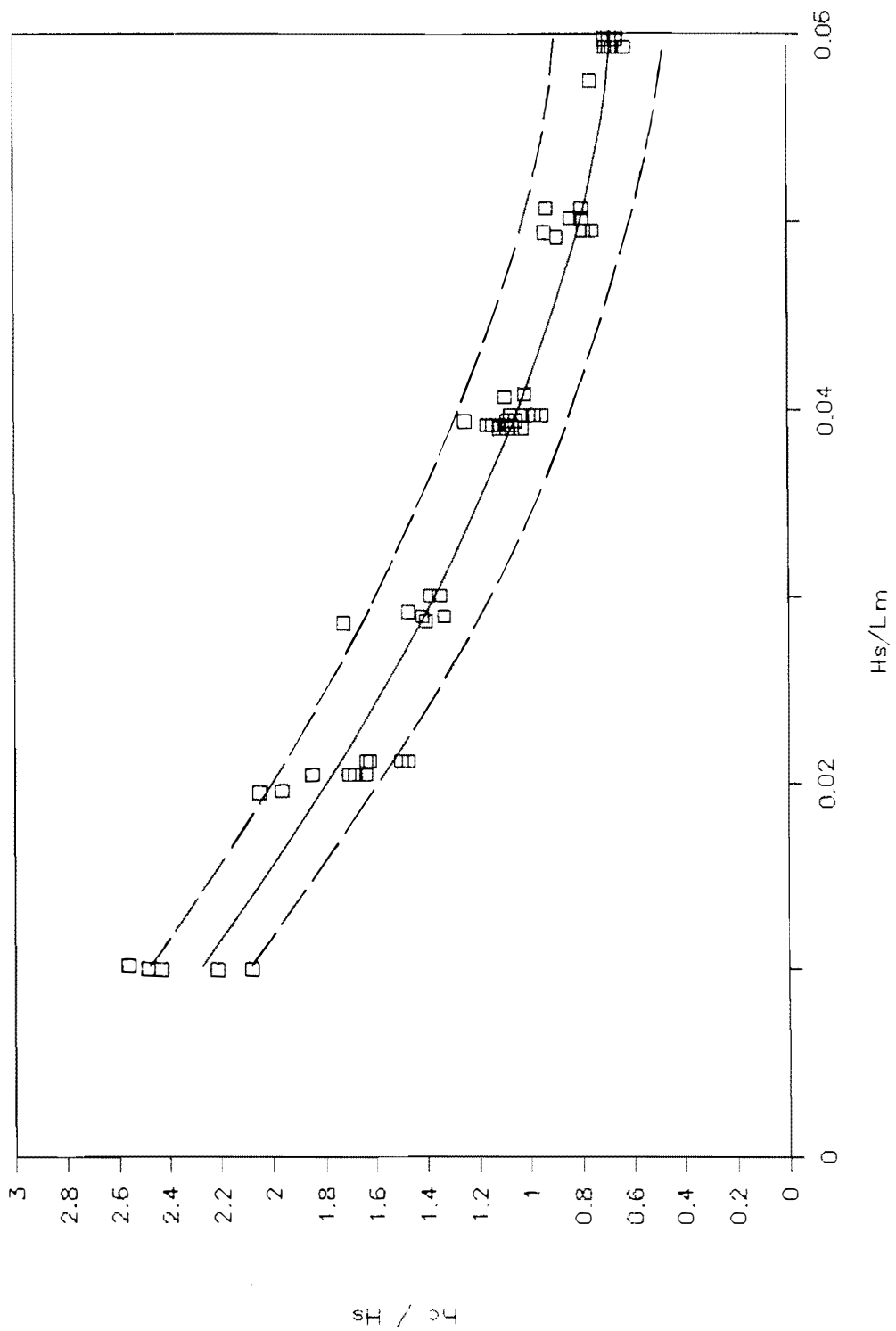


Fig 4.4 Crest elevation

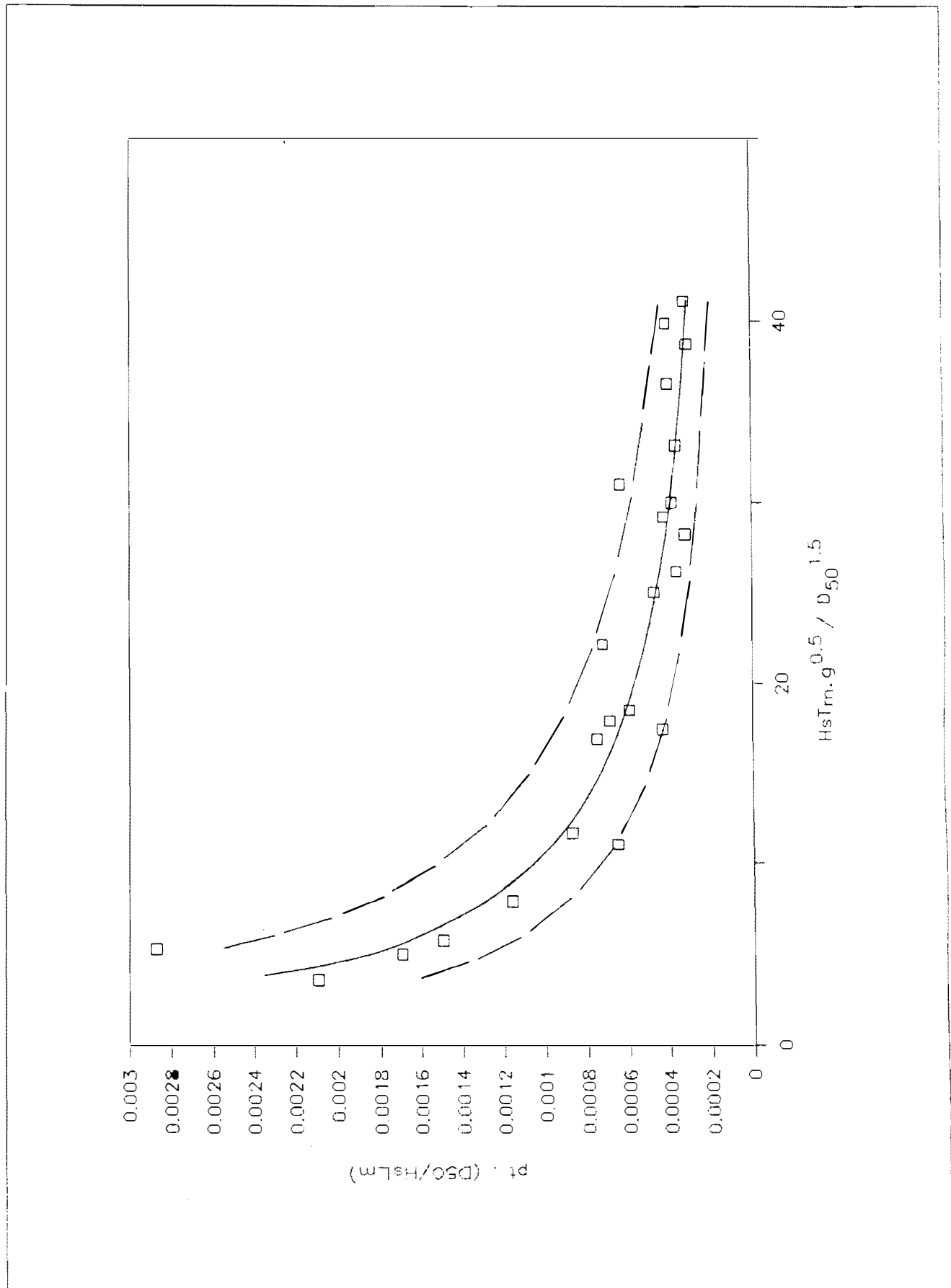


Fig 4.5 Step position ( $Hs/Lm < 0.03$ )

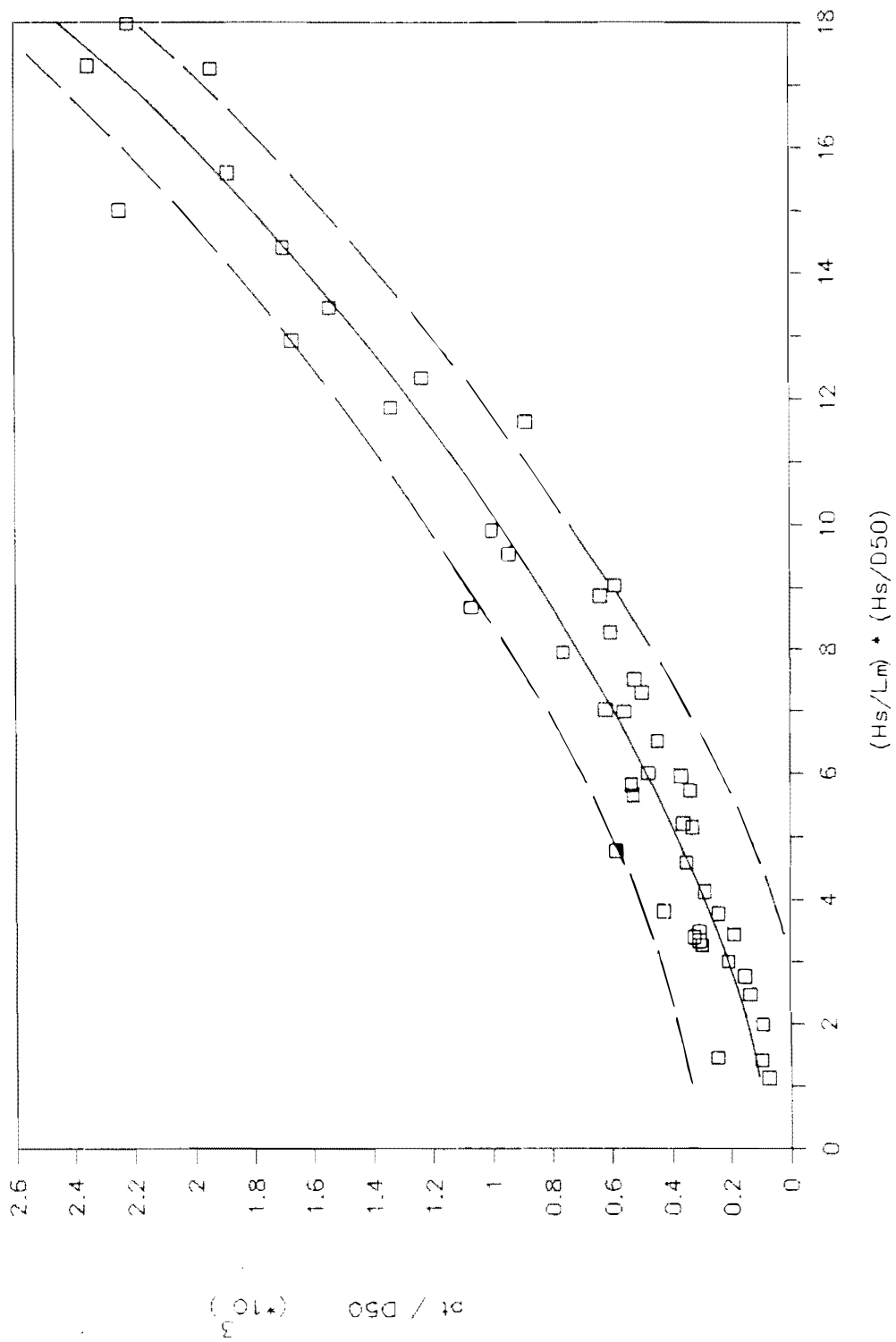


Fig 4.6 Step position ( $H_s/L_m \geq 0.03$ )

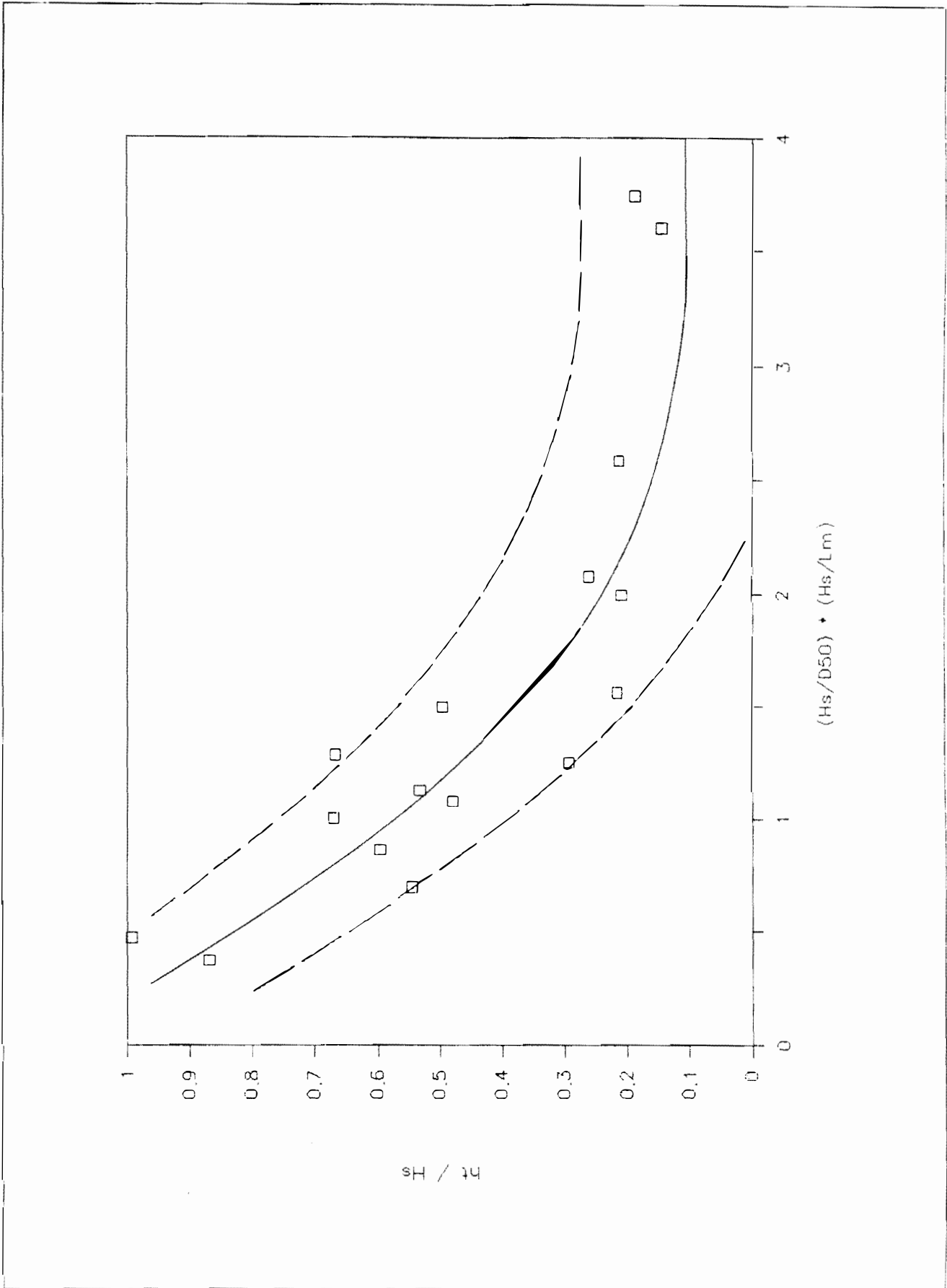


Fig 4.7 Step elevation ( $H_s/L_m < 0.03$ )

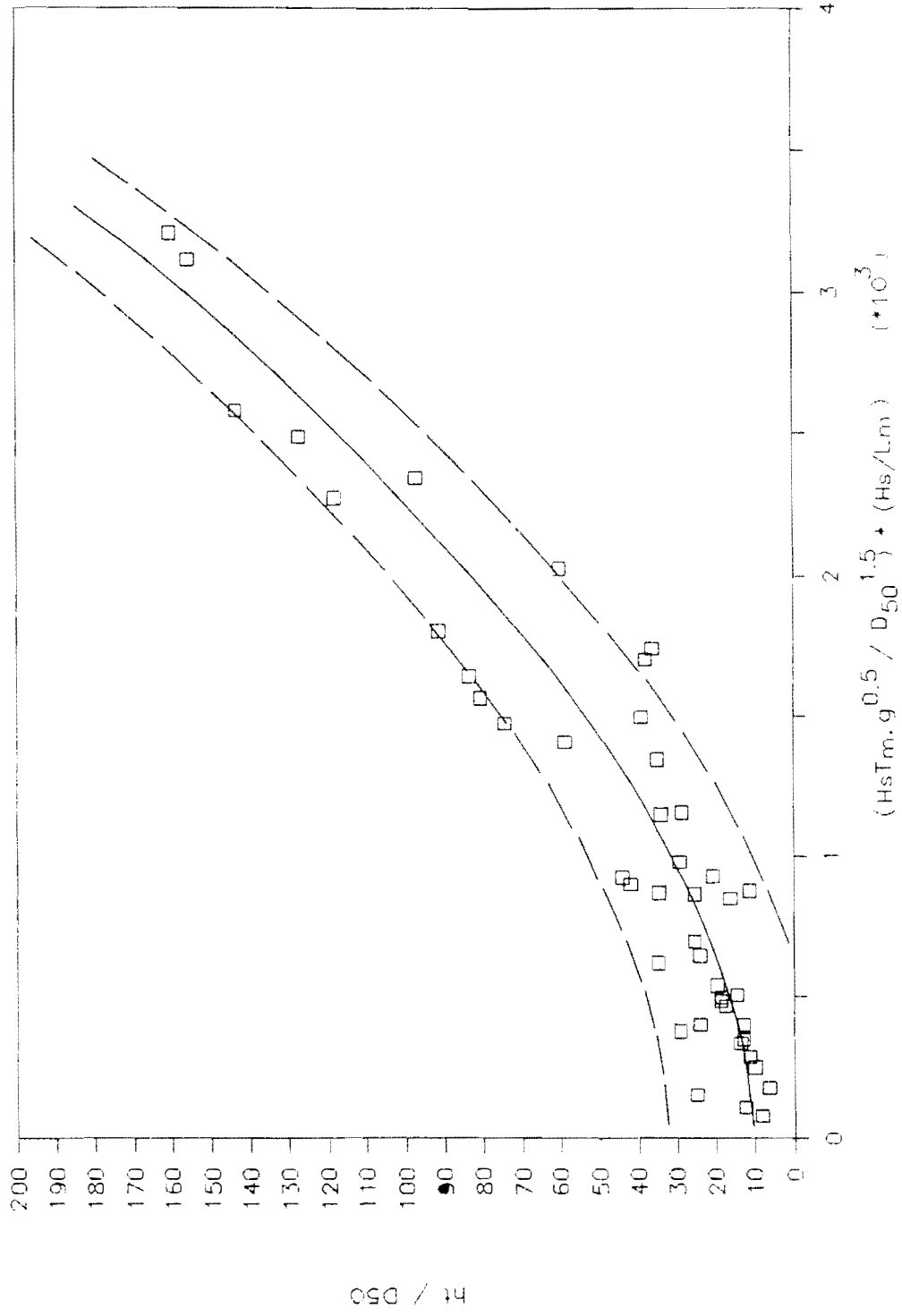


Fig 4.8 Step elevation ( $H_s/L_m \geq 0.03$ )

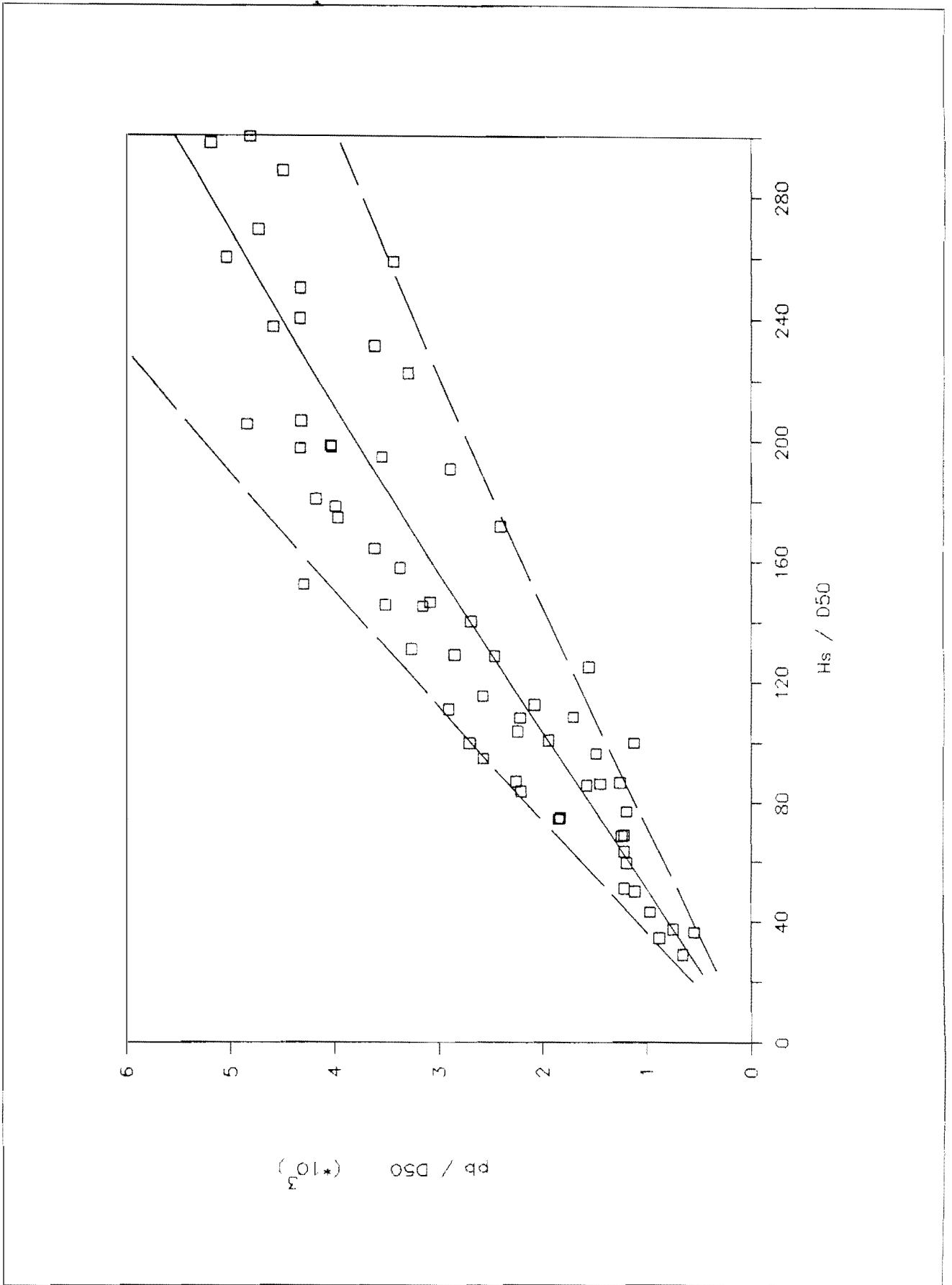


Fig 4.9 Wave base position

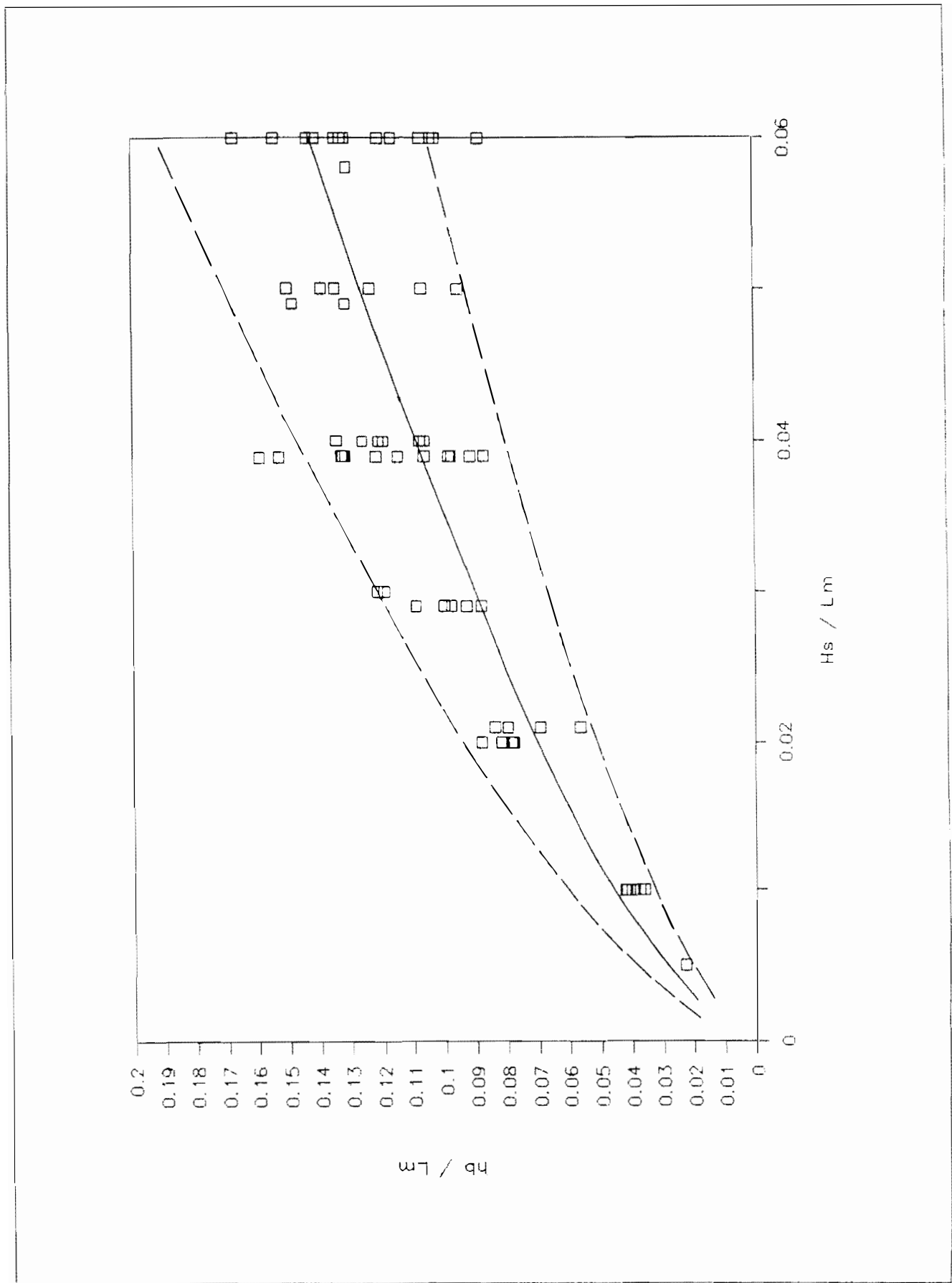


Fig 4.10 Wave base

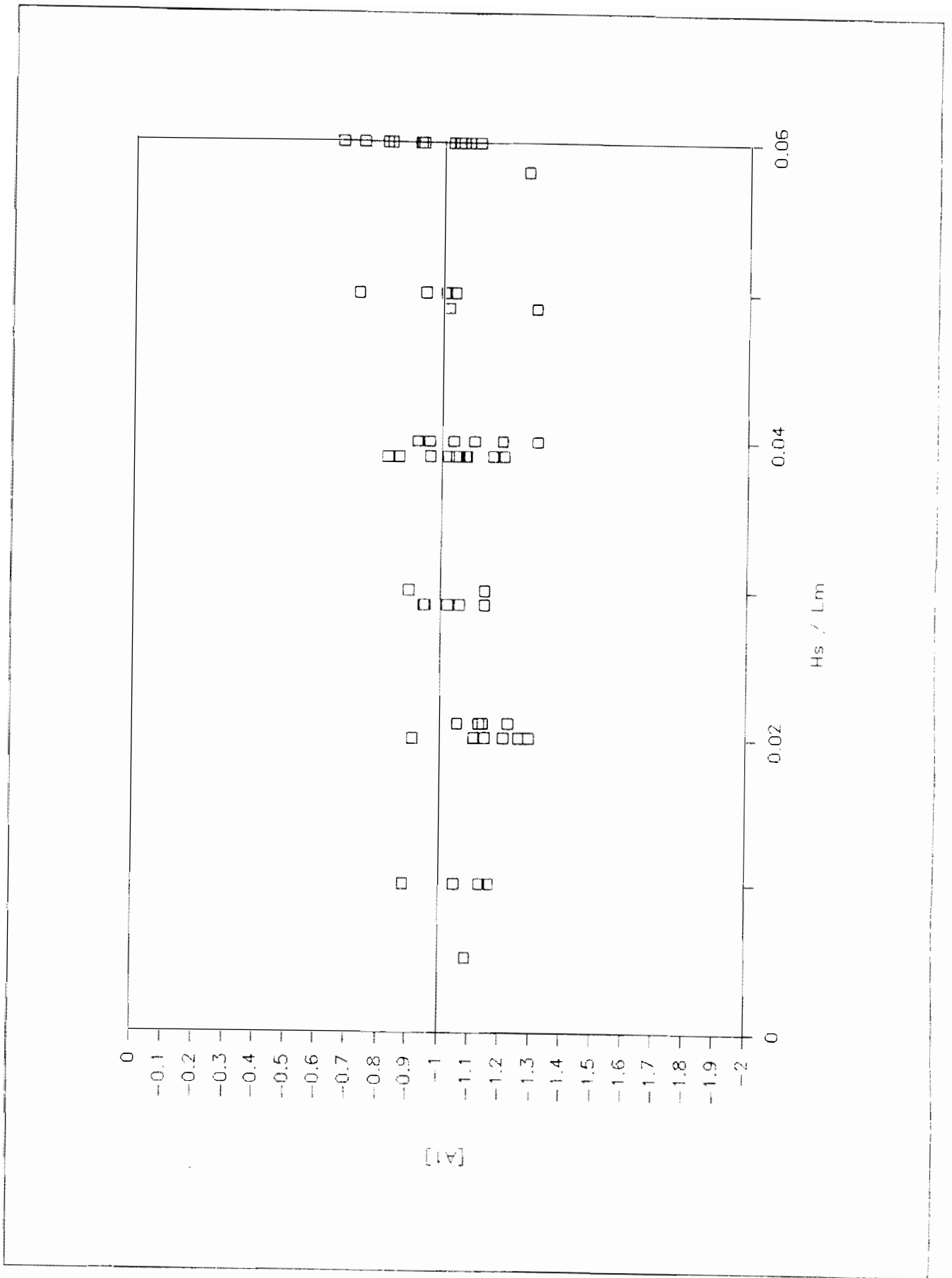


Fig 4.11 Curve A1

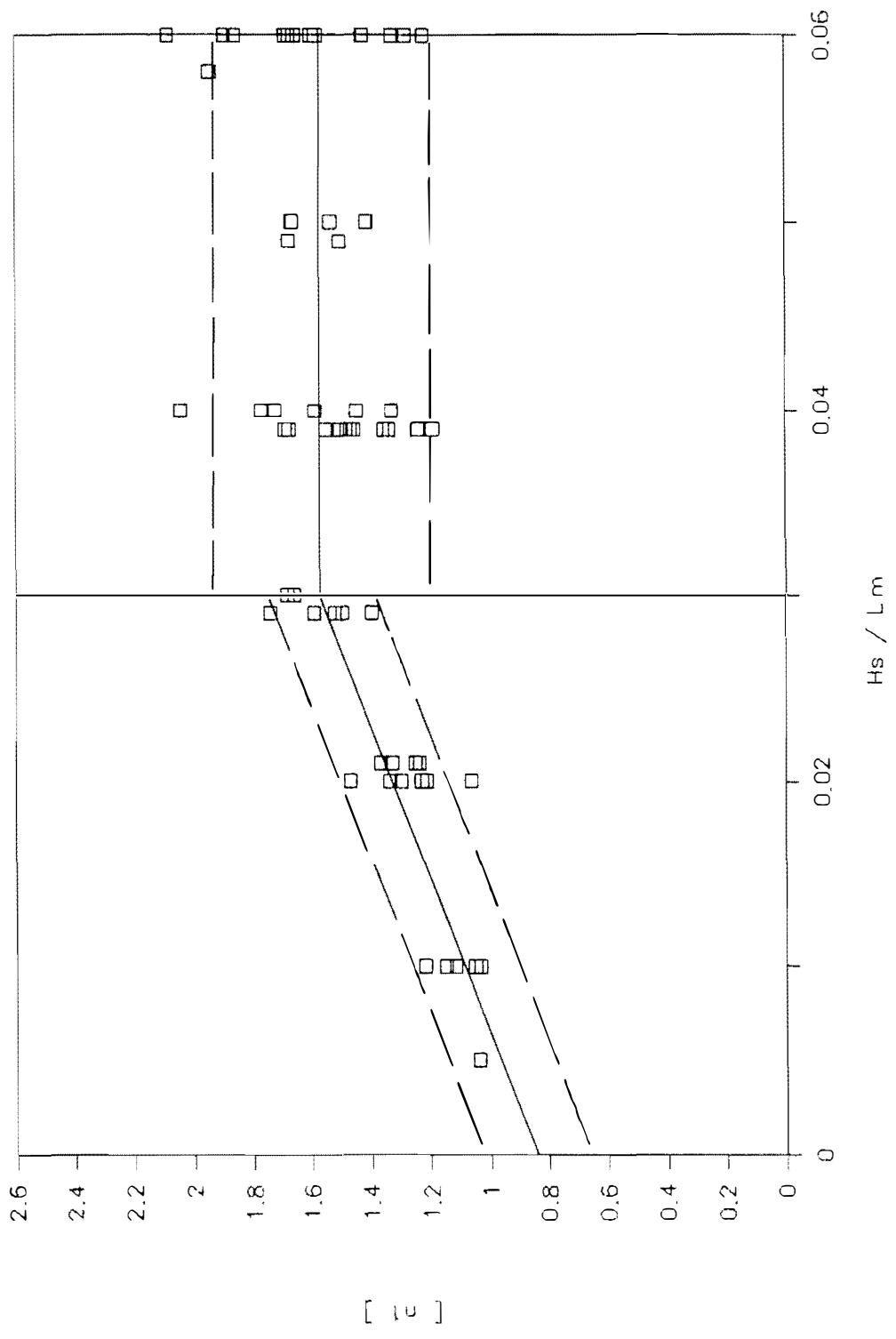


Fig 4.12 Curve n1

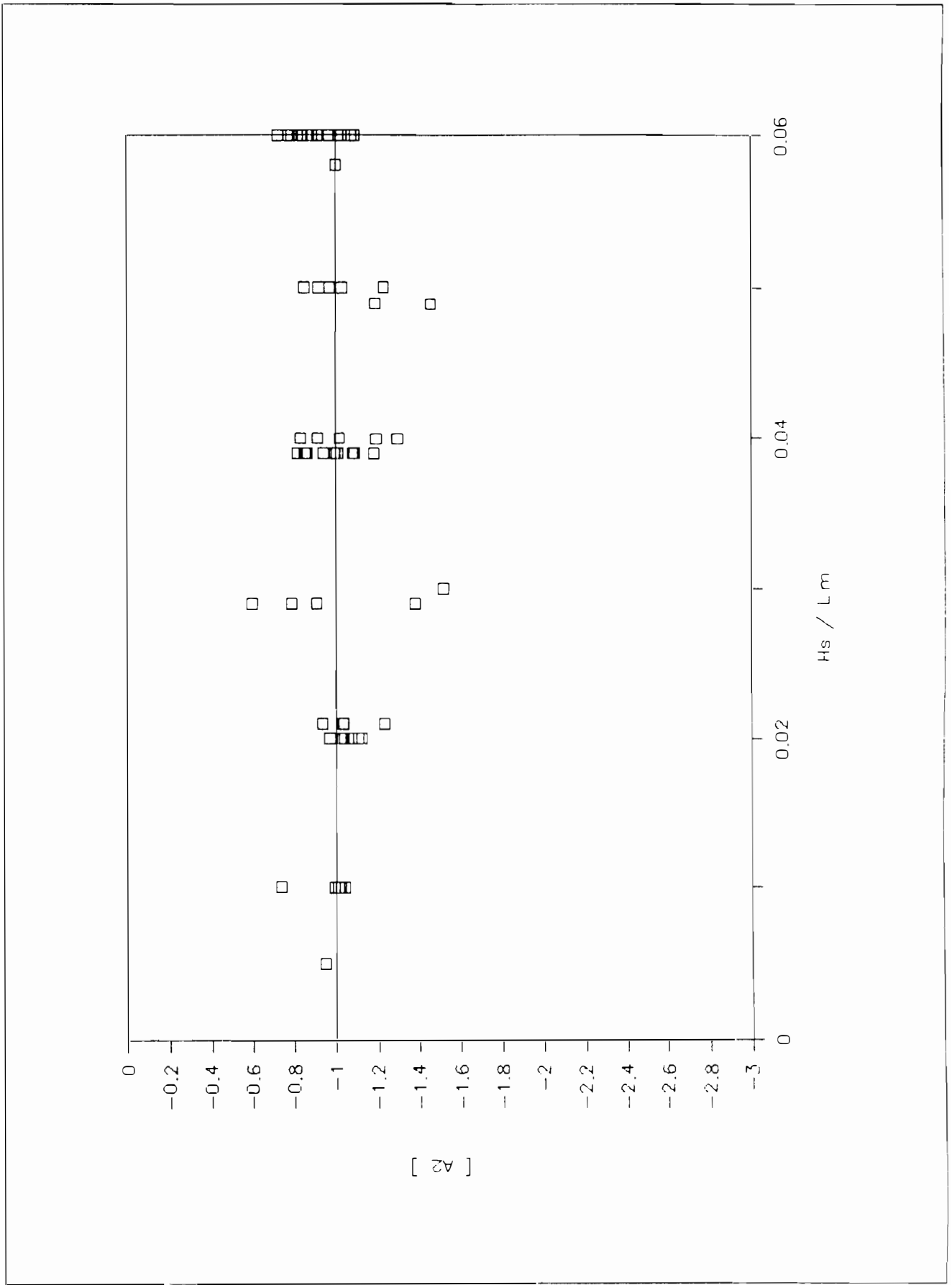


Fig 4.13 Curve A2

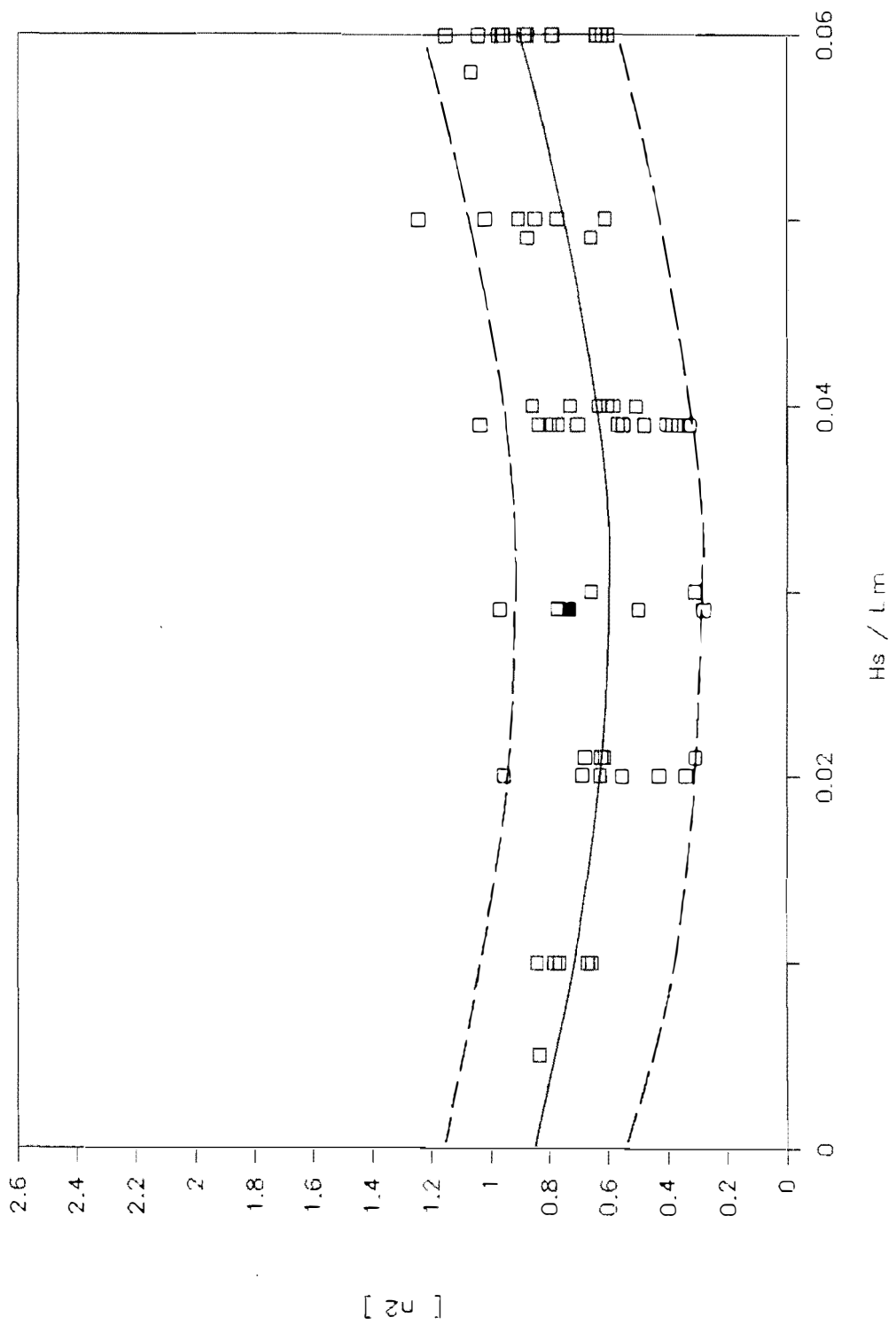
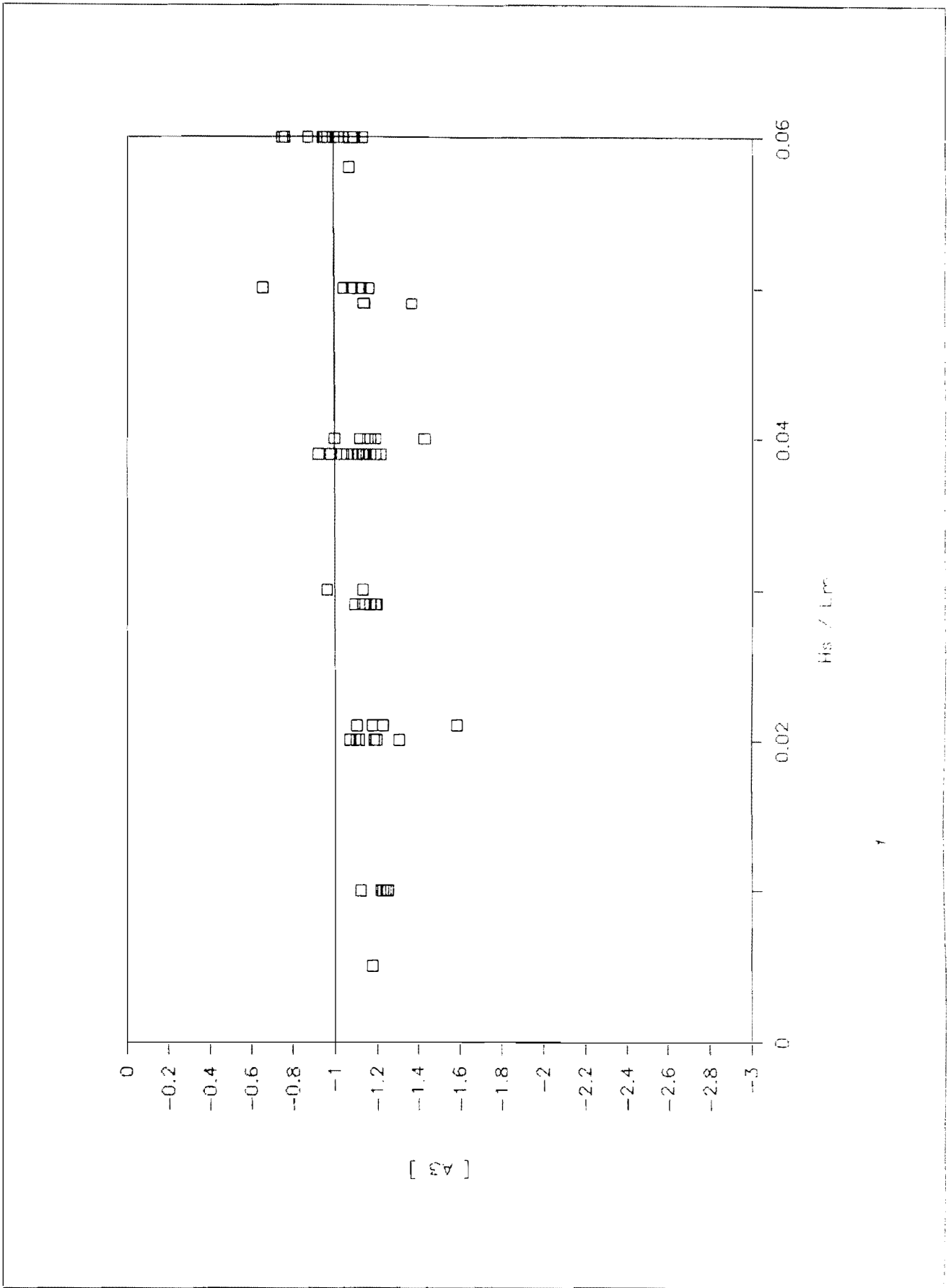


Fig 4.14 Curve n2



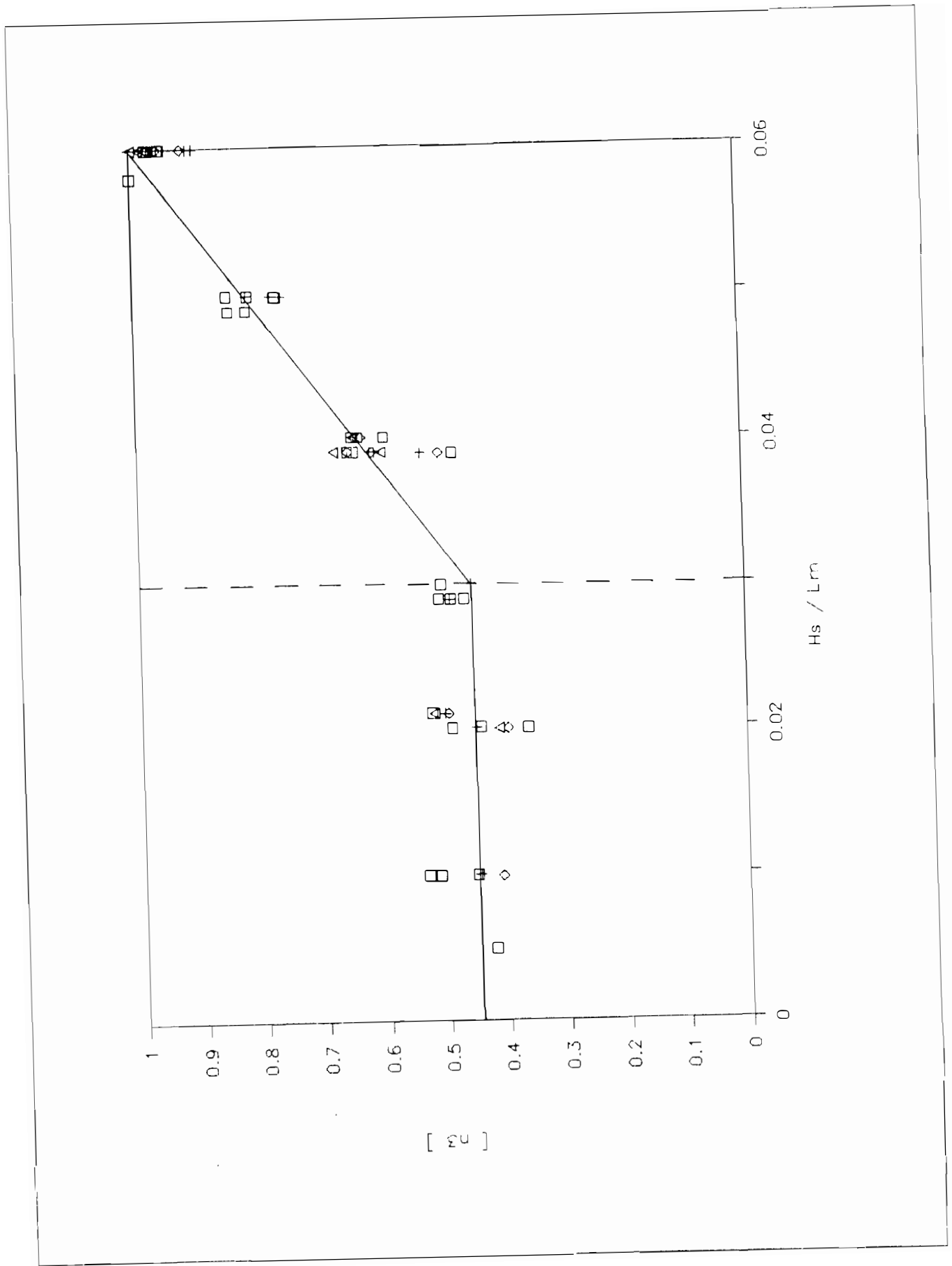


Fig 4.16 Curve n3

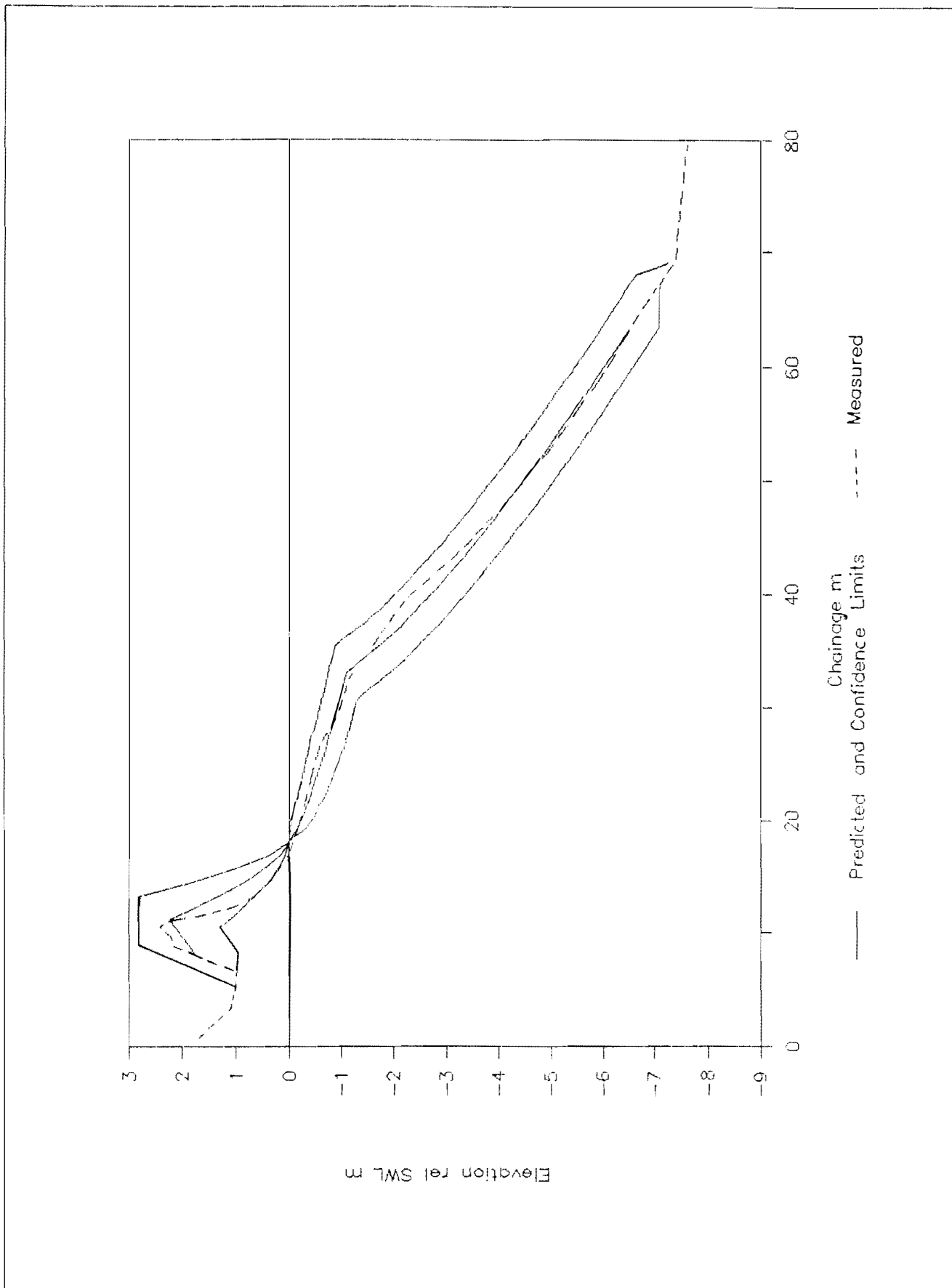


Fig 4.17 Confidence limits on predicted profile  
-wave steepness 0.05.

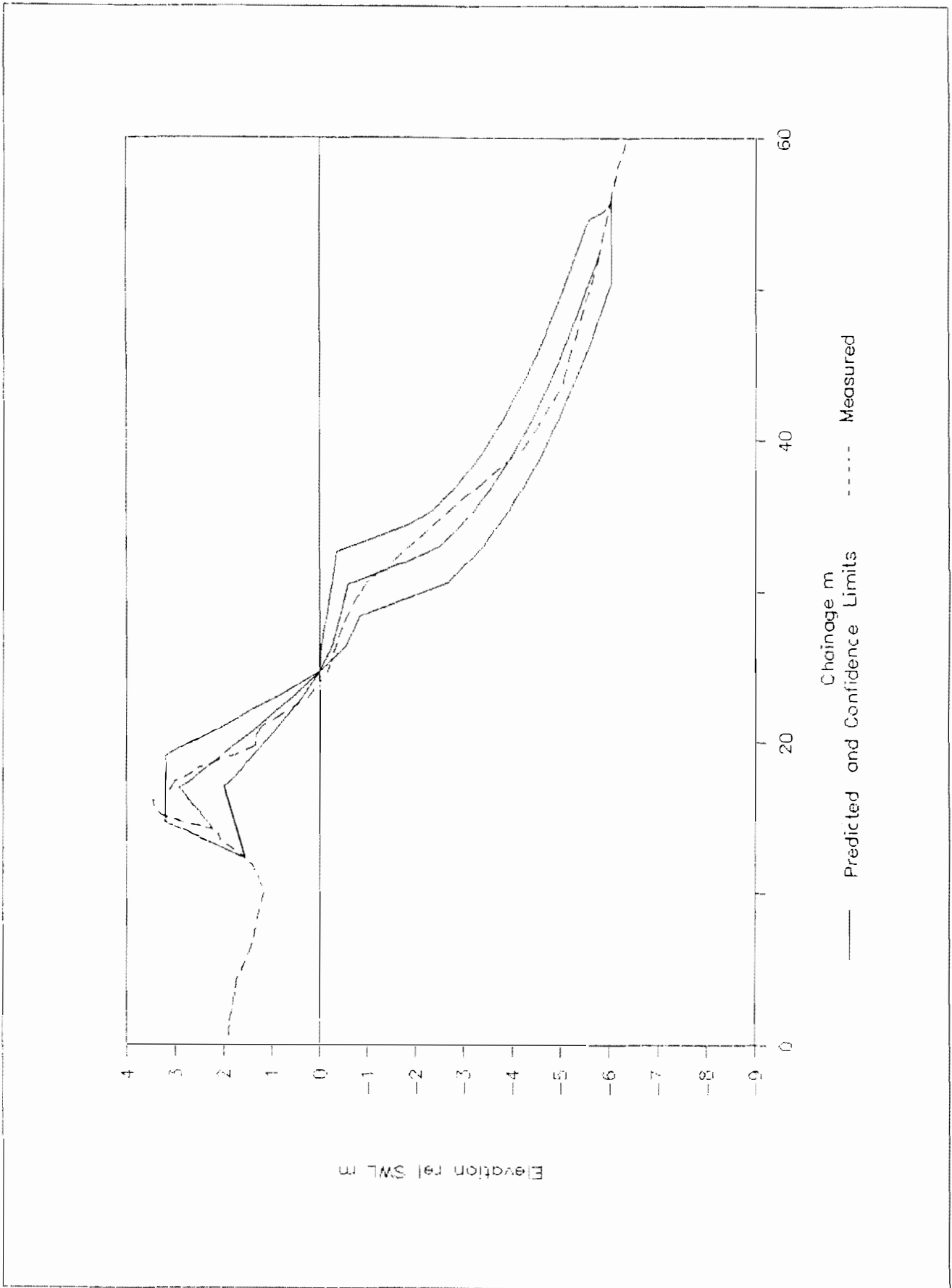


Fig 4.18 Confidence limits on predicted profile  
-wave steepness 0.01

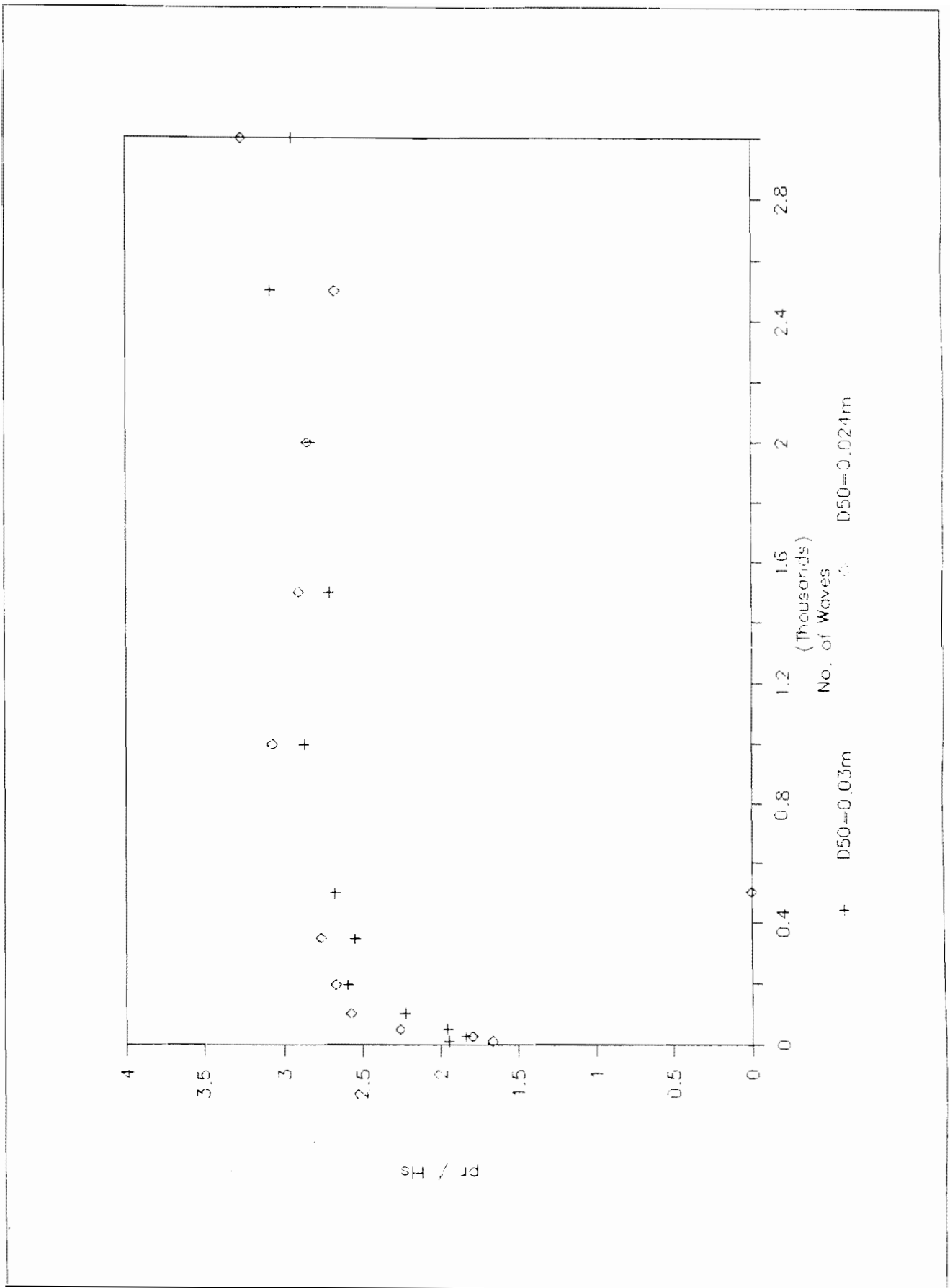


Fig 4.19 Typical wave duration trend- $pr/H_s$

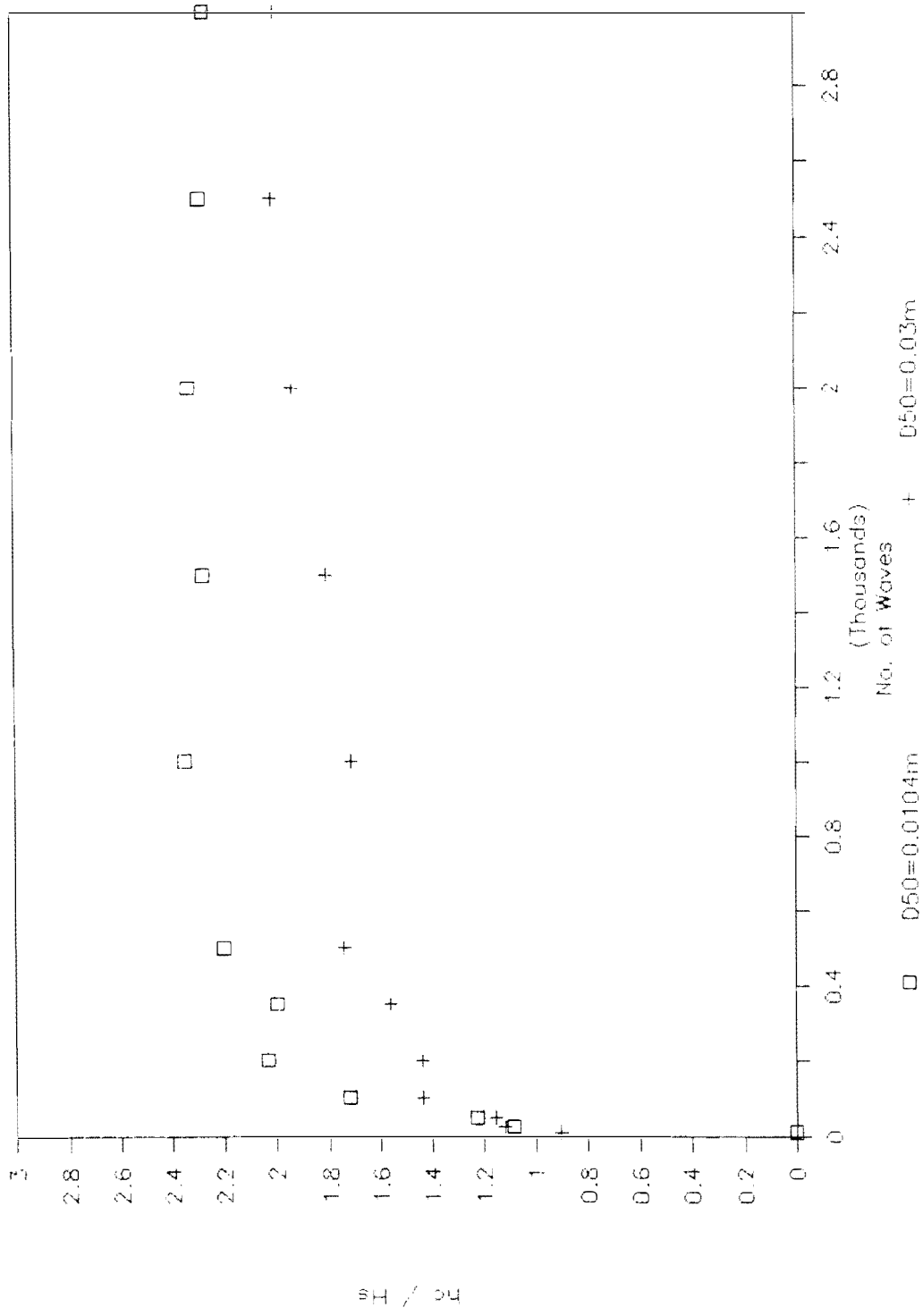


Fig 4.20 Typical wave duration trend- $hc/H_s$

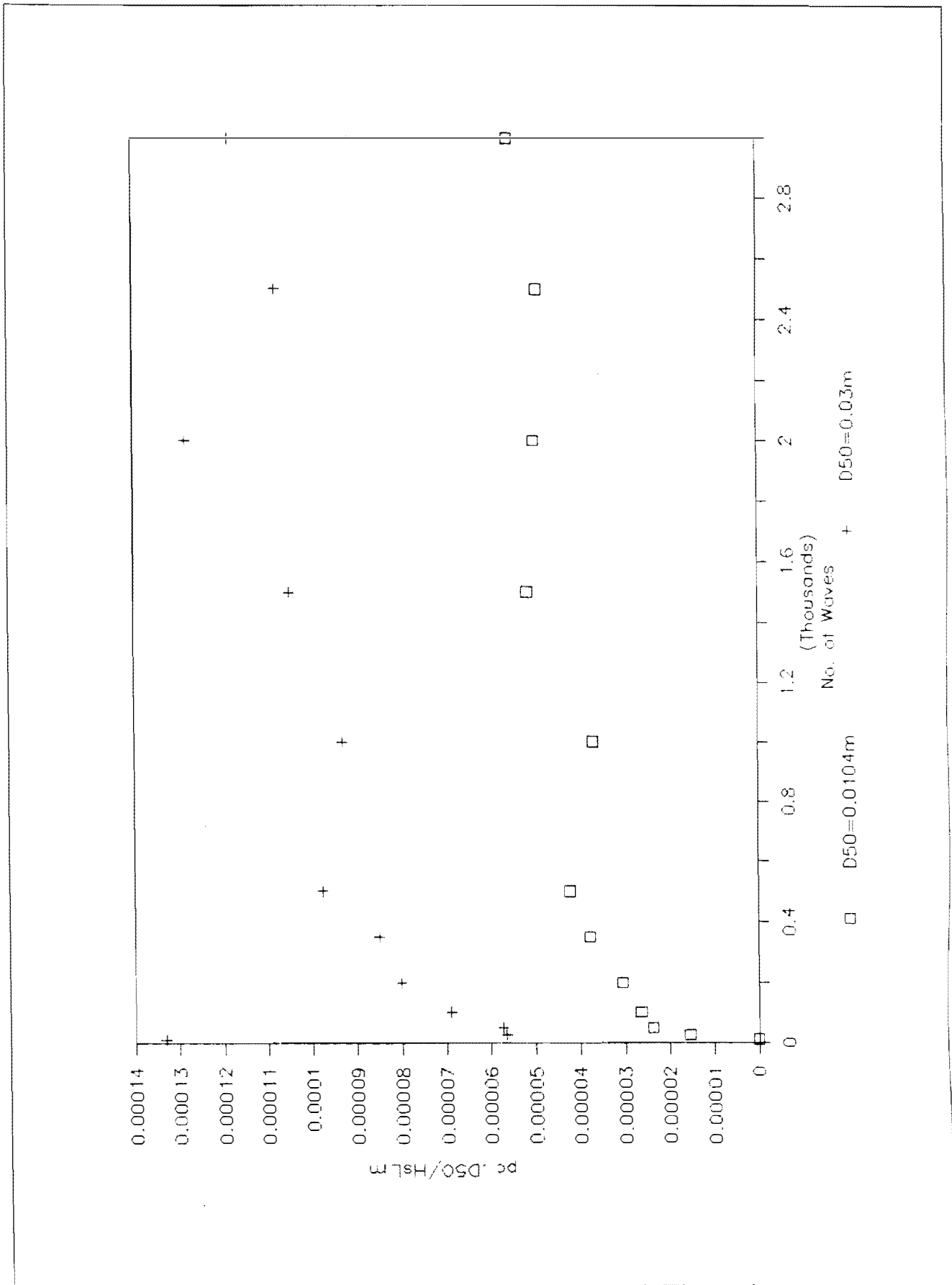


Fig 4.21 Typical wave duration trend -pcD50/HsLm

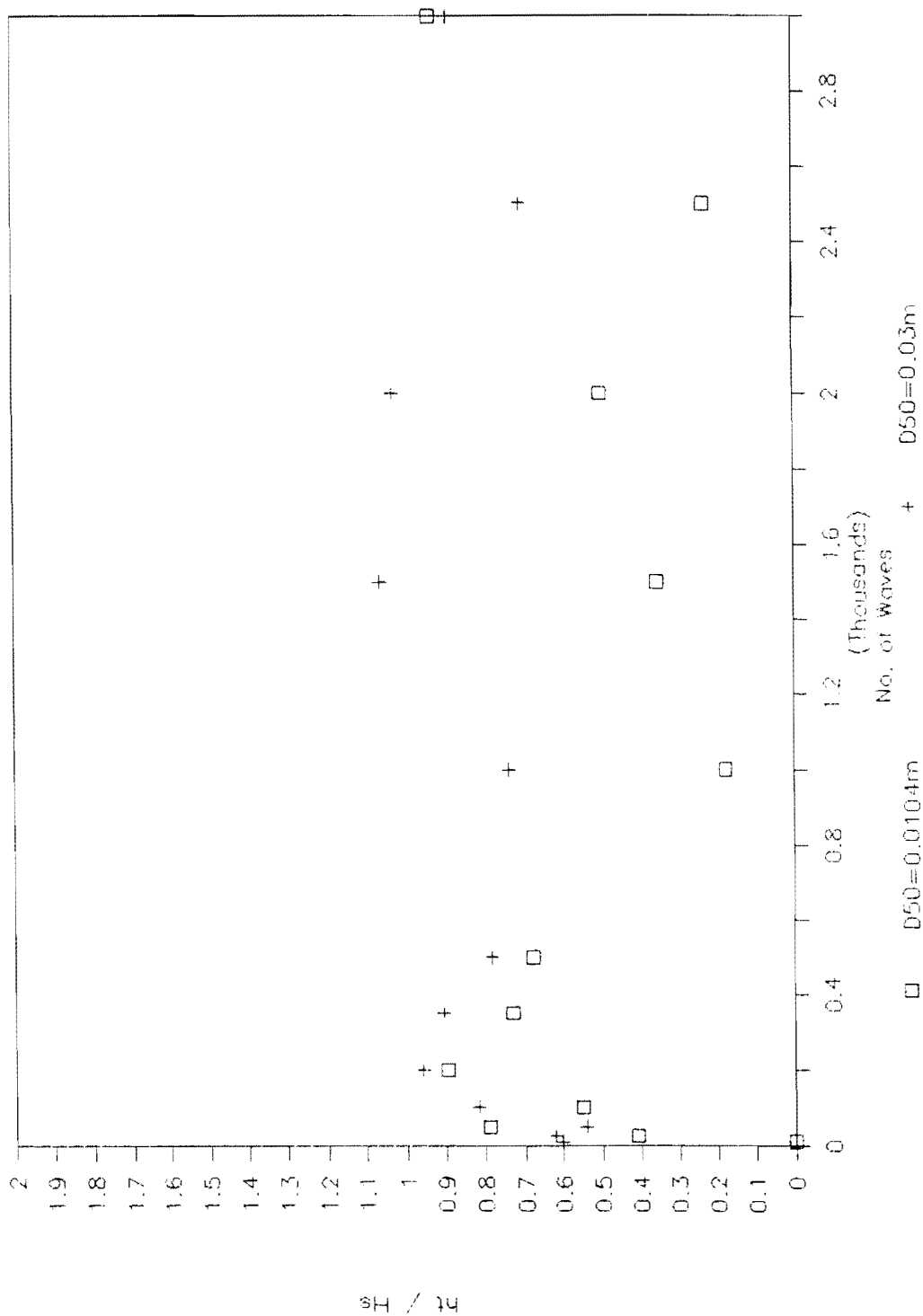


Fig 4.22 Typical wave duration trend- $ht/H_s$

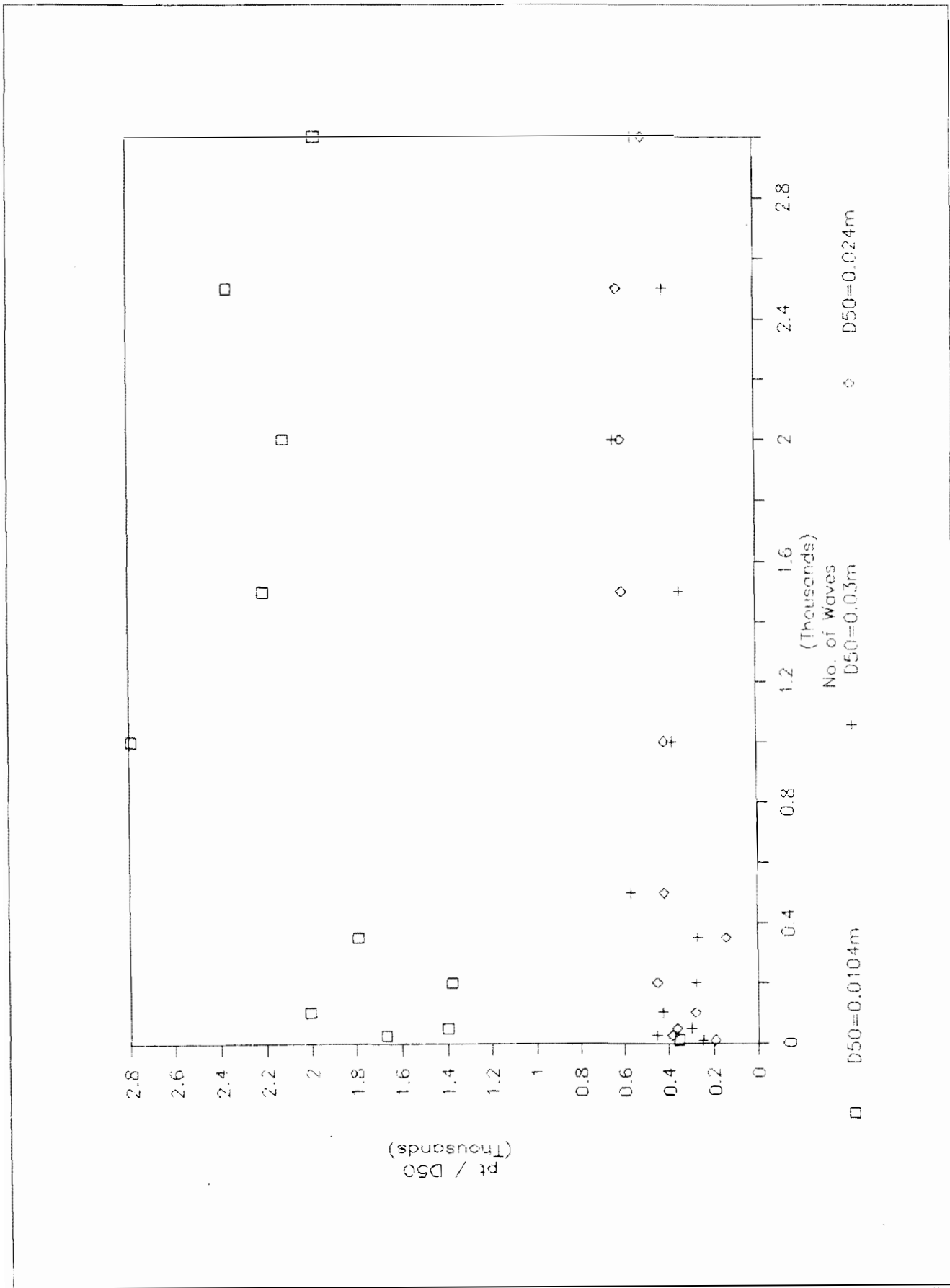


Fig 4.23 Typical wave duration trend-pt/D50

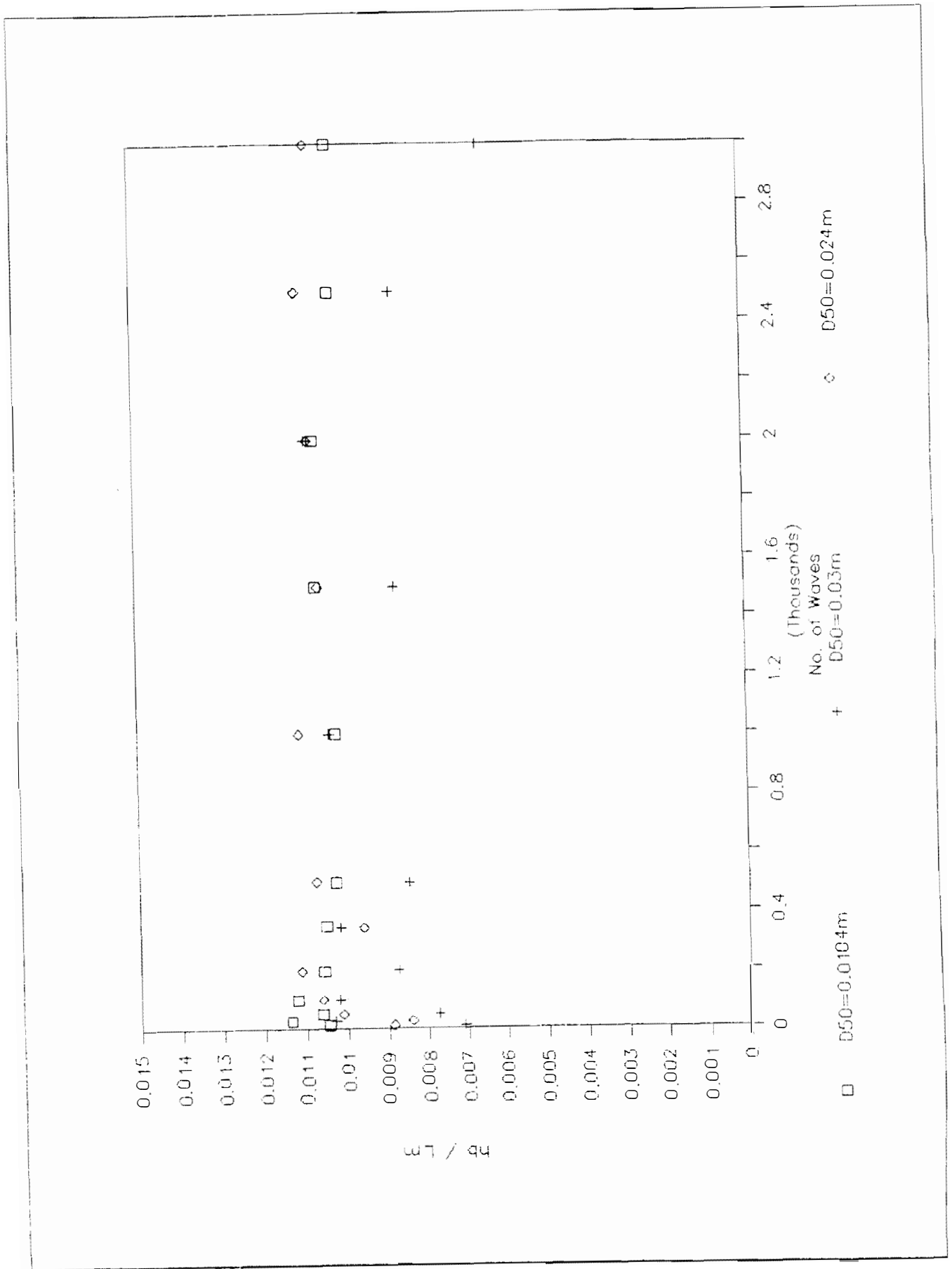


Fig 4.24 Typical wave duration trend- $hb/Lm$

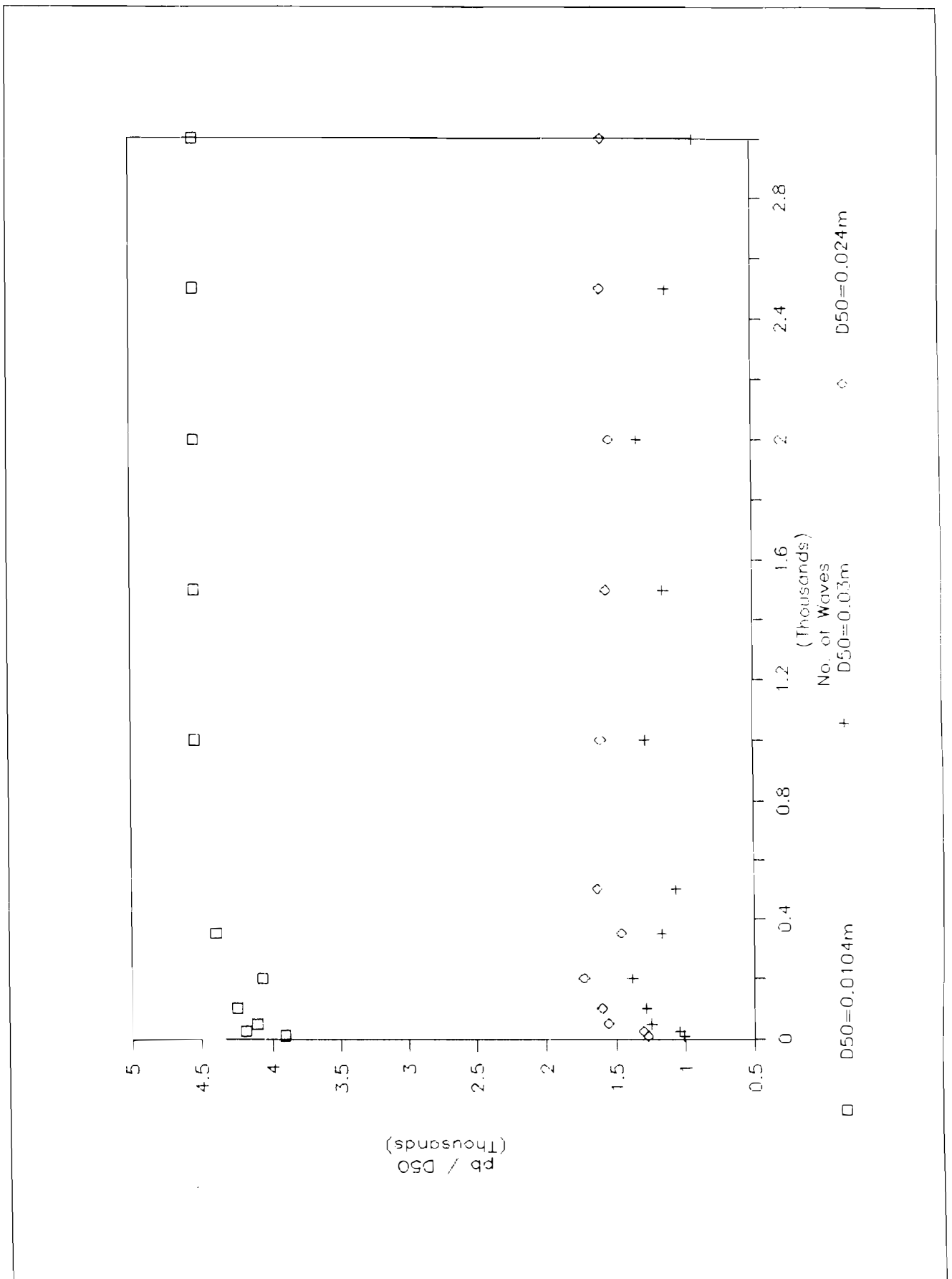


Fig 4.25 Typical wave duration trend-pb/D50

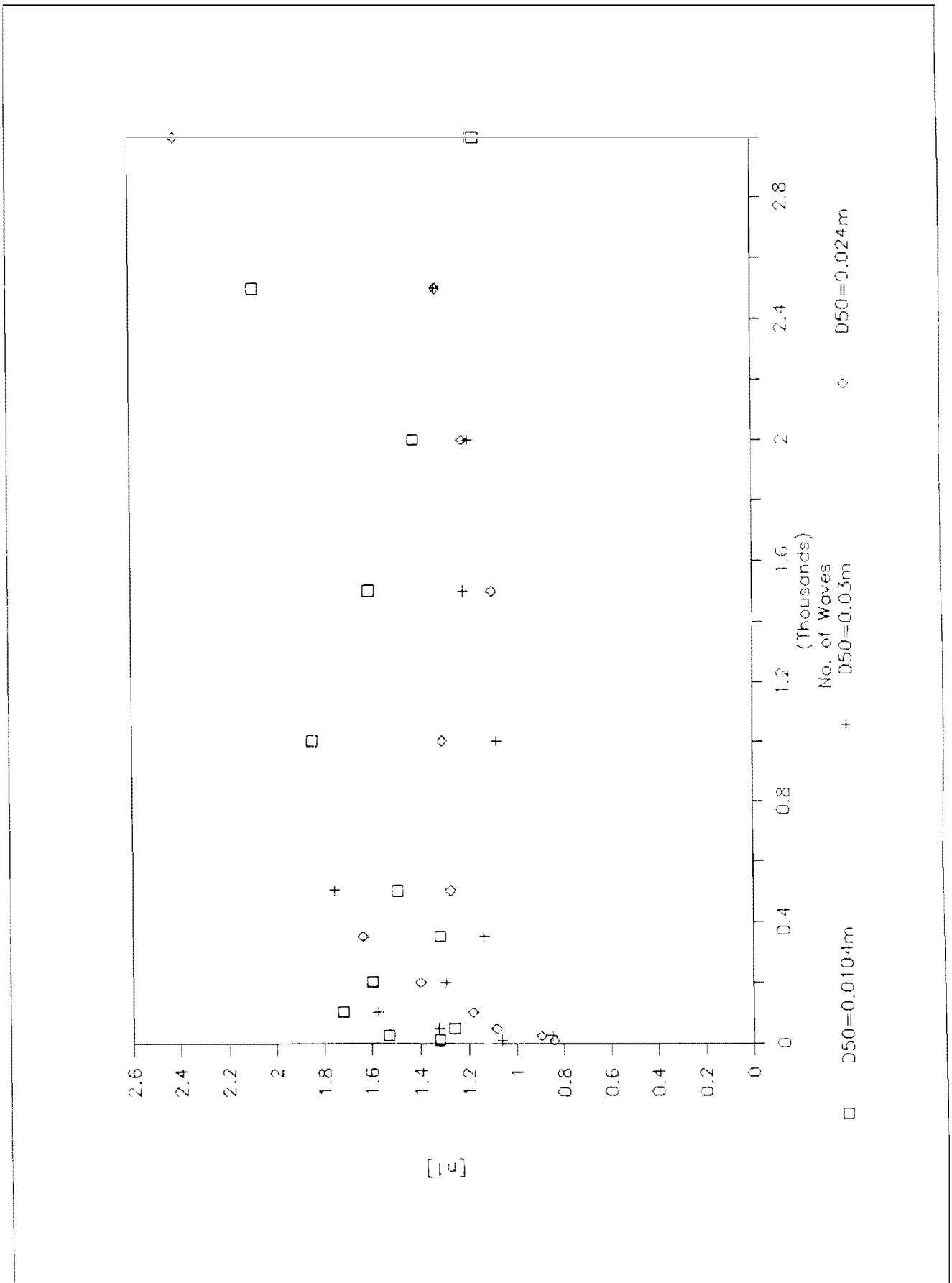


Fig 4.26 Typical wave duration trend-n1

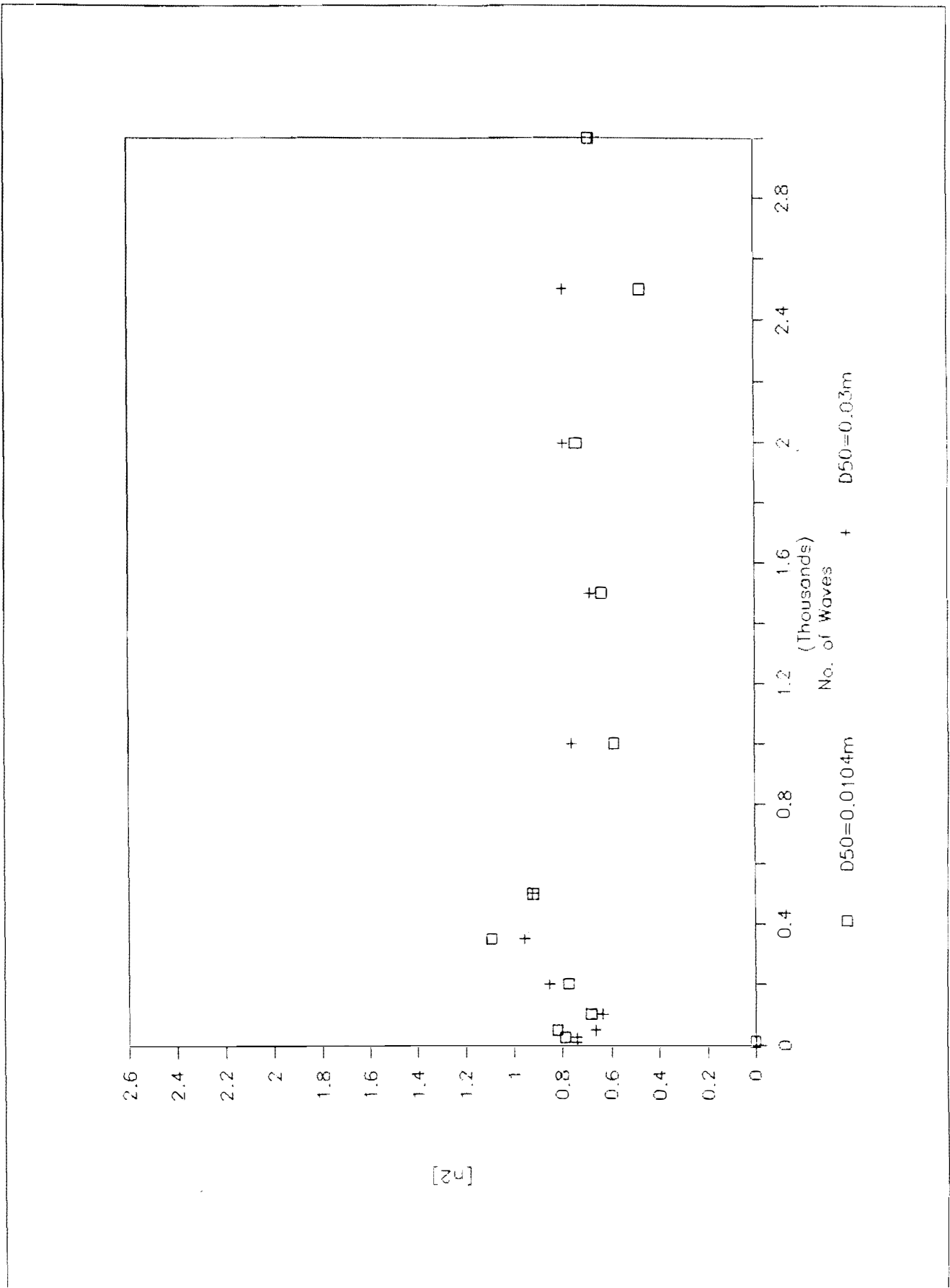


Fig 4.27 Typical wave duration trend- $n_2$

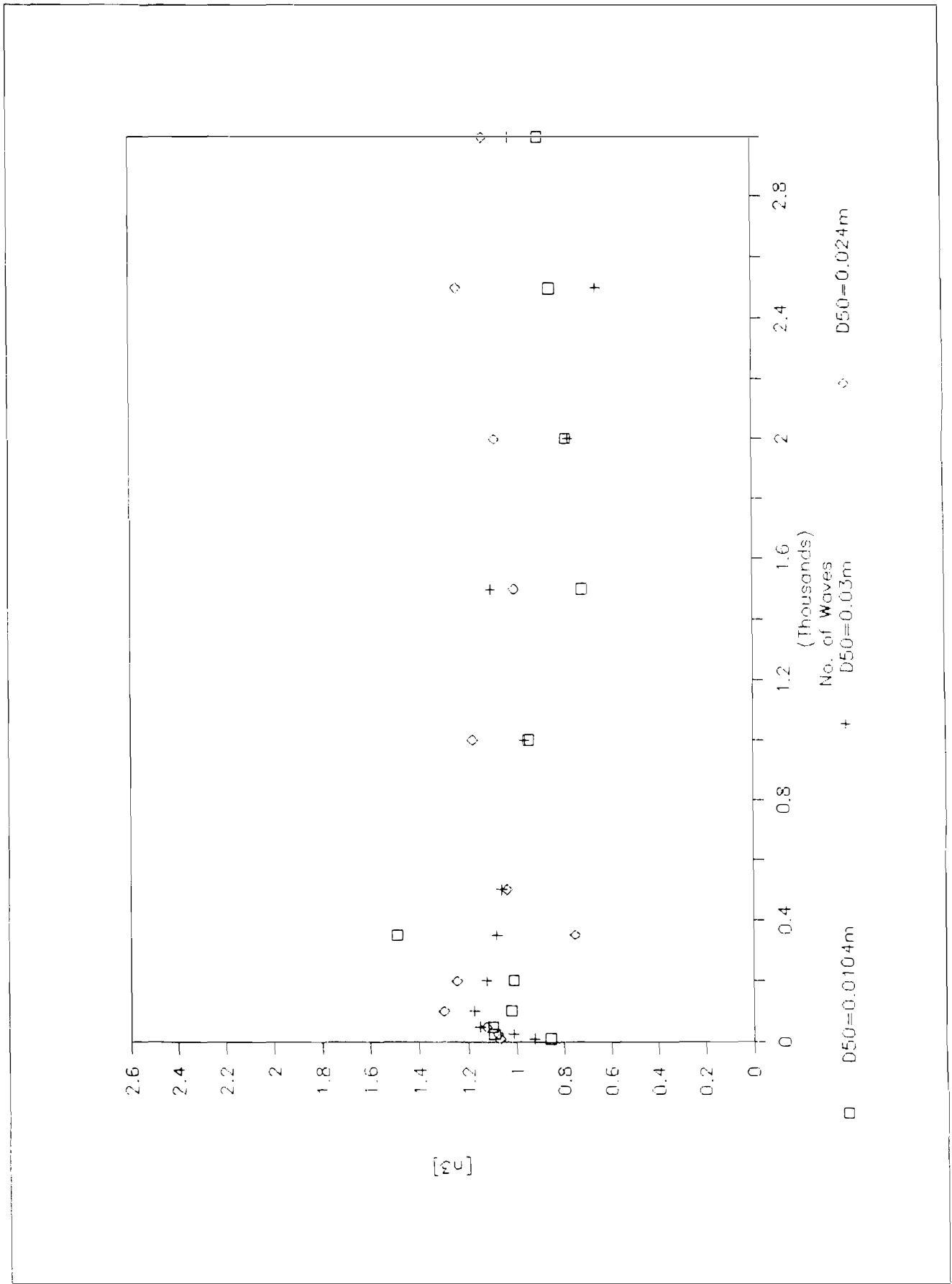


Fig 4.28 Typical wave duration trend-n3

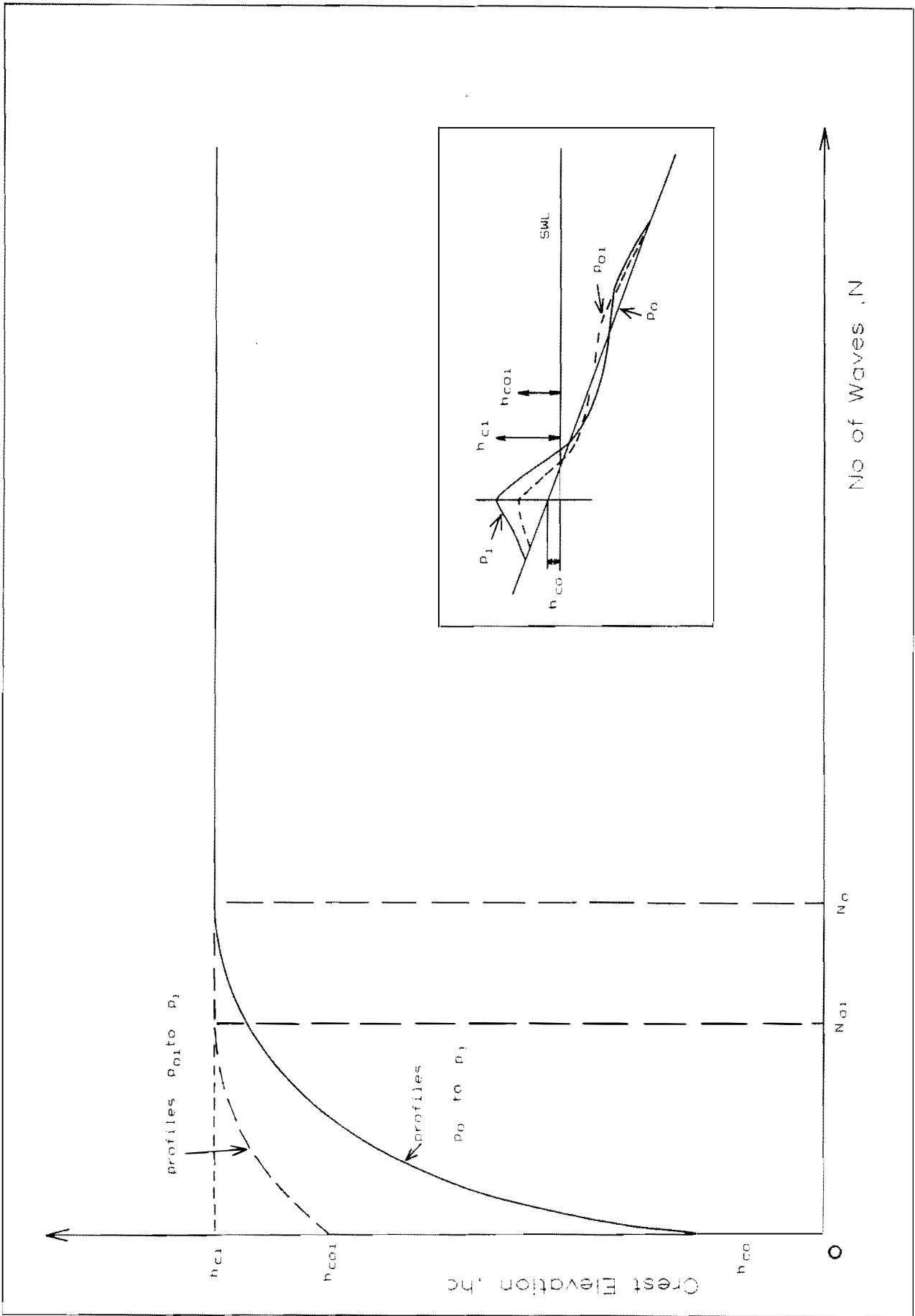


Fig 4.29 Schematic representation of wave duration and profile similarity dependence

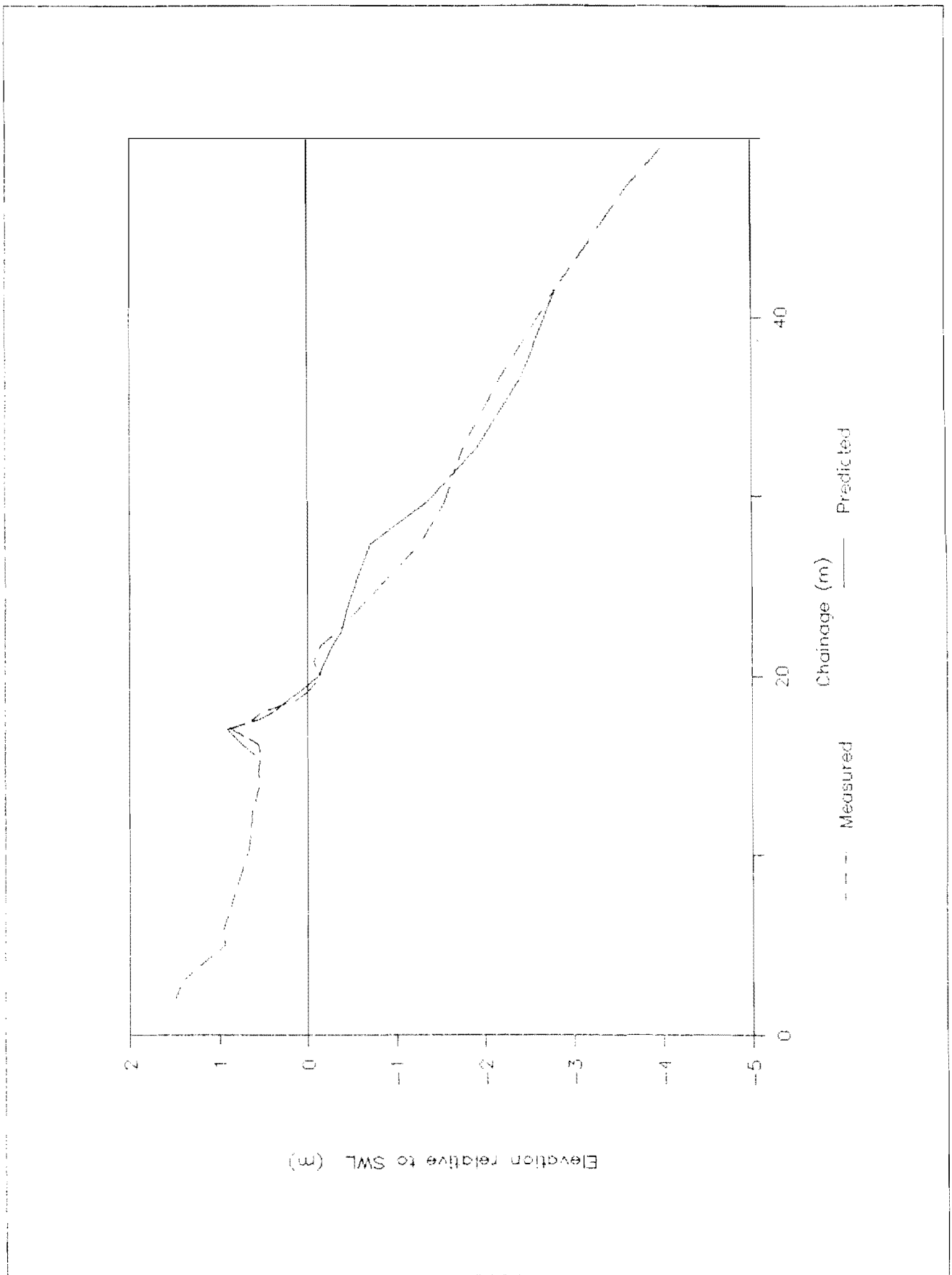


Fig 4.30 Wave duration limited profile  
 -Test No.16 500 waves.

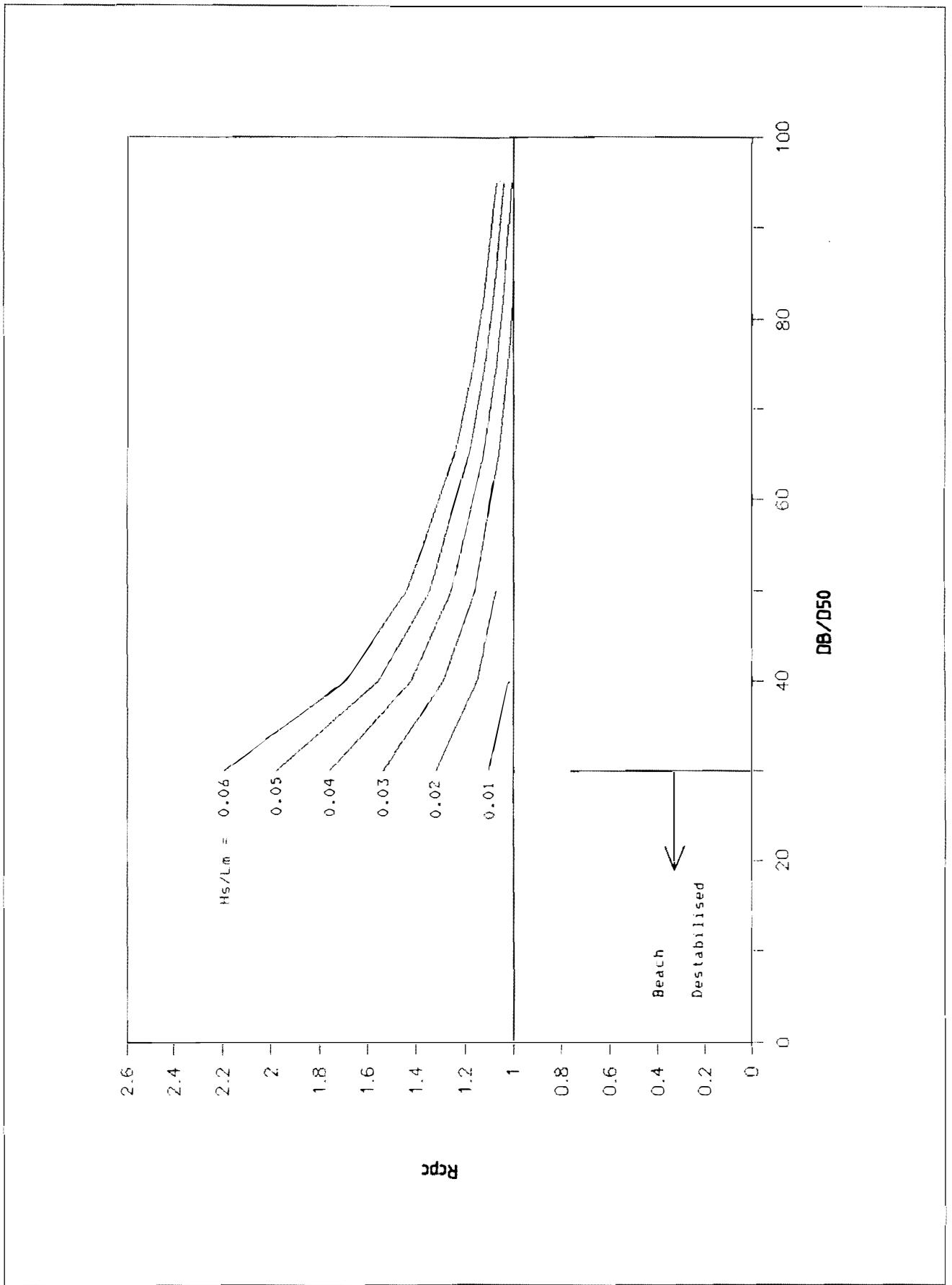


Fig 4.31 Effective beach thickness correction factor for crest position

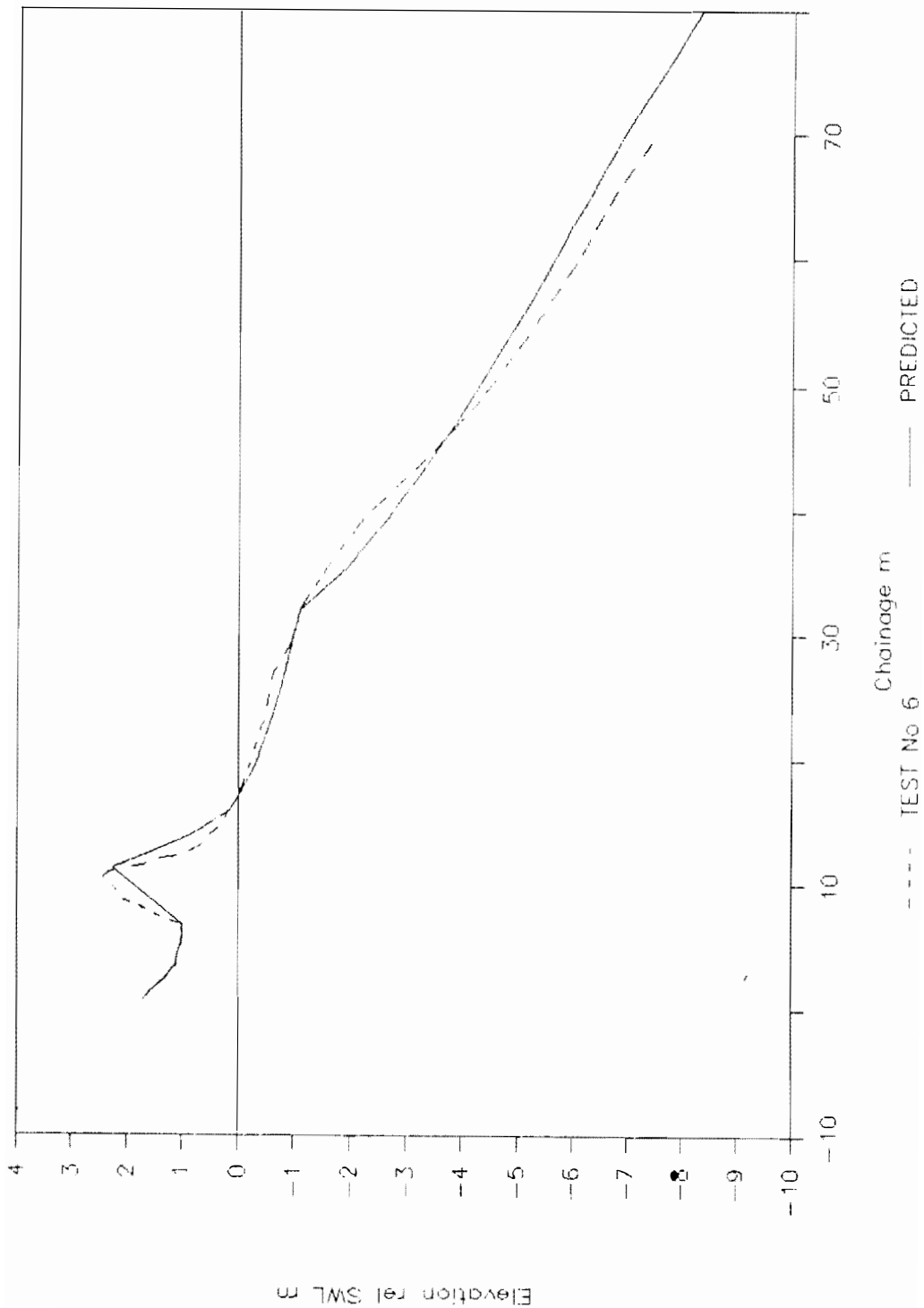


Fig 4.32 Comparison, measured and predicted profiles-Test 6.

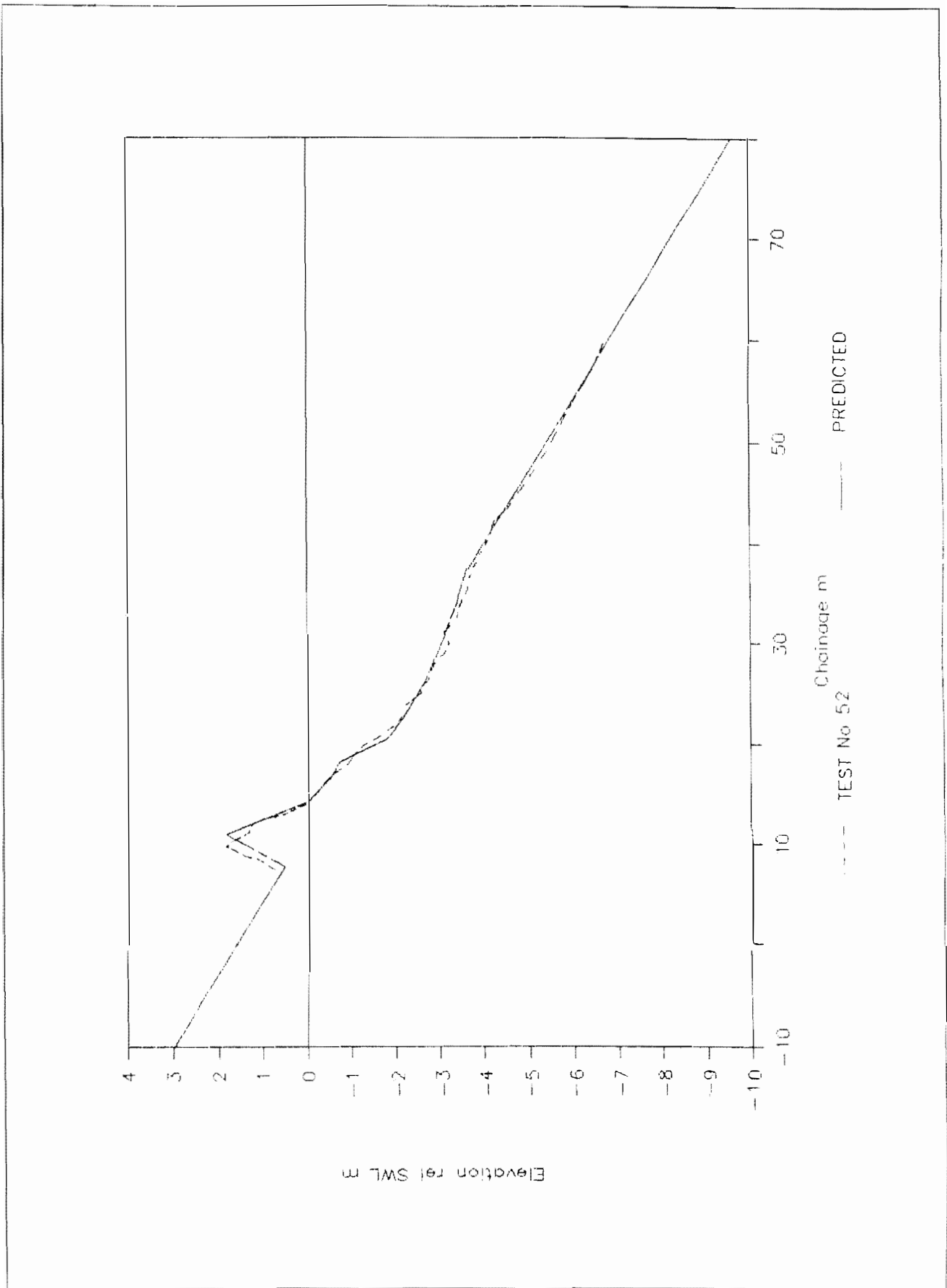


Fig 4.33 Comparison, measured and predicted profiles-Test 52

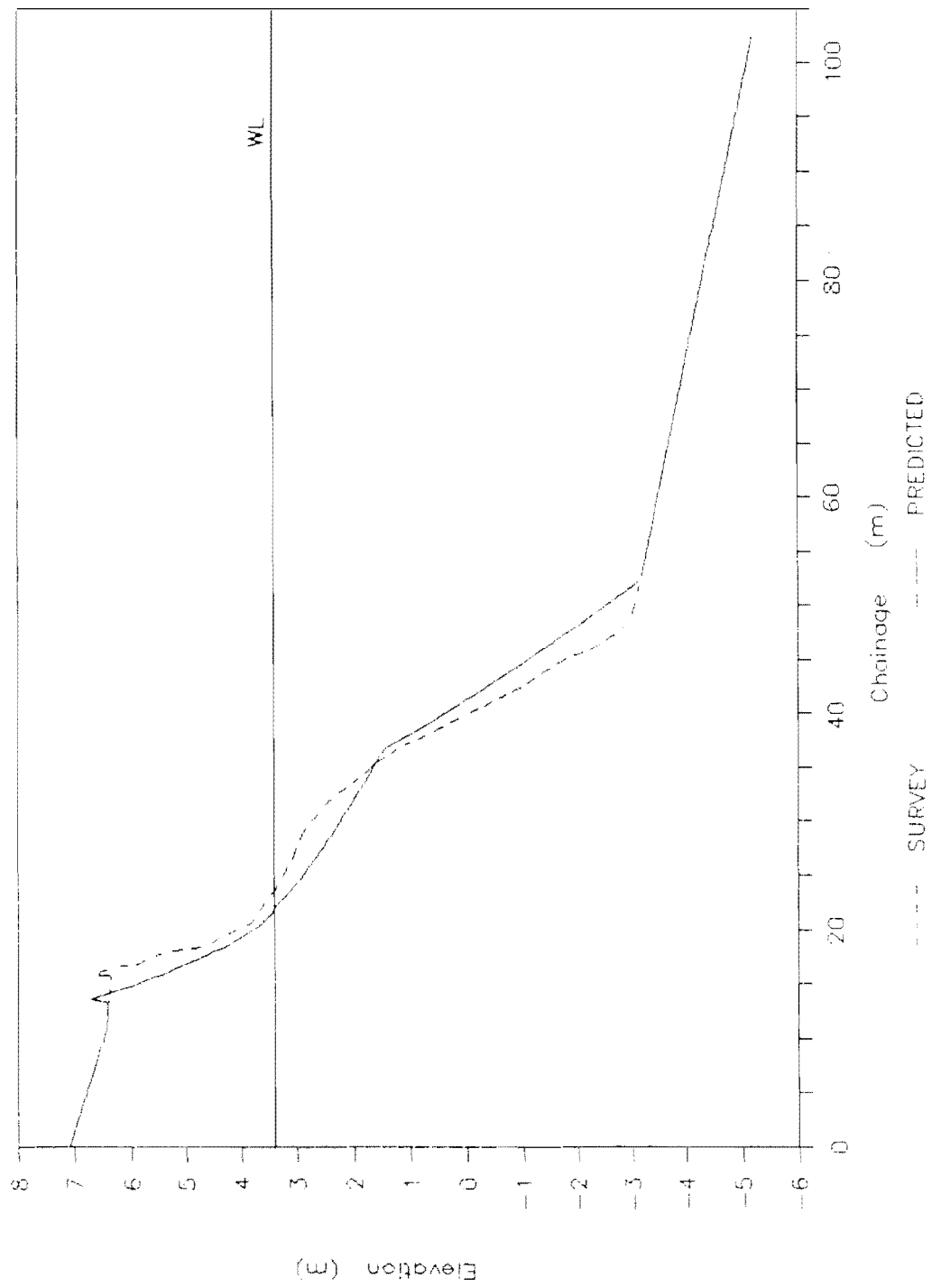


Fig 4.34 Comparison, measured and predicted profiles-Depth limited foreshore

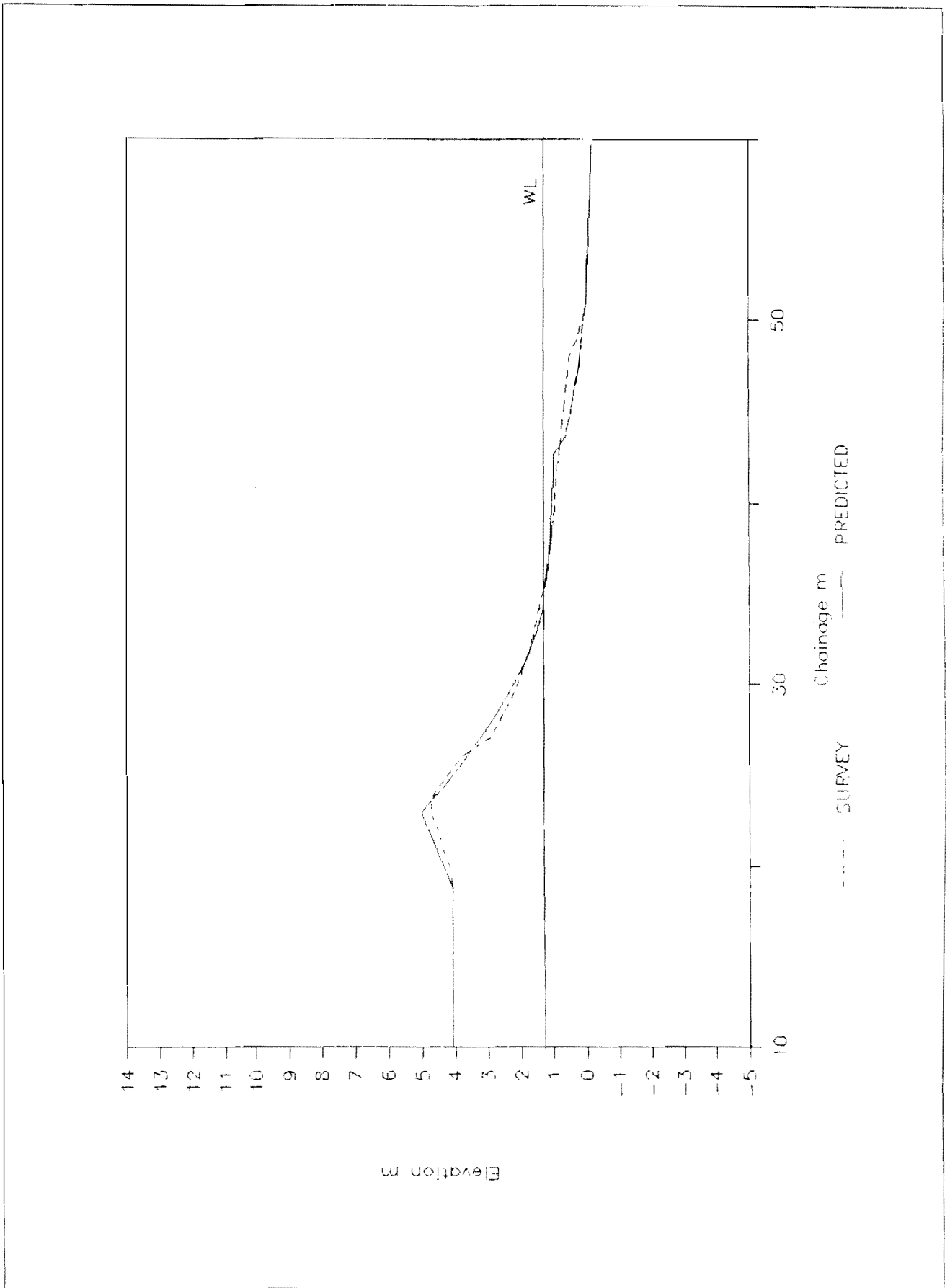


Fig 4.35 Comparison, measured and predicted profiles-Depth limited foreshore

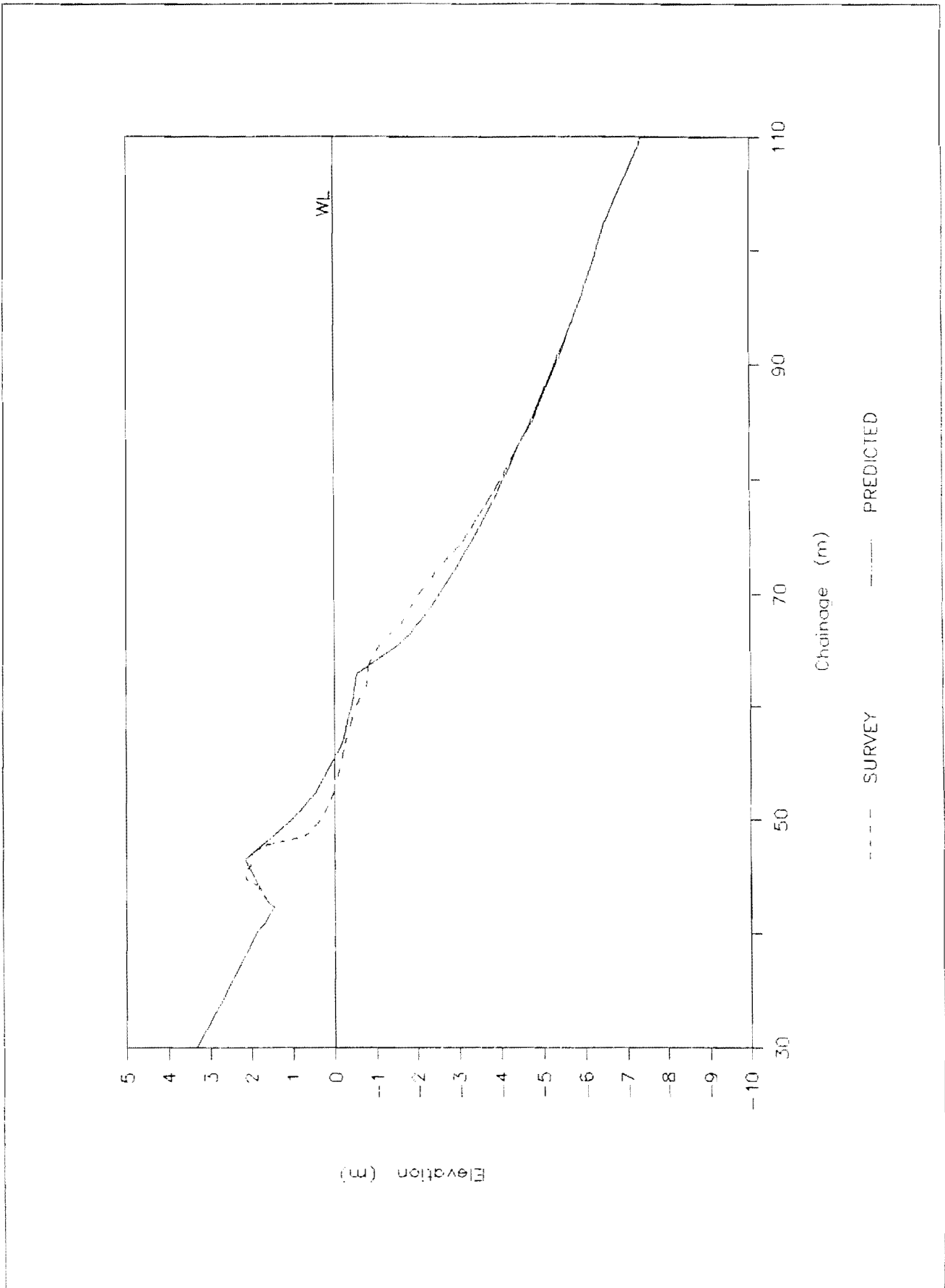


Fig 4.36 Comparison, measured and predicted profiles-Limited beach thickness

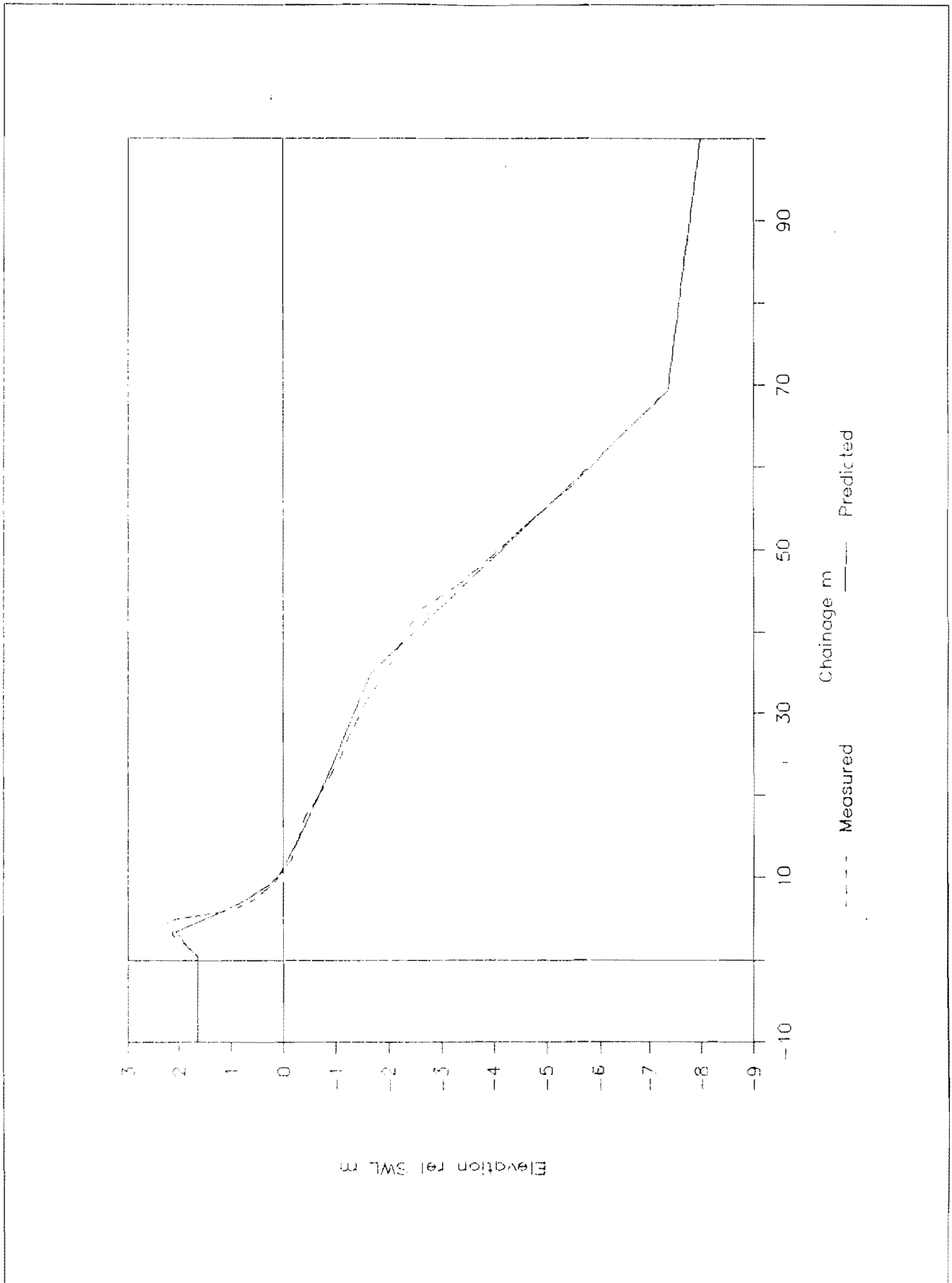


Fig 4.37 Comparison, measured and predicted profiles-Wave steepness 0.06

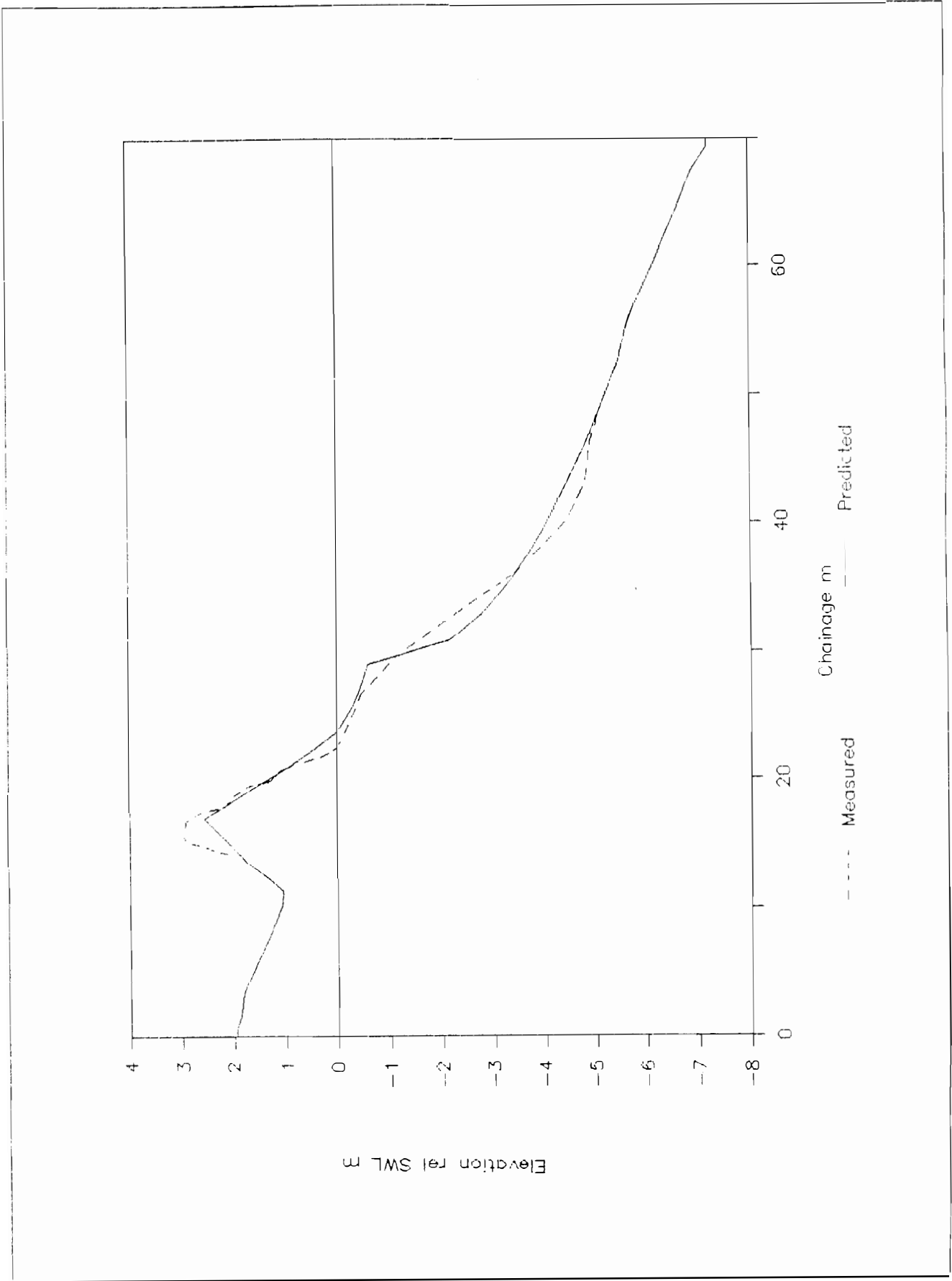


Fig 4.38 Comparison, measured and predicted profiles-Wave steepness 0.01

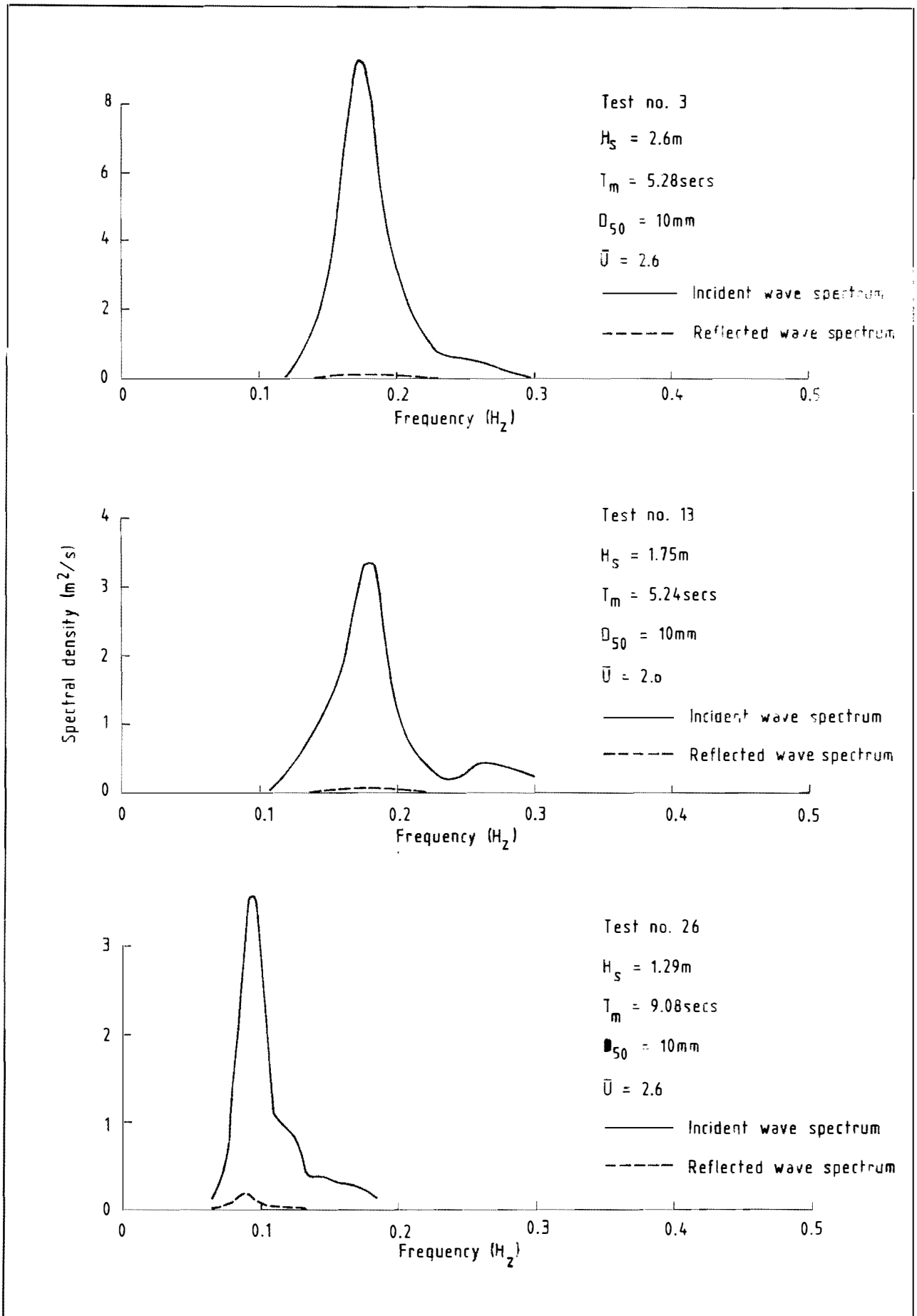


Fig 5.1 Typical incident and reflected wave spectra

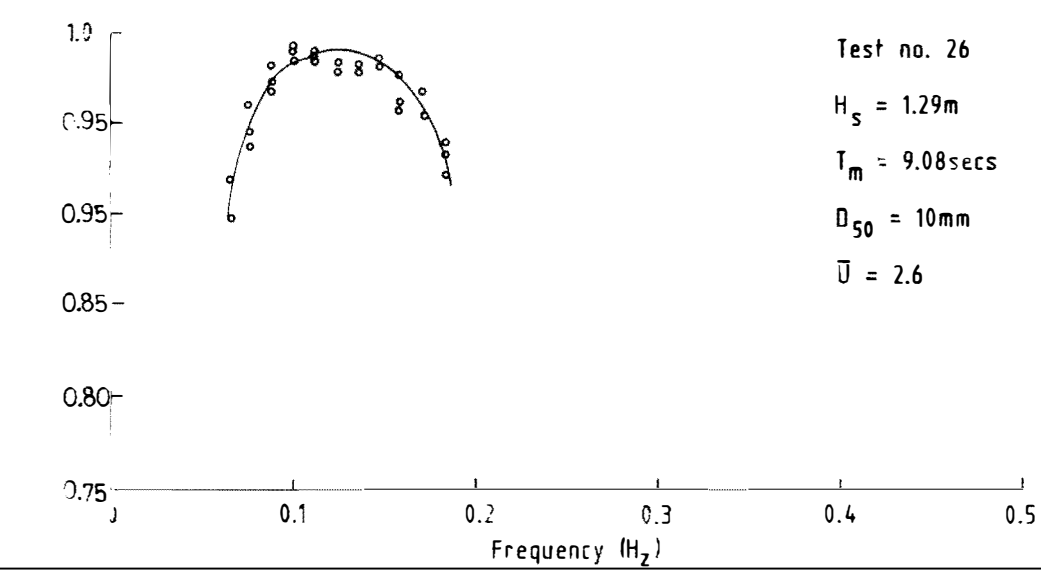
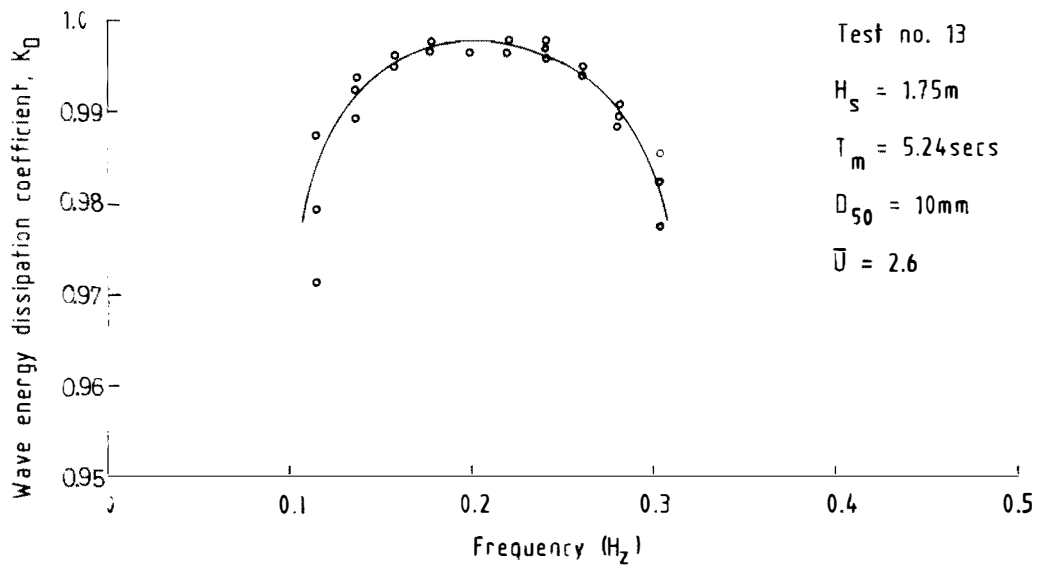
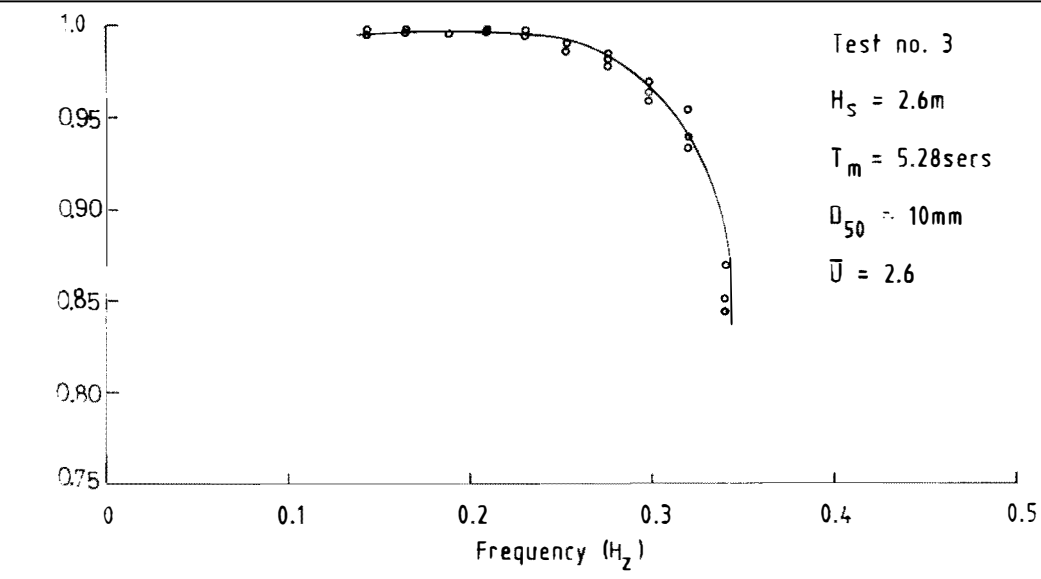
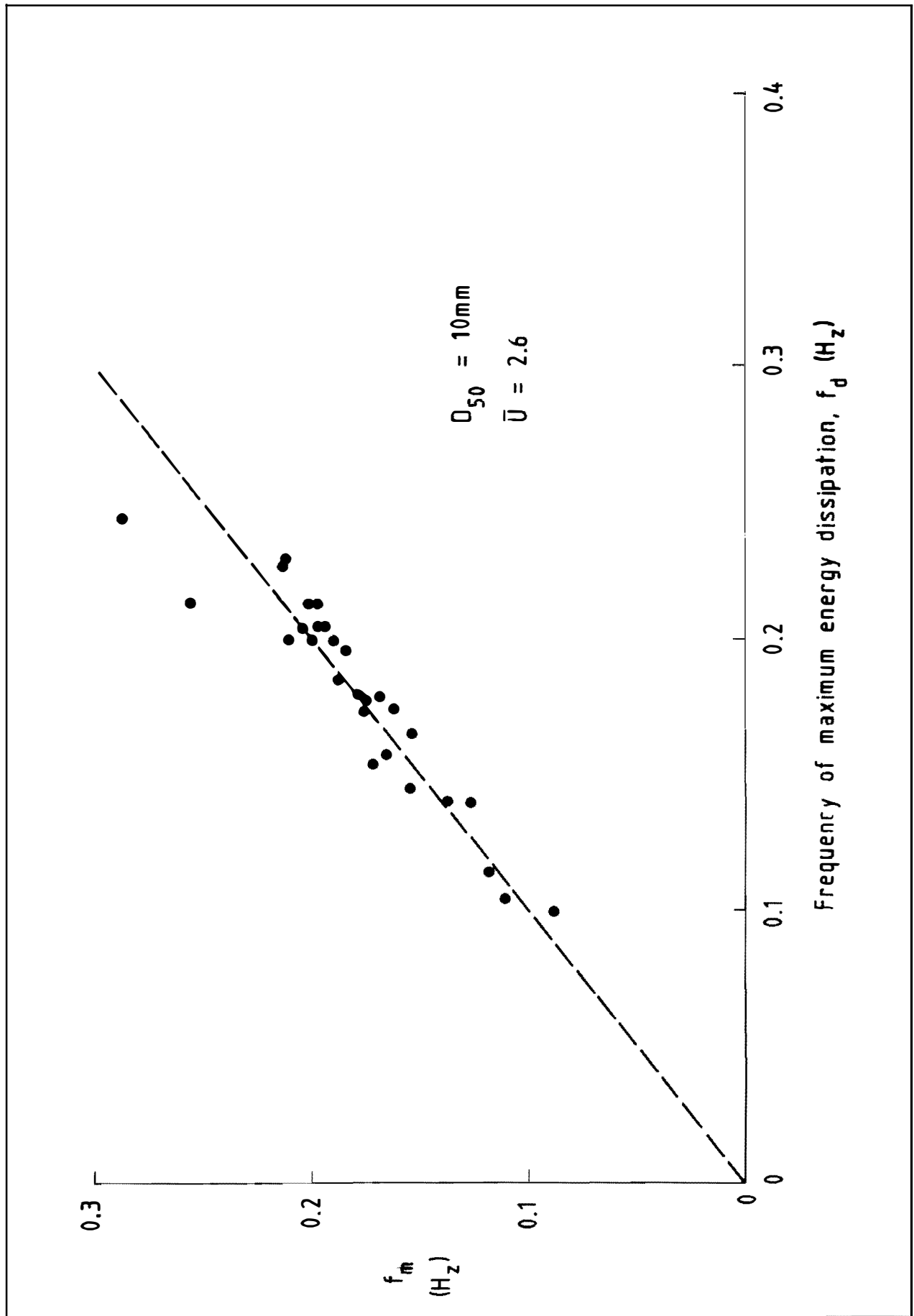


Fig 5.2 Typical wave energy dissipation curves - JONSWAP spectra.



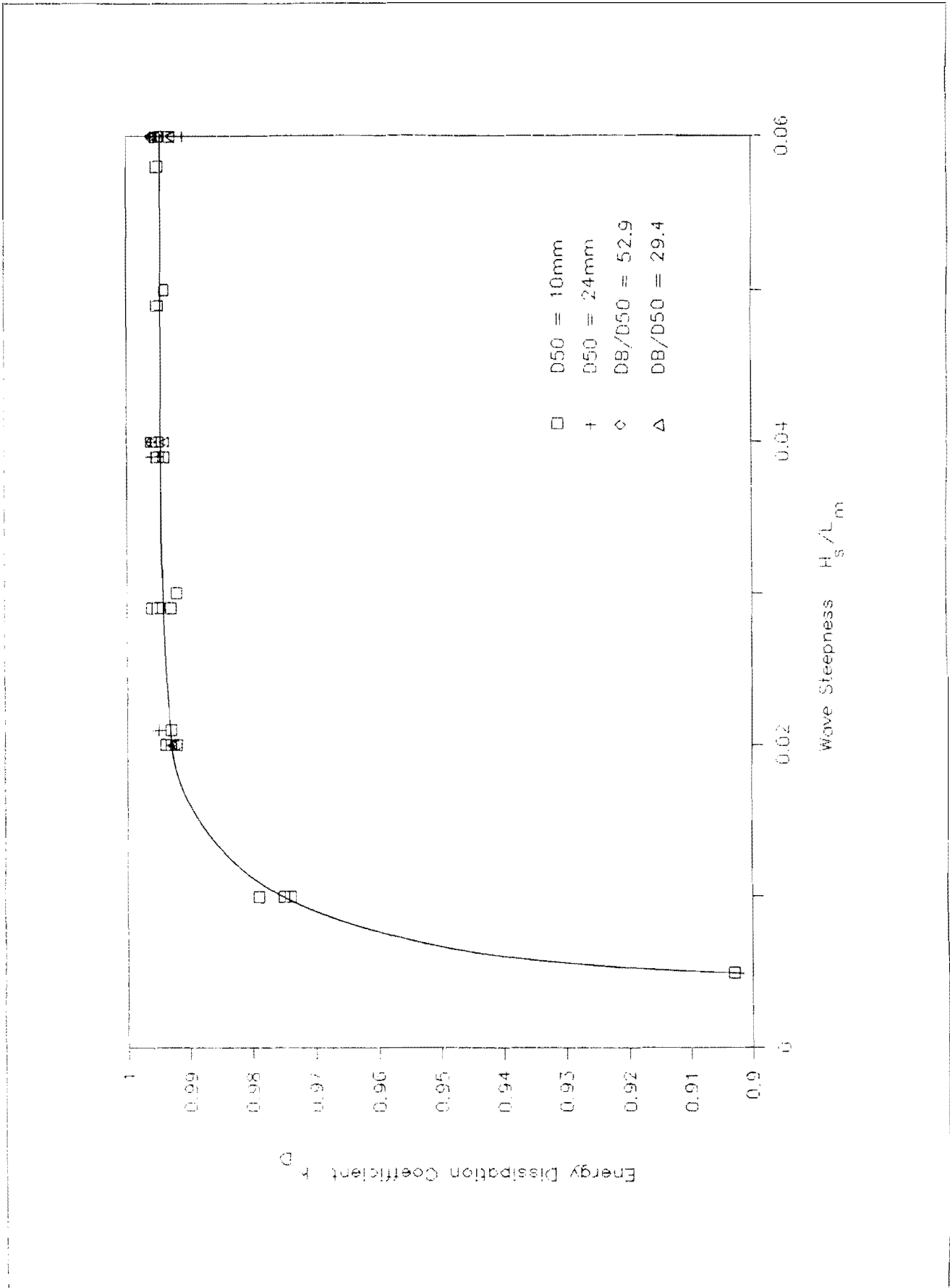


Fig 5.4 Wave energy dissipation as a function of mean sea steepness

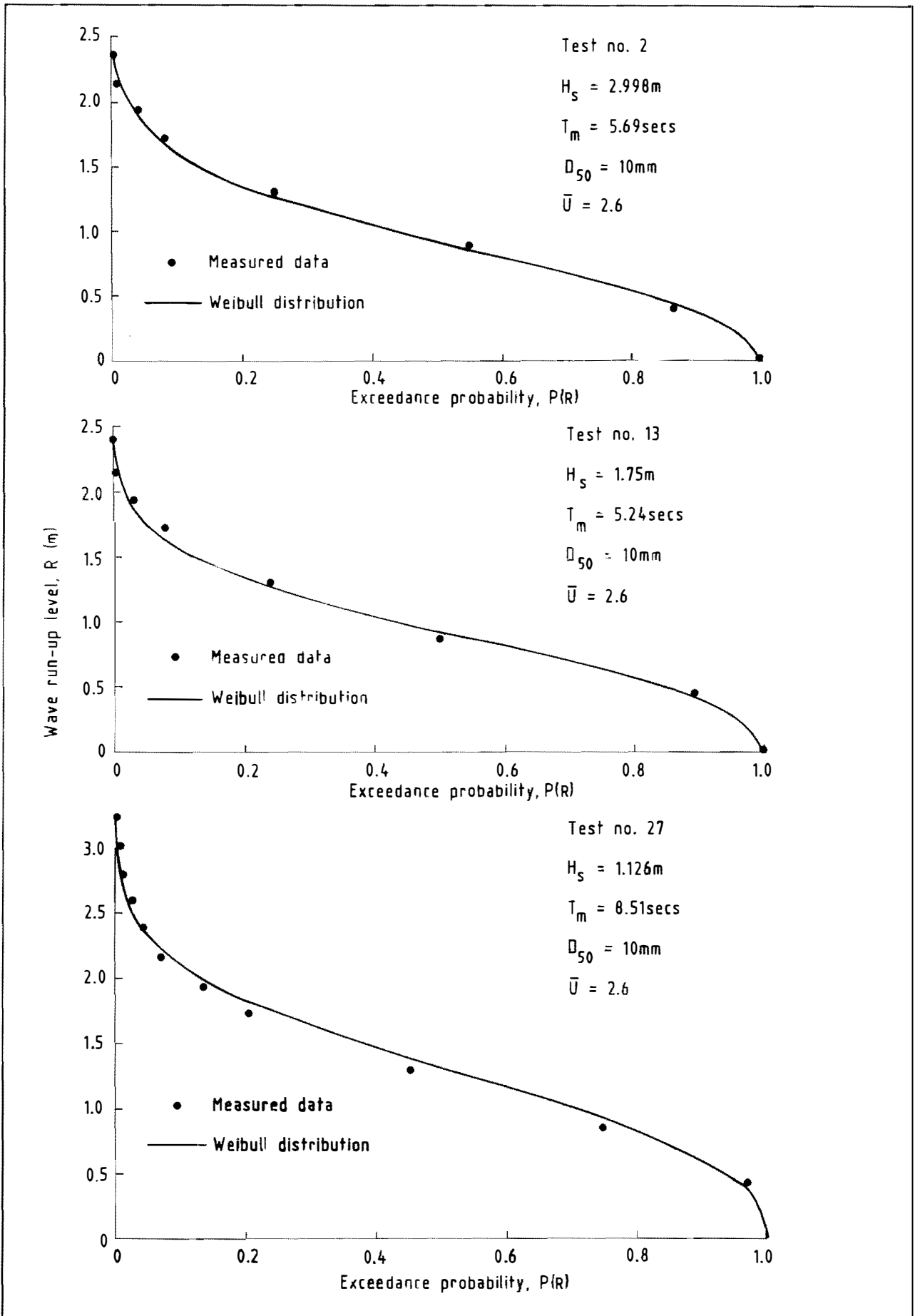


Fig 6.1 Typical wave run-up distributions

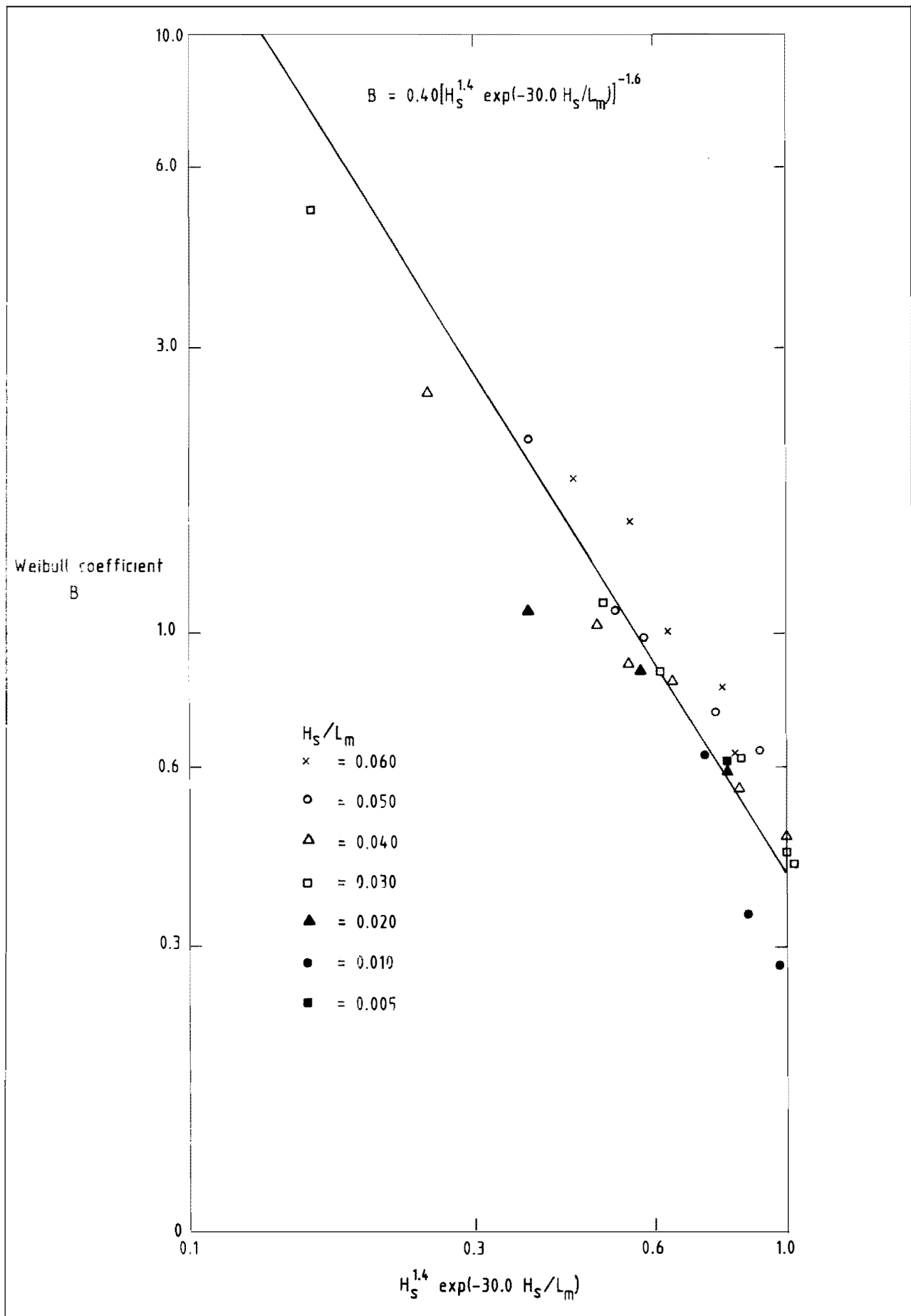


Fig 6.2 Variation in Weibull coefficient B.

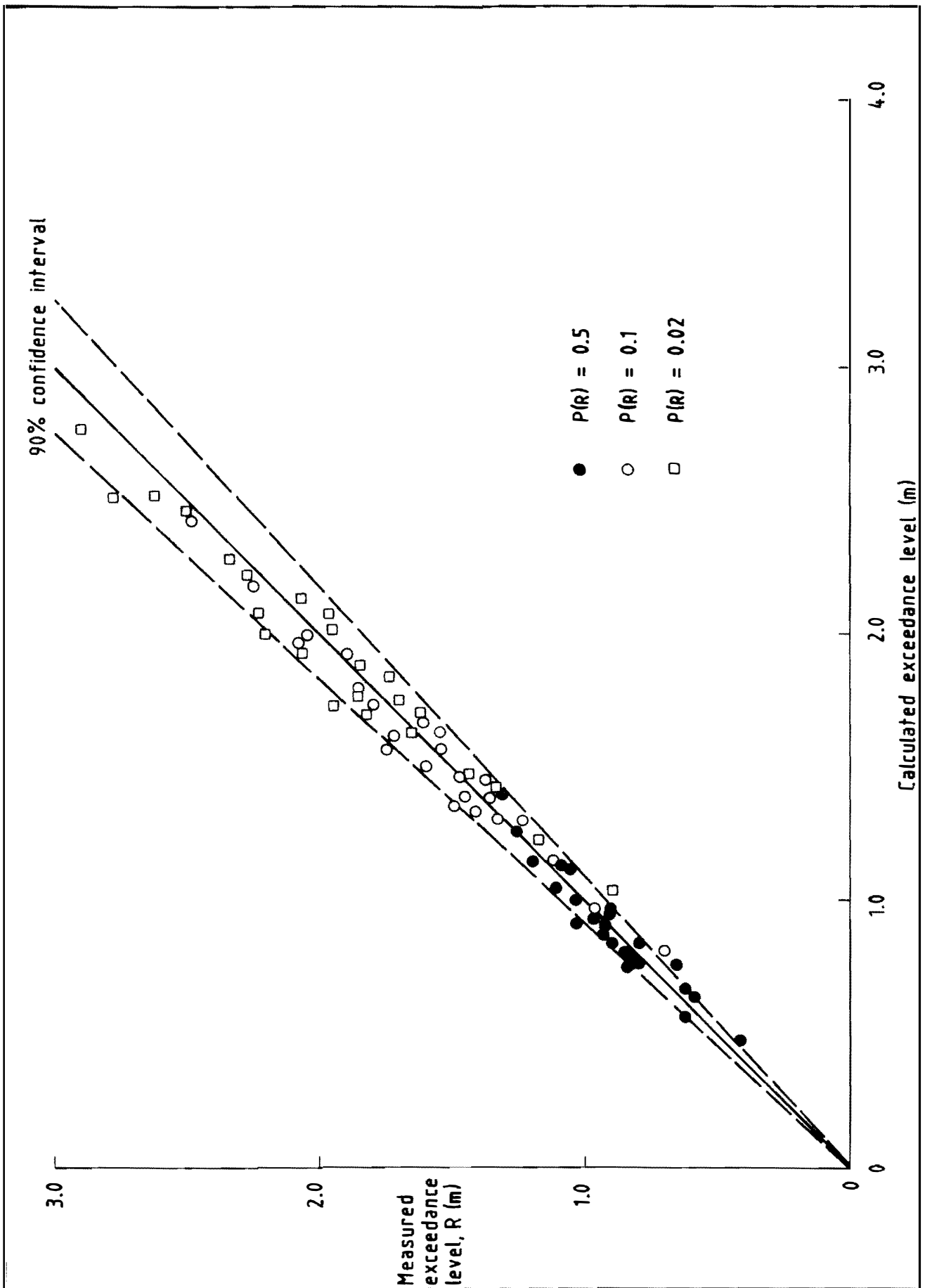
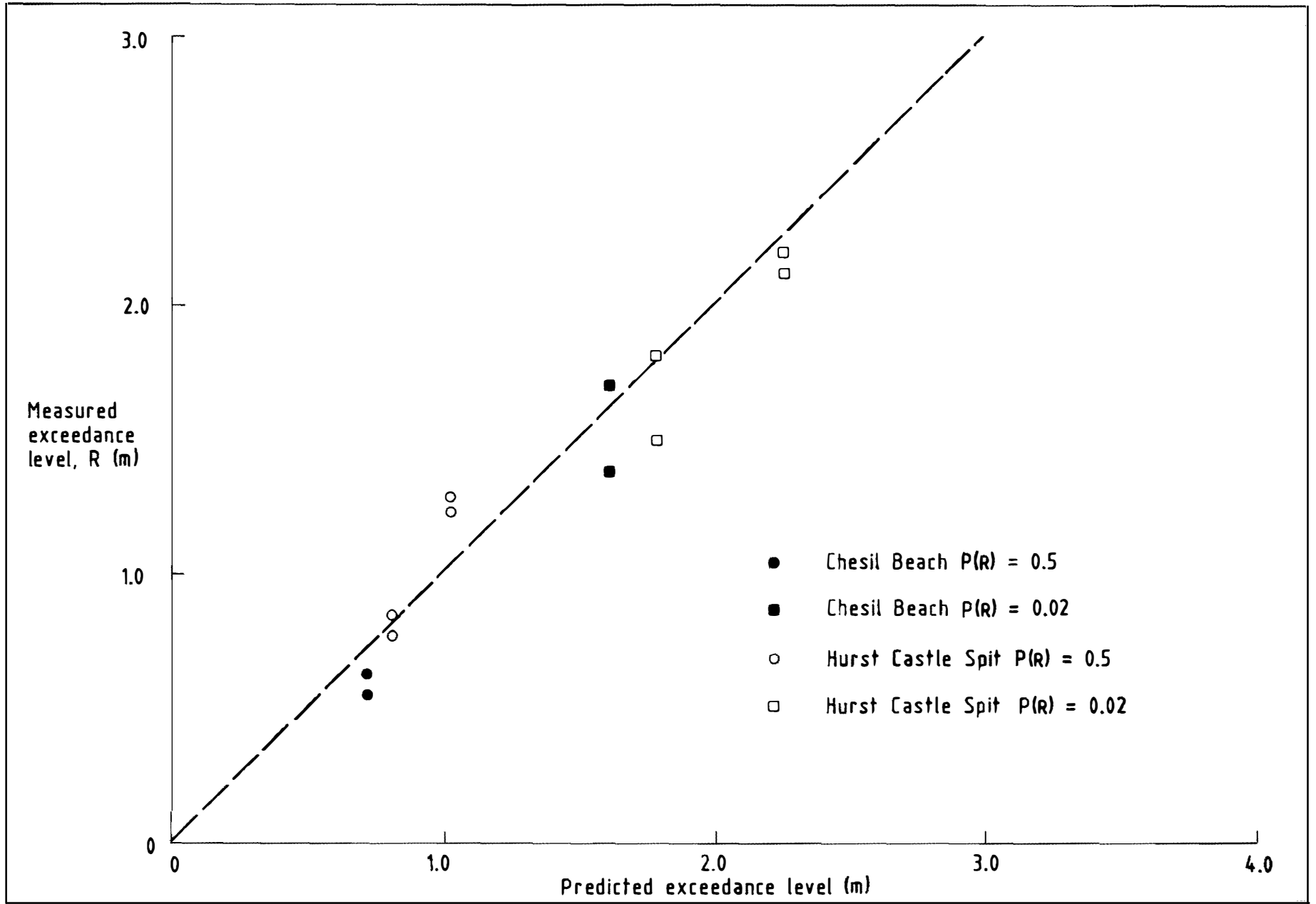


Fig 6.3 Measured versus back-calculated run-up exceedance levels

Fig 6.4 Comparison of field measurement and predicted run-up exceedance levels



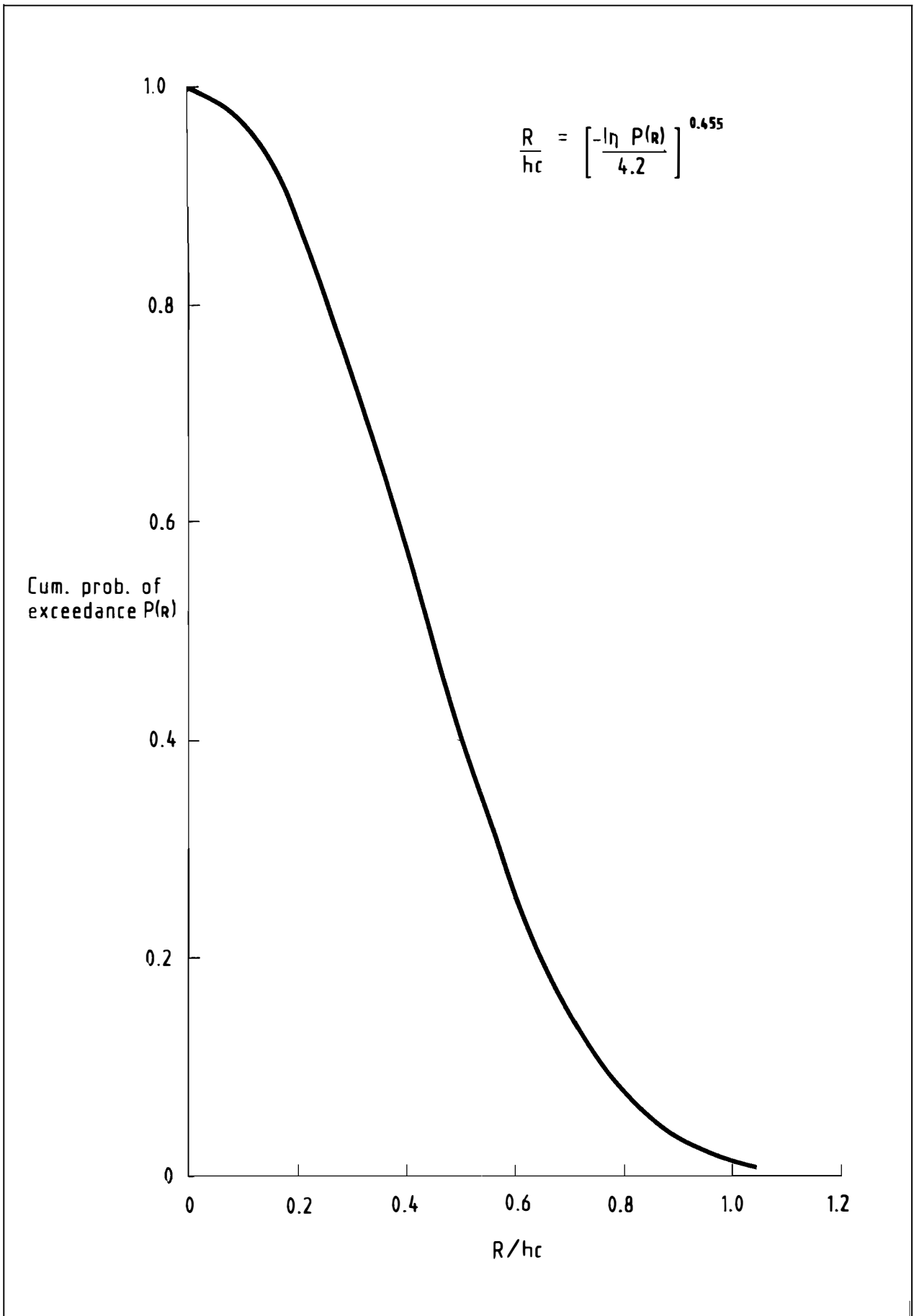


Fig 6.5 Wave run-up exceedance levels - cumulative probability distribution

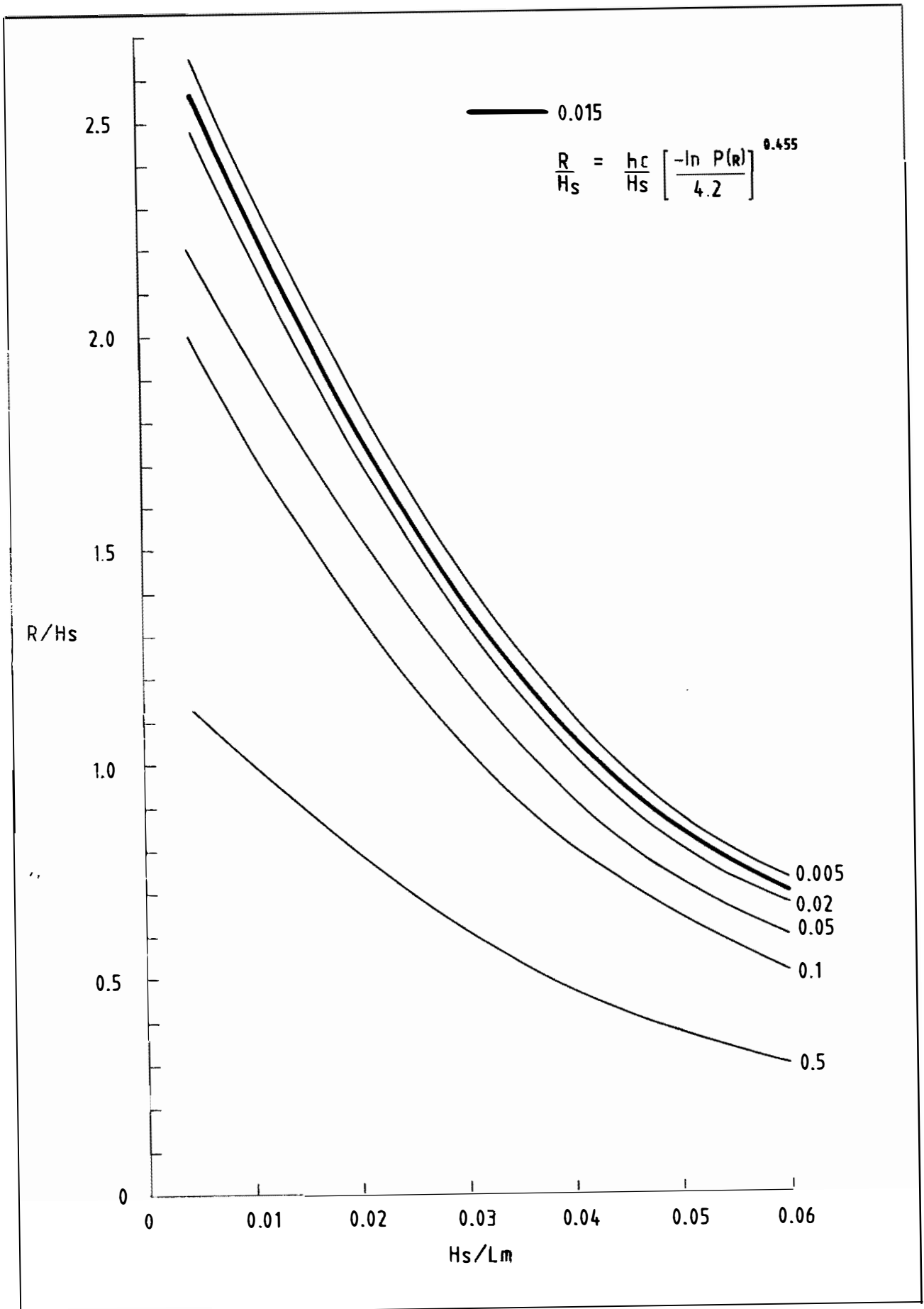


Fig 6.6 Wave run-up exceedance levels - wave steepness dependency

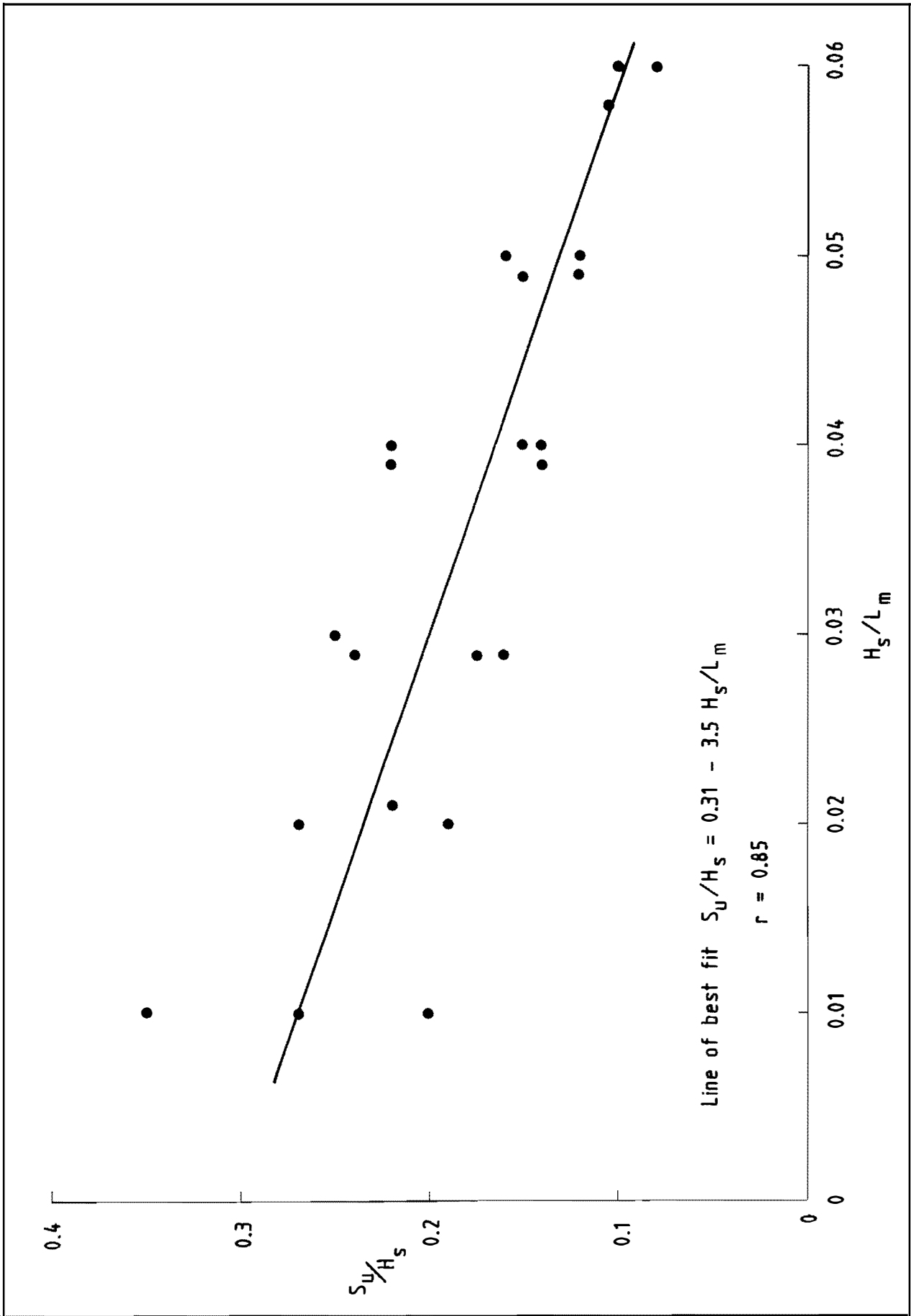


Fig 6.7 Correlation between measured wave set-up and mean sea steepness

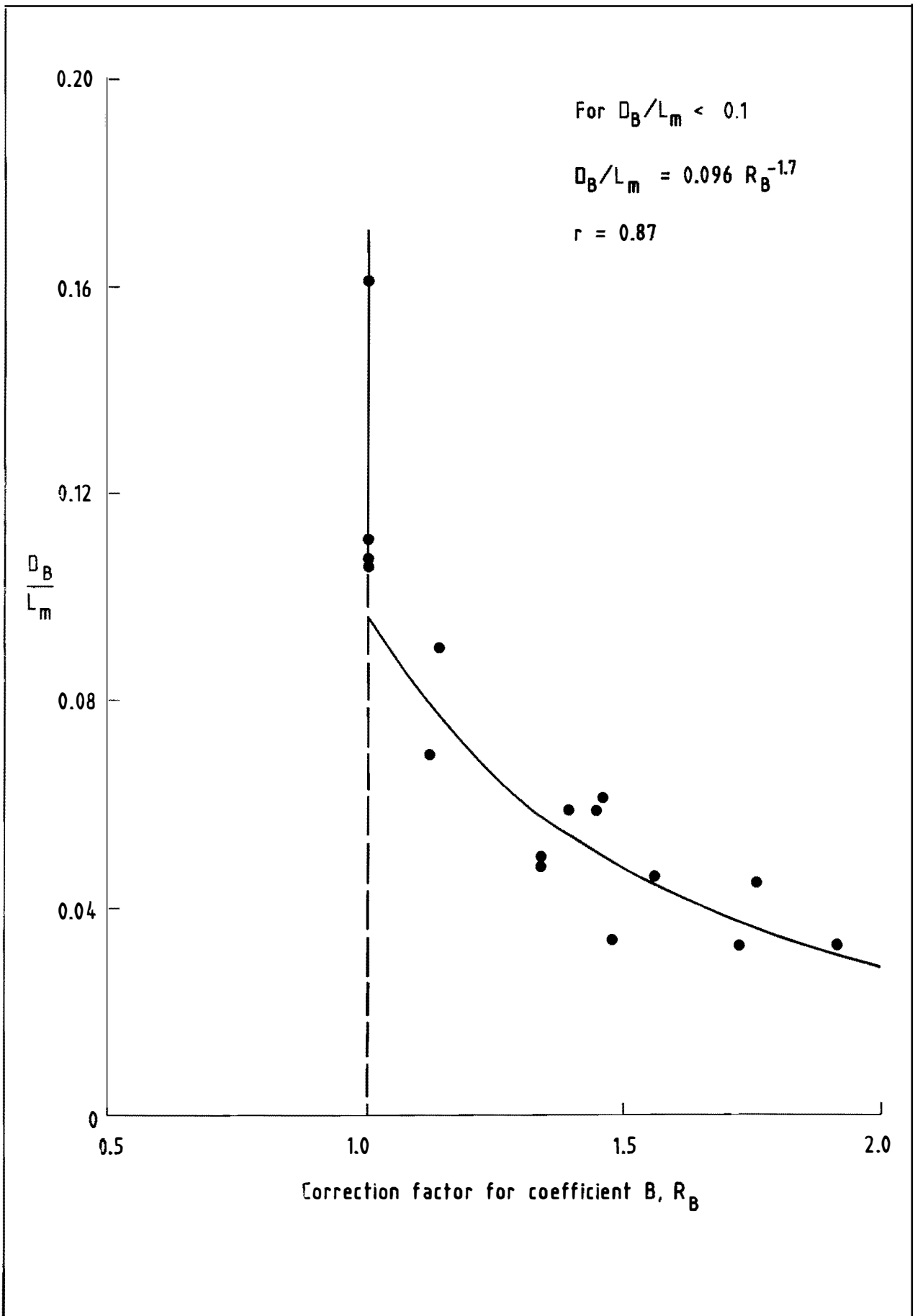


Fig 6.8 Beach depth correction factor for Weibull probability distribution coefficient B

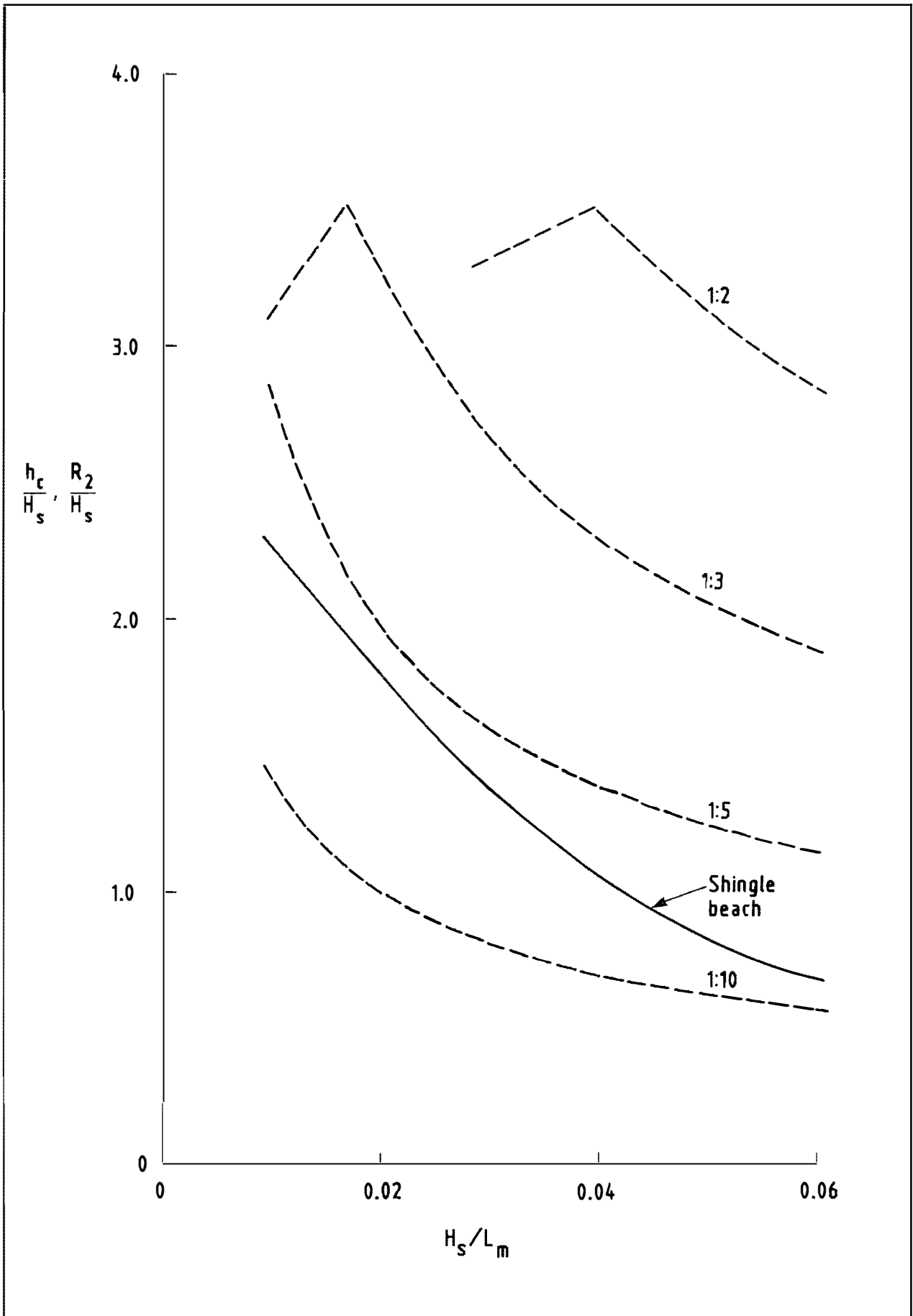


Fig 6.9 Comparison of smooth slope and shingle beach run-up

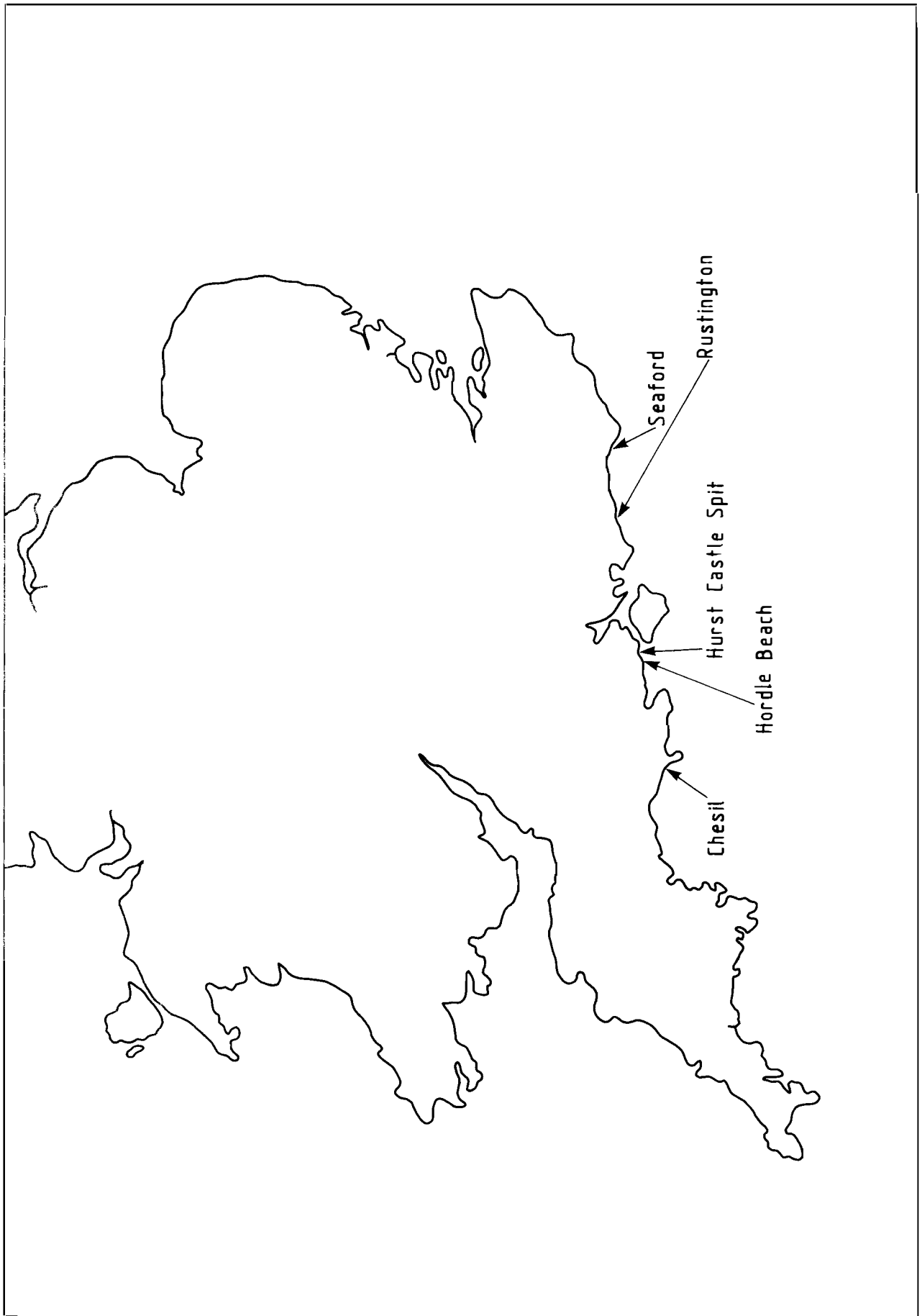


Fig 7.1 Location of field measurement sites

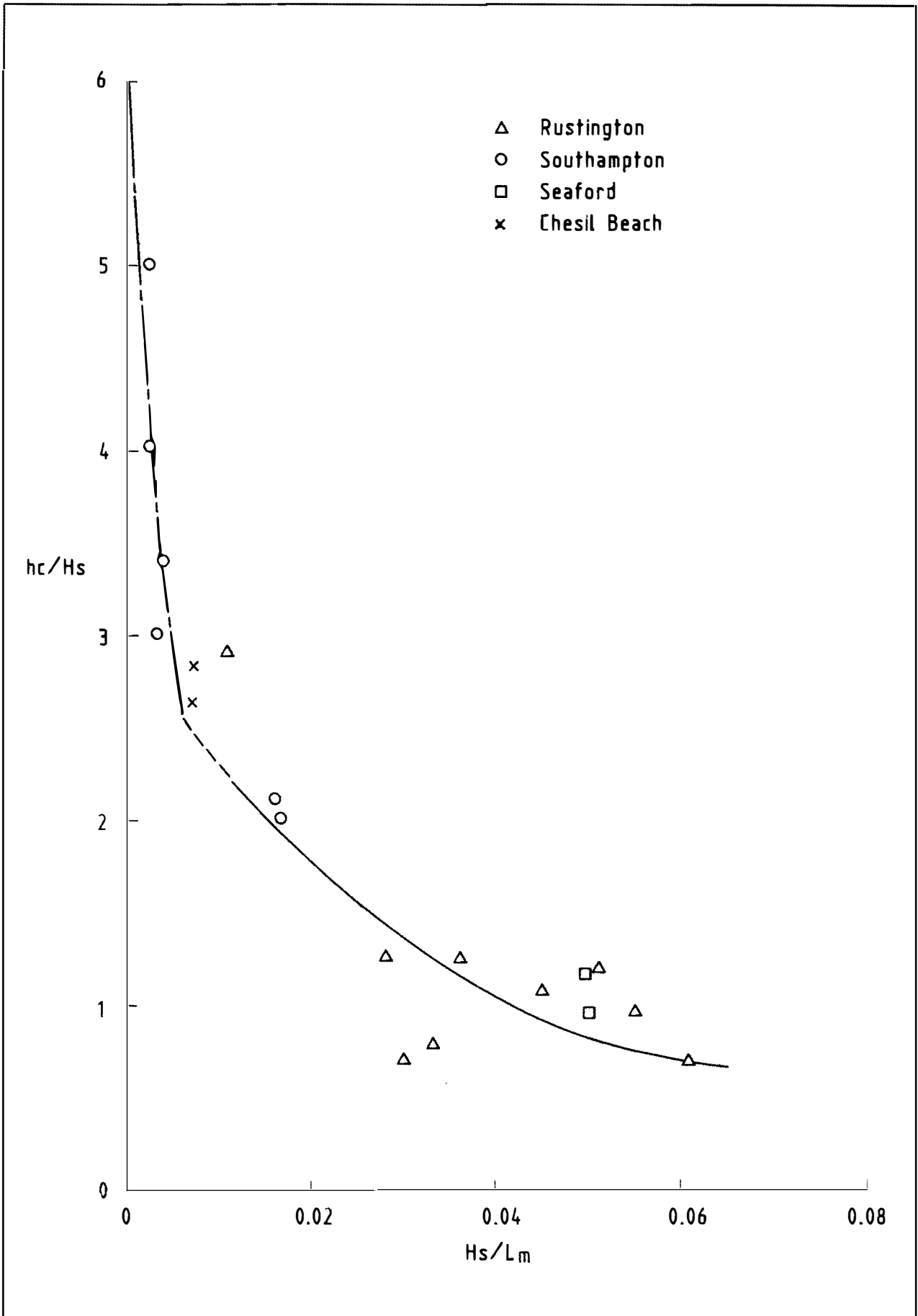


Fig 7.2 Beach crest elevation - comparison of predicted and field data

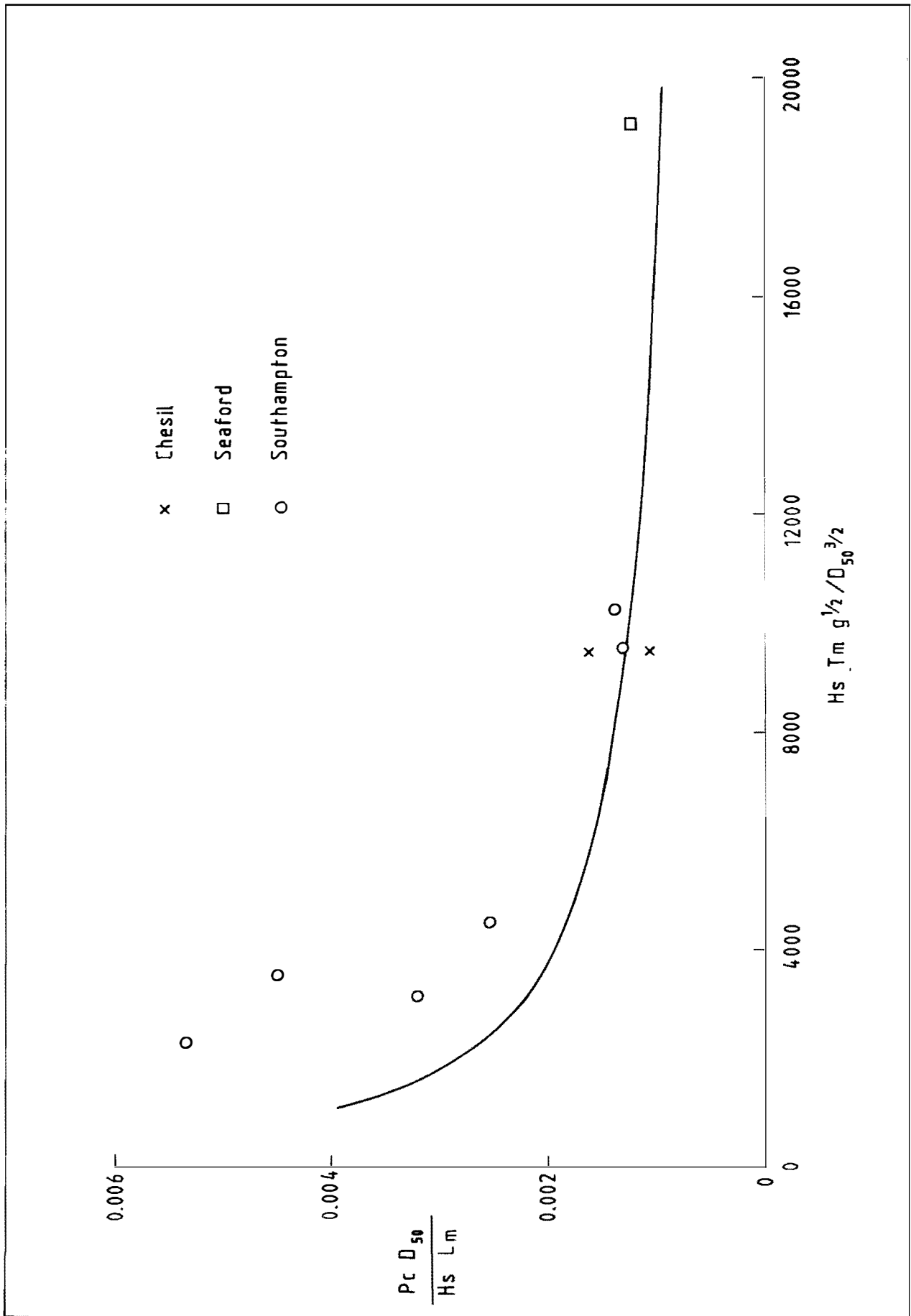


Fig 7.3 Beach crest position - comparison of predicted and field data

## APPENDICES



## APPENDIX 1

### Review of previous studies

Although many authors have commented upon the concave profile of natural beaches few have attempted to describe this curve mathematically. In the few cases where the profile shape has been studied in detail, it has generally been concluded that a hyperbolic curve of the form,

$$y = Ax^n \quad (A.1)$$

where A and n are functions of the beach material and incident wave conditions, and y and x are vertical and horizontal distances respectively, provides the best description.

Keulegan and Krumbein (1949) presented the following equation for the curve of a beach profile:

$$y^{1/4} = \frac{x}{4.86} (v^{2/9})^{0.25} \quad (A.2)$$

where  $v$  is the kinematic viscosity of water ( $9.68 \times 10^{-6}$  ft<sup>2</sup>/s) and x and y are in feet.

This equation was derived using the solitary wave theories of Boussinesq and Russell, together with laboratory tests of the energy loss in a solitary wave. However the assumptions made in the theoretical derivation do not appear to be compatible with the actual experimental conditions used for the laboratory tests. Nevertheless equation A2 is of the same general format as equation A.1 and as such may be rewritten as,

$$y = 0.007 x^{0.57} \quad (\text{A.3})$$

where  $y$  and  $x$  are in metres.

Bruun (1954) derived a theoretical expression for the equilibrium profiles of sand beaches based on the assumptions that:

1. The beach profile is formed only by the onshore/offshore component of the shear stress due to wave action.
2. The shear stress per unit area of seabed is constant both in time and along the onshore axis.
3. There is a uniform loss of wave energy as the wave approaches the shoreline ie spilling waves.

From these assumptions Bruun arrived at the general equation,

$$y = Ax^{2/3} \quad (\text{A.4})$$

which he then proceeded to fit to beach profile data obtained from the North Sea coast of Denmark and from Mission Bay, California. The results of the curve fitting are summarised below:-

Site	A	$D_{50}$ (mm)	$H_o/L_o$
Denmark	0.131	0.26	0.0340
Mission Bay - Winter	0.141	0.14	0.0020
Mission Bay - Summer	0.145	0.14	0.0014

From this table it appears that  $A$  is partly dependent upon wave steepness: increasing with decreasing steepness.

Dean (1977) suggested three possible models for sand beach equilibrium profiles in the region between the wave break point and the shoreline. All three model derivations require that the ratio of breaker height to water depth is constant, landward of the first break point. This effectively limits the models to spilling breakers. Such a limitation is perfectly reasonable for flat sand beaches, though it may not be so for steeper shingle beaches where spilling breakers are unusual.

Dean's first model assumed that the beach profile was due to a uniform longshore shear stress. However, since beach processes are considered here only on an onshore/offshore basis, this model is not applicable. The second model considered that the profile was the result of a uniform energy dissipation per unit surface area of seabed, with the energy first being transferred into turbulence and then, through viscous action, into heat. The final result was an equation of the form:

$$d_n = Ax^{2.5} \quad (A.5)$$

where  $d_n$  is depth below mean sea level  
 $x$  is horizontal range directed seaward  
and  $A$  is a function primarily of grain size.

The derivation of the third model proceeded along the same lines, however, this time, the profile was considered to be the result of uniform energy dissipation per unit volume of water within the surf zone. This resulted in an equation of the form,

$$d_n = Ax^{2.3} \quad (A.6)$$

Subsequent evaluation of a large number of beach profiles by Hughes and Chiu (1978) found that equation

A.6 provided the best fit to the data in the majority of cases. This implies that the mechanism of sand beach profile formation within the surf zone is best described, in the simplest of approximations, as a uniform energy dissipation per unit volume.

Dean's actual derivation of equation A.6 gives,

$$A = \frac{(4.8 D(d))^{2/3}}{\gamma K^2 g} \quad (\text{A.7})$$

where  $K$  is a constant ( $= H_n/d_n$ )

$H_n$  is wave height within the surf zone

$\gamma$  is density of water

$D(d)$  is rate of wave energy dissipation per unit volume as a function of grain size.

Thus  $A$  would appear to be a function only of sediment size. However, as stated earlier, shingle beaches are rarely subjected to spilling waves, and therefore any constant used within the formulation must include a measure appropriate to a wider range of incident wave conditions. It should also be noted that  $A$ , as defined, is not dimensionless and has units of  $m^{1/3}$ .

Hughes and Chiu (1978) analysed over 400 beach profiles taken from along the Florida coast and from a small section of the Lake Michigan shoreline. The median size ( $D_{50}$ ) of the beach material was approximately 0.27mm. From the analysis they found that a curve of the form,

$$y = 0.10 x^{2/3} \quad (\text{A.8})$$

ie  $A = 0.10 m^{1/3}$

provided the best fit to the data.

Hughes and Chiu (1981) conducted a series of experiments related to the formation of laboratory sand beach ( $D_{50} = 0.15\text{mm}$ ) profiles. Provided that the criterion for spilling breakers was met, they found that equation A.6, as derived by Dean, gave a reasonable fit to the data, with  $A = 0.132\text{m}^{1/3}$ . Moreover, in line with Dean's derivation, the coefficient A was found to be neither a function of breaking wave height nor wave period. This prompted the authors to suggest that the extra surf zone volume necessary to dissipate an increased incident wave energy was obtained by a lengthening of the surf zone rather than by a change in profile. Thus for increasing incident wave energy the position of the bar trough moves offshore and becomes deeper in such a manner that the curve  $y = Ax^{2/3}$  can be extended seaward to intersect this position without changing the value of A. The increased energy is then dissipated by the increased surf zone volume.

Following an extensive investigation into the scale factors pertaining to the laboratory modelling of sand dune erosion under storm surges, Vellinga (1984) derived an empirical scale factor through curve fitting of the dune erosion profiles and erosion quantities;

$$\frac{y_p}{y_m} = \left(\frac{x_p}{x_m}\right)^{0.78} \quad (\text{A.9})$$

where the suffixes p and m refer to prototype and model respectively.

Assuming that the erosion profiles can be described by a power curve of the form  $y = Ax^n$ , equation A.9

results in:-

$$y = Ax^{0.78} \quad (\text{A.10})$$

For sand beaches with  $D_{50} = 0.225\text{mm}$  and  $H_o/L_o = 0.034$ , equation A.10 becomes,

$$y = 0.08x^{0.78} \quad (\text{A.11})$$

This equation gives a curve in close agreement with that obtained by Bruun (1954) for the very similar Danish beaches. Hughes and Chiu's 1978 formulation of equation A.6 does not however show such good agreement, giving profiles that are much more gentle than those of Vellinga and Bruun. This discrepancy is probably due to differences in wave climates along the North Sea and Florida coasts, with the Florida profiles being formed and maintained by waves of generally smaller steepness than those of the North Sea. On this basis there would appear to be a steepness effect.

From considerations of the scaling relationships obtained by himself, and Hughes and Chiu (1981), Vellinga attempted to establish the form of this steepness effect assuming that the steepness effect was described solely by the coefficient and not by the exponent. He found that:

$$y = A_1 (H_o/L_o)^{0.17} x^{0.78} \quad (\text{A.12})$$

$$\text{ie } A = A_1 (H_o/L_o)^{0.17} \quad (\text{A.13})$$

It should however be noted that these equations are based on results from model tests run with a constant wave steepness of 0.034. As such their general applicability is somewhat limited.

Vellinga further attempted to incorporate the effect of material size within the coefficient A by means of a similar consideration of the original scaling relationships to that which yielded the steepness effect. From these considerations Vellinga derived a universal erosion profile of the form,

$$y = 0.7 (H_o/L_o)^{0.17} V_s^{0.44} x^{0.78} \quad (\text{A.14})$$

where  $V_s$  is fall velocity of a beach material particle of size  $D_{50}$ .

This equation gives reasonable results in the field for conditions with  $0.025 < H_o/L_o < 0.04$  and  $0.16\text{mm} < D_{50} < 0.4\text{mm}$ . However, comparison with the shingle beaches measured in the present study is poor; with equation A.14 yielding very much shallower profiles. Furthermore this equation is only applicable below the still water level, as indeed are all those previously given, and has only been formulated on the basis of, and checked against, sand beach profiles formed by waves with a steepness in the order of 0.034.

More recently attention has focussed on the application of similar analysis techniques to shingle beach profiles. Van Hijum and Pilarczyk (1982) and Powell (1986) report on the results of physical model tests intended to provide a description of shingle beach profiles. In both cases the profiles were schematised as two hyperbolic curves, one from the beach crest to the step, the other from the step to lower profile limit. Equations relating these curves to the wave and sediment characteristics were then determined. Although good agreement with the model results was obtained, much of the work contained in these studies was undertaken with regular waves. It

is therefore difficult to relate these studies directly to natural conditions.

Van der Meer (1988) extended work he was undertaking on the dynamic stability of rock slopes to natural gravel beaches. His profiles were schematised as three separate curves,

- from crest to SWL
- from SWL to transition
- from transition to lower profile limit.

The results of an extensive series of random wave tests provided relationships between profile parameters and either of two dimensionless terms:

1. Wave steepness,  $H_s/L_m$

2. Combined wave height - wave period,  $\frac{H_s T_m g^{1/2}}{\Delta D_{50}^{3/2}}$

where  $\Delta$  is relative mass density  $(\rho_s - \rho_f)/\rho_f$   
and  $\rho_s$  is density of sediment  
 $\rho_f$  is density of fluid

All length parameters were found to be described by the combined wave height - wave period function, whilst the profile elevation parameters were best described by the wave steepness parameter.

In order to extend the results to a wider range of situations, van der Meer also derived correction factors for shallow foreshores and oblique wave attack. However in the extension of his work to gravel beaches he failed to allow for the scale effects that become increasingly important with

material of this size. In particular it is to be expected that the permeability, and hence slope, of the beaches employed in the study, will be incorrect. Attempts to validate the model results against large scale tests are also suspect, given that the material used in the large scale tests was a very fine shingle - fine enough to cross the behavioural border between sand and shingle beaches (Van Hijum, 1974).

## References

- A1. Keulegan G H and Krumbein W C. Stable configuration of bottom slope in shallow water and its bearing on geological processes. Trans Amer Geophys Union, 30, No 6, 1949.
- A2. Bruun P. Coast erosion and the development of beach profiles. US Army Corps of Engrs, BEB, TM-44, 1954.
- A3. Dean R G. Equilibrium beach profiles: US Atlantic and Gulf coasts. Univ of Delaware, Dept of Civil Engrg, Ocean Engrg, Report No 12, 1977.
- A4. Hughes S A and Chiu T S. The variations in beach profiles when approximated by a theoretical curve. Univ of Florida, Coastal and Oceanographic Engrg Dept, Report No 78/010, 1978.
- A5. Hughes S A and Chiu T S. Beach and dune erosion during severe storms. Univ of Florida, Coastal and Oceanographic Engrg Dept, Report No TR/043, 1981.
- A6. Vellinga P. A tentative description of a universal erosion profile for sandy beaches and rock beaches. Coastal Engrg 8, 1984.

- A7. Van Hijum E and Pilarczyk K W. Equilibrium profile and longshore transport of coarse material under regular and irregular wave attack. Delft Hyd Lab Pub No 274, 1982.
- A8. Powell K A. The hydraulic behaviour of shingle beaches under regular waves of normal incidence. PhD Thesis, Univ of Southampton, 1986.
- A9. Van der Meer J W. Rock slopes and gravel beaches under wave attack. Delft Hyd Comm No 396, 1988.
- A10. Van Hijum E. Equilibrium profiles of coarse material under wave attack. Proc 14th Conf on Coastal Eng, 2, 1974.

## APPENDIX 2

### Selection of model sediment

Ideally the model sediment should satisfy three criteria:

- Permeability of the shingle beach should be correctly reproduced
- The relative magnitudes of the onshore and offshore motion should be correct
- The threshold of motion should be correctly scaled

The first of these basically governs the beach slope, the second determines whether the beach will erode or accrete under given wave conditions, and the third determines the wave velocity at which sediment motion will begin.

### Reproduction of Permeability

Yalin published a paper in 1963 describing a method for modelling shingle beaches with the correct permeability and drag forces. For the permeability he said that in an undistorted model the percolation slope must be identical to the prototype, where

$$J = k(\text{Re}_v)v^2/gD_{10}$$

with  $J$  = percolation slope

$k$  = permeability, a function of .....

$\text{Re}_v$  = voids Reynolds Number  $vD_{10}/\nu$

$v$  = velocity through the voids

$D_{10}$  = 10% undersize of the sediment

$\nu$  = kinematic viscosity

For identical percolation slopes in model and prototype this gives

$$\lambda_v^2 \lambda_k / \lambda_D = 1$$

where  $\lambda$  is the model scale (prototype value/model value). Assuming that the model is operated according to Froude's Law then  $\lambda_v^2 = \lambda$ , the geometric scale, so that

$$\lambda \lambda_k / \lambda_D = 1 \quad (\text{A.1})$$

Unfortunately permeability is a non-linear function of Reynolds Number. For example, Yalin proposed a steady-flow law, and produced a recommended curve of  $k$  against  $Re_v$ . This curve can be approximated by the expression

$$\log k = 3.17 - 1.134 \log Re_v + 0.155 \log^2 Re_v,$$

within the range  $1 \leq Re_v \leq 200$

With such a non-linear expression the scaling law will depend on the representative value of the prototype permeability. If this is designated  $k_p$ , and the Reynolds Number is  $Re_p$ , then

$$\lambda_k = k_p / k_m = \lambda_D / \lambda$$

$$\text{or } \lambda_D = \lambda k_p / k_m$$

Now  $k_m = k(Re_m)$  where  $Re_m$  is the model Reynolds Number, so

$$k_m = k(Re_p / \lambda_v \lambda_D) = k(Re_p / \lambda^{1/2} \lambda_D)$$

By substituting this expression the implied equation for  $\lambda_D$  is obtained as

$$\lambda_D = \lambda k_p / k(Re_p / \lambda^{1/2} \lambda_D) \quad (A.1a)$$

Assuming that  $k_p$  and  $Re_p$  are known, and the form of the function  $k(Re_v)$  is known then this equation can be solved by successive approximation to define the particle size for the model sediment.

### Reproduction of Onshore/Offshore Movement

Several authors have postulated that the relative tendency for sediments to move onshore or offshore depends on the dimensionless parameter  $H_b/wT$ , where  $H_b$  is the wave height at breaking,  $T$  is the wave period and  $w$  is the settling velocity of the sediment particles. Roughly speaking if  $H_b/wT \leq 1$  then the sediment moves onshore, and if  $H_b/wT \geq 1$  then offshore movement occurs (see for example Shore Protection Manual, section 4.525). In physical terms the parameter represents the ratio between the wave height and the distance which the sediment particle can settle during one wave period. For correct reproduction of the relative magnitudes of onshore and offshore movement the model scales must therefore be such that

$$\lambda_{H_b} / \lambda_w \lambda_T = 1$$

With a Froudian model  $\lambda_T = \lambda^{1/2}$ , and assuming that the beach slope is correctly modelled then  $\lambda_{H_b} = \lambda$ , so

$$\text{that we have } \lambda_w = \lambda^{1/2}$$

In general, the settling velocity is given by

$$w = \left( \frac{1.33gD \cdot \rho_s - \rho_f}{C_D \rho_f} \right)^{1/2}$$

where  $\rho_s$  and  $\rho_f$  are specific gravities of the sediment and fluid respectively, and  $C_D$  is the drag coefficient for the settling particles.

For modelling purposes we therefore have

$$\lambda_w = \lambda_D^{1/2} \lambda_\Delta^{1/2} / \lambda_{C_D}^{1/2} = \lambda^{1/2}$$

$$\text{or } \lambda_\Delta = \lambda \lambda_{C_D} / \lambda_D \quad (\text{A.2})$$

where  $\Delta$  is  $(\rho_s - \rho_f) / \rho_f$

Unfortunately  $C_D$  is also a non-linear function, in this case a function of the sediment particle Reynolds Number  $Re_s = wD/\nu$ . The actual scaling will again therefore depend on the typical value of the prototype drag coefficient. Denoting this prototype value as  $C_{D_p}$ , and the appropriate Reynolds Number  $Re_p$  we therefore have

$$\begin{aligned} \lambda_{C_D} &= C_{D_p} / C_{D_m} = C_{D_p} / C_D(Re_m) \\ &= C_{D_p} / C_D(Re_p / \lambda_w \lambda_D) \end{aligned}$$

$$\lambda_{C_D} = C_{D_p} / C_D(Re_p / \lambda^{1/2} \lambda_D) \quad (\text{A.2a})$$

If  $C_{D_p}$  and  $Re_p$  are known, and  $\lambda_D$  has also been determined (for example from the permeability scaling) then equation A.2a can be solved for  $\lambda_{C_D}$ , and the value then inserted in equation A.2 to derive  $\rho_s$ , the specific gravity of the model sediment. If both model and prototype sediments are coarse grained (roughly

greater than 4 mm) then  $\lambda_{C_D} \sim 1$ , thus giving  $\lambda_{\Delta} = \lambda/\lambda_D$

**Threshold of Motion** For oscillating flow Komar and Miller (1973) proposed that for sediment sizes greater than 0.50 mm, which is expected to be the case for both model and prototype sediments, the threshold of movement was defined by the expression

$$\frac{U_m^2}{\Delta g D} = 0.46 \pi \left(\frac{d_o}{D}\right)^{1/4}$$

where  $U_m$  is the peak value of the near-bed orbital velocity at the threshold of motion

and  $d_o$  is the near-bed orbital diameter.

Since  $U_m = \pi d_o/T$ , this expression can be re-written

$$U_m^{7/4} / (\Delta D^{3/4} T^{1/4}) = 0.46 \pi^{3/4} g$$

To the first order, the maximum orbital velocity near the bed is given by

$$U_m = \frac{\pi H}{T \sinh(2\pi d/L)}$$

where  $L$  is the wavelength.

Substituting this expression, and rearranging, gives the threshold in terms of wave height and period as

$$H^{7/4} A^{7/4} / (\Delta D^{3/4} T^2) = 0.46 g/\pi$$

where A is the depth attenuation factor  $1/\sinh(2\pi d/L)$

For correct modelling we therefore have

$$\lambda_H^{7/4} \lambda_A^{7/4} / (\lambda_\Delta \lambda_D^{3/4} \lambda_T^2) = 1$$

In a Froudian model  $\lambda_H = \lambda_L = \lambda_d = \lambda$  and  $\lambda_T = \lambda^{1/2}$ .

Therefore  $\lambda_A = 1$ . This then gives

$$\lambda_\Delta \lambda_D^{3/4} = \lambda^{3/4} \quad (\text{A.3})$$

### Summary of Scaling Laws

The preceding paragraphs have given the following equations for scaling the model material

For correct permeability:  $\lambda_D = \lambda k_p / k(\text{Re}_p / \lambda^{1/2} \lambda_D)$  (A.1a)

For correct onshore/offshore movement:

$$\lambda_\Delta = \lambda \lambda_{C_D} / \lambda_D \quad (\text{A.2})$$

where  $\lambda_{C_D} = C_{D_p} / C_D (\text{Re}_p / \lambda^{1/2} \lambda_D)$  (A.2a)

For correct threshold of motion:

$$\lambda_\Delta \lambda_D^{3/4} = \lambda^{3/4} \quad (\text{A.3})$$

Assuming that the prototype values  $k_p$ ,  $\text{Re}_p$  etc are known, we then have four equations to solve for the four scale factors  $\lambda$ ,  $\lambda_D$ ,  $\lambda_\Delta$  and  $\lambda_{C_D}$ . However the

only solution to these four equations is the prototype situation, ie  $\lambda = \lambda_D = \lambda_\Delta = \lambda_{C_D} = 1$ . In practice it

is necessary to select one of the scales (usually  $\lambda$ ), and then decide which of the various scaling requirements are most important. Clearly, having selected one scale we have four equations to solve for three variables, and one of the equations therefore has to be relaxed.

### Application

Application of these equations to the four beach gradings selected for the present study yields the following sediment requirements at a model scale of 1:17.

Mix	Model $D_{50}$ (mm)	$\rho_s$ Threshold of motion	$\rho_s$ Onshore/Offshore movement
1	3.2	1.42	1.37
2	3.3	1.43	1.38
3	6.7	1.56	1.35
4	6.2	1.51	1.33

Anthracite has a specific gravity of 1.39 and thus satisfies most of the requirements for reproducing the correct onshore/offshore movement and threshold of motion. Moreover it is commercially available in a number of size gradings from which the required model mixes can be blended. It is therefore ideally suited for modelling shingle beaches at this scale.



## APPENDIX 3

### Summary of prediction equations

This appendix summarises the prediction equations and correction factors derived in this report. It should be read in conjunction with Figure 4.1 and the listing of the notation given in the front of the report.

#### A. Beach profile prediction

1. Run-up limit,  $p_r$

$$p_r/H_s = 6.38 + 3.25 \ln(H_s/L_m)$$

2. Crest position,  $p_c$

$$p_c D_{50}/H_s L_m = -0.23 (H_s T_m g^{1/2}/D_{50}^{3/2})^{-0.588}$$

3. Crest elevation,  $h_c$

$$h_c/H_s = 2.86 - 62.69 (H_s/L_m) + 443.29 (H_s/L_m)^2$$

4. Transition position,  $p_t$

For  $H_s/L_m < 0.03$ :

$$p_t D_{50}/H_s L_m = 1.73 (H_s T_m g^{1/2}/D_{50}^{3/2})^{-0.81}$$

For  $H_s/L_m \geq 0.03$ :

$$p_t/D_{50} = 55.26 + 41.24 (H_s^2/L_m D_{50}) + 4.90 (H_s^2/L_m D_{50})^2$$

5. Transition elevation,  $h_t$

For  $H_s/L_m < 0.03$ :

$$h_t/H_s = -1.12 + 0.65 (H_s^2/L_m D_{50}) - 0.11 (H_s^2/L_m D_{50})^2$$

For  $H_s/L_m \geq 0.03$ :

$$h_t/D_{50} = -10.41 - 0.025 (H_s^2/D_{50}^{3/2} L_m^{1/2}) - 7.5 \times 10^{-5} (H_s^2/D_{50}^{3/2} L_m^{1/2})^2$$

6. Wave base position,  $p_b$

$$p_b/D_{50} = 28.77 (H_s/D_{50})^{0.92}$$

7. Wave base elevation,  $h_b$

$$h_b/L_m = -0.87 (H_s/L_m)^{0.64}$$

8. Curve 1, crest to still water level

$$\frac{y}{h_c} = \left(\frac{x}{p_c}\right)^{n_1}$$

where  $n_1 = 0.84 + 23.93 H_s/L_m$  for  $H_s/L_m < 0.03$   
and  $n_1 = 1.56$  for  $H_s/L_m \geq 0.03$

9. Curve 2, still water level to transition

$$\frac{y}{h_t} = \left(\frac{x}{p_t}\right)^{n_2}$$

where  $n_2 = 0.84 - 16.49 H_s/L_m + 290.16 (H_s/L_m)^2$

10. Curve 3, transition to wave base

$$\frac{y - h_t}{h_b - h_t} = \left(\frac{x - p_t}{p_b - p_t}\right)^{n_3}$$

where  $n_3 = 0.45$  for  $H_s/L_m < 0.03$   
and  $n_3 = 18.6 (H_s/L_m) - 0.1$  for  $H_s/L_m \geq 0.03$

B. Confidence limits

1) Curve 0:

$$V(X_0) = (1-t)^2 V(p_c) + t^2 V(p_r) + 2.34 t(1-t)$$

$$V(Y_0) = (1-t)^2 V(h_c) + a_o t^2 V(p_r) + 0.49 a_o t(1-t)$$

2) Curve 1:

$$V(X_1) = t^2 V(p_c)$$

$$V(Y_1) = t^{2n_1} V(h_c) + (y_1 \log t)^2 V(n_1)$$

3) Curve 2:

$$V(X_2) = t^2 V(p_t)$$

$$V(Y_2) = t^{2n_2} V(h_t) + 0.037 (y_2 \log t)^2 + 0.062 t^{n_2} y_2 \log t$$

4) Curve 3:

$$V(X_3) = (1-t)^2 V(p_t) + \frac{t^2}{a_3} V(h_b)$$

$$V(Y_3) = (1-t^{n_3})^2 V(h_t) + t^{2n_3} V(h_b) + [(y_3 - h_t) \log t]^2 V(n_3) \\ - 0.44 t^{n_3} (1-t^{n_3}) + (y_3 - h_t) \log t [0.036 t^{n_3} - 0.014]$$

C. Correction for effective beach thickness

To be applied when  $30 D_{50} \leq D_B \leq 100 D_{50}$ . For values of  $D_B < 30 D_{50}$  the beach is destabilised.

Correction,  $R_{c_{p_c}}$  applies only to beach crest position,  $P_c$ .

$$R_{c_{pc}} = \frac{P^c(D_B/D_{50})}{P^c(D_B/D_{50} \geq 100)} = 6646 H_s/L_m (D_B/D_{50})^{-1.68} + 0.88$$

D. Correction for depth limited foreshore

Correction factors necessary for positional parameters when  $H_s/D_w > 0.3$ , and for elevation parameters when  $H_s/D_w > 0.55$ .

$$\text{Correction factor, } R_{c_d} = \text{Par}_{\text{meas}}/\text{Par}_{\text{pred}}$$

where the predicted parameter value uses the wave conditions at the toe of the beach.

Depth limited wave height,

$$H_{s_b} = 0.12 L_m [1.0 - \exp(-4.712 D_w (1.0 + 15m^{1.33})/L_m)]$$

Depth limited wave length,

$$L_{m_s} = T_m (g D_w)^{1/2}$$

1. Upper profile limit correction,

$$R_{c_d} = 1.08 (H_s/D_w) + 0.72$$

$$\text{for } 0.3 < H_s/D_w < 2.5$$

2. Crest position correction,

$$R_{c_d} = 3.03 (H_s/D_w) + 0.12$$

$$\text{for } 0.3 < H_s/D_w < 2.5$$

3. Crest elevation correction,

$$R_{c_d} = (H_s/D_w) + 0.41$$

$$\text{for } 0.55 < H_s/D_w < 2.5$$

4. Transition position correction,

$$R_{c_d} = 0.007 (L_m/D_w)^{1.2} + 0.45$$

$$\text{for } 40 < L_m/D_w < 130$$

5. Transition elevation correction,

$$R_{c_d} = 1.0$$

$$\text{for } 0.55 < H_s/D_w < 2.5$$

6. Wave base position correction,

$$\text{for } 0.3 < H_s/D_w < 0.8$$

$$R_{c_d} = -1.14 (H_s/D_w) + 1.31$$

$$\text{for } 0.8 < H_s/D_w < 2.5$$

$$R_{c_d} = 0.20 (H_s/D_w) + 0.28$$



## APPENDIX 4

### Details of Field Surveys

This appendix contains details of the field surveys undertaken to collect validation data for the physical model tests. Data from two earlier field surveys has also been used in this study, and is detailed below.

The sites for which field measurements were taken, or are available, are:

1. West Bexington, Chesil Beach
2. Hordle Beach, Christchurch Bay
3. Hurst Castle Spit, Christchurch Bay
4. Rustington, Littlehampton
5. Seaford

The location of these sites is shown in Figure 7.1. The calibration data for Seaford was obtained from an earlier report (Hydraulics Research Report No EX 1346, Seaford Frontage Study, 1986) and is not described further in this appendix.

1. West Bexington, Chesil Beach

Location: Two survey lines set up perpendicular to beach and approximately 100 metres apart, just to the west of West Bexington Car Park.

Date: 1-2 April 1987.

Personnel: Survey measurements taken by Dr K A Powell and Mr A R Channell from the Coastal Engineering Group at Hydraulics Research. Wave

recorders installed and monitored by staff from the Proudman Oceanographic Laboratory, POL (formerly IOS Bidston).

Conditions:

- Waves of normal incidence with  $H_s \sim 0.5\text{m}$  and  $T_m \sim 6.0$  secs.
- Spring tide, no significant surge.
- Strong onshore wind.

Beach:

Steeply shelving, composed of fine, well sorted shingle ( $D_{50} = 10\text{mm}$ ,  $\bar{U} = 1.36$ ). Effective thickness of beach reported by staff from POL to vary from 1.0 to 1.5 metres.

Survey technique:

- Wave and water level data collected throughout survey by an array of inshore pressure transducers.
- Beach profiles at two survey locations recorded at low tide immediately before and after survey.
- Wave run-up exceedance levels recorded, over high tide, by visual observation against a line of marker poles installed across the beach at preceding low tide.
- Beach samples collected from swash zone, on completion of monitoring.

## 2. Hordle Beach, Christchurch Bay

Location: Two profile lines set up, 50 metres apart, on Hordle beach to the west of Milford-on-Sea coast defences. Westernmost line located at 427515E, 91831N.

Dates: 23 December 1987 and 7 January 1988.

Personnel: Surveys undertaken by staff from the Civil Engineering Department at Southampton University under the direction of Mr M Riley and Mr J Cross. Wave Rider Buoy installed by Hydraulics Research for New Forest District Council at 50°42.5'N, 1°35.6'W.

Conditions: 23/12/87 - Waves of normal incidence to beach with  $H_s \sim 0.5\text{m}$  and  $T_m \sim 6.0$  to 8.0 secs. A long swell component with  $T_m \sim 15.0$  secs also observed.

- Spring tide.
- Onshore wind (S-SE).

7/1/88 - Waves of normal incidence with observed  $H_s \sim 1.5$  to 2.0 metres. Wave Rider not operational.

- Spring tide.
- Very strong offshore wind (N-NW).

Beach: On both occasions the beach was steeply shelving in front of crest, before levelling out onto a sand foreshore. Pronounced cusping was evident with the westernmost profile line being set out over a cusp and the eastern line through the cusp bay.

Survey technique:

- Wave data collected by Wave Rider Buoy.
- Water levels recorded using visually observed tide pole located on nearby groyne.
- Beach profiles at two survey locations recorded at low tide immediately before and after survey.
- Wave run-up exceedance levels recorded, over high tide, by visual observation against a line of marker poles installed across the beach at the preceding low tide.
- Beach samples collected from swash zone on completion of monitoring.

### 3. Hurst Castle Spit, Christchurch Bay

Location: Two profile lines set up, 50 metres apart, on Hurst Castle Spit to the east of Milford-on-Sea coast defences. Westernmost line located at 430110E, 90632N.

Dates: 24 December 1987 and 23 January 1988.

Personnel: Surveys undertaken by staff from the Civil Engineering Department at Southampton University under the direction of Mr M Riley and Mr J Cross. Wave Rider buoy installed by Hydraulics Research for New Forest District Council at 50°42.5'N, 1°35.6'W.

Conditions: 24/12/87 - Waves breaking nearly parallel to beach, observed breaking height 1.5-2.0m. Wave Rider records show offshore conditions to be  
 $H_s \sim 0.5-1.0m,$   
 $T_m \sim 4.0-5.0 \text{ secs.}$   
- Spring tide.  
- Onshore wind (S-SW).

23/1/88 - Waves approaching at 5° to beach with  
 $H_s \sim 0.5-1.0m,$   
 $T_m \sim 5.0-7.0 \text{ secs.}$   
- Spring tide.  
- Very strong offshore wind (NW).

Beach: 24/12/87 - Gently shelving, mixed sand/shingle with  
 $D_{50} \sim 6-10mm.$

23/1/88 - Steeply shelving down to sand foreshore. Upper beach composed of well graded shingle with  
 $D_{50} \sim 15-20mm.$

Survey technique: As at Hordle Beach.

4. Rustington, Littlehampton

Location: Three survey lines located 15 metres apart in a groyne bay 2.5km east of the River Arun. Grid Reference 101400N, 505300E.

Date: Surveyed at fortnightly intervals between October 1985 and March 1986.

Personnel: Survey measurements and Wave Rider installation undertaken by staff from the Coastal Engineering and Field Studies Groups at Hydraulics Research.

Conditions:

- Wave conditions recorded continuously over survey period, maximum Hs ~ 3.2m.
- All surveys carried out after highest spring tide.

Beach: Poorly graded shingle beach overlying sand foreshore. D<sub>50</sub> ~ 12.0 to 20.0mm. Beach heavily groyned.

Survey technique:

- Wave data collected by Wave Rider Buoy sited offshore in 10 metres of water at 50°43.7'N, 0°25.7'W.
- No direct water level measurements taken.
- Beach profile survey lines recorded at low water as soon as

possible after the highest spring  
tide.

- Beach samples collected from  
various locations along the  
central profile.



## APPENDIX 5

### Derivation of confidence limits for predicted profiles

From the regression analysis outlined in Section 4.3 it is possible to establish the variation, measured within the model tests, in X and Y at any point along the predicted beach profile. With this variation obtained, confidence limits on the predicted profile can be determined.

Regarding the variations in X and Y separately, and assuming dependent variables, equation 4.14 for curve 1 (crest to SWL) can be re-written as:

$$X_1 = p_c t \quad \text{and} \quad Y_1 = h_c t^{n_1}$$

where  $0 \leq t \leq 1$

The variations in  $X_1$  and  $Y_1$  ie  $V(X_1)$  and  $V(Y_1)$  are then given by,

$$V(X_1) = \left(\frac{dx_1}{dp_c}\right)^2 V(p_c) \quad (\text{A5.1})$$

and

$$V(Y_1) = \left(\frac{dy_1}{dh_c}\right)^2 V(h_c) + \left(\frac{dy_1}{dn_1}\right)^2 V(n_1) + 2 \frac{dy_1}{dh_c} \frac{dy_1}{dn_1} C(y_1, n_1) \quad (\text{A5.2})$$

where  $C_{ij}$  is the cross co-variance given by

$$C_{ij} = \overline{\Delta_{\alpha_i} \Delta_{\alpha_j}} = \sum (i-\bar{i})(j-\bar{j})/N$$

$\alpha_{i,j}$  is a given parameter  
 $\Delta_{\alpha_{i,j}}$  deviation of that parameter about its mean  
 value  
 and N is the number of data points.

[Note also that  $V(\alpha_i) = C_{ii}$ ]

Resolving the differentials allows equations A5.1 and A5.2 to be re-written as:

$$V(X_1) = t^2 V(p_c) \quad (A5.3)$$

and

$$V(Y_1) = t^{2n_1} V(h_c) + (y_1 \log t)^2 V(n_1) + 2t^{n_1} y_1 \log t C(h_c, n_1) \quad (A5.4)$$

Curve 2, from the SWL to the transition, can be treated similarly to yield:

$$V(X_2) = t^2 V(p_t) \quad (A5.5)$$

and

$$V(Y_2) = t^{2n_2} V(h_t) + (y_2 \log t)^2 V(n_2) + 2t^{n_2} y_2 \log t C(h_t, n_2) \quad (A5.6)$$

Curve 3, from the transition to wave base, is slightly different in that its component equations become,

$$X_3 = p_t(1-t) + p_b t$$

$$\text{and } Y_3 = h_t + (h_b - h_t)t^{n_3}$$

and that  $h_b, p_b$  are assumed to lie on the fixed line  $h_b = a_3 p_b$ , leading to variations in  $X_3$  and  $Y_3$  given by:

$$V(X_3) = (1-t)^2 V(p_t) + \frac{t^2}{a^3} V(h_b) + \frac{2t}{a^3} (1-t) C(p_t, h_b) \quad (A5.7)$$

and,

$$\begin{aligned} V(Y_3) &= (1-t^{n_3})^2 V(h_t) + t^{2n_3} V(h_b) + [(y_3-h_t)\log t]^2 V(n_3) \\ &+ 2t^{n_3} (1-t^{n_3}) C(h_t, h_b) + 2(1-t^{n_3}) (y_3-h_t) \log t C(h_t, n_3) \\ &+ 2t^{n_3} (y_3-h_t) \log t C(h_b, n_3) \end{aligned} \quad (A5.8)$$

Similarly the component equations for curve 0, from the crest to the run-up limit can be written as:

$$X_0 = p_c (1-t) + p_r t$$

$$\text{and } Y_0 = h_c (1-t) + a_o p_r t$$

where  $n_o = 1$  and  $h_r, p_r$  are assumed to lie on the fixed line  $h_r = a_o p_r$ .

This gives,

$$V(X_0) = (1-t)^2 V(p_c) + t^2 V(p_r) + 2(1-t)t C(p_c, p_r) \quad (A5.9)$$

and

$$V(Y_0) = (1-t)^2 V(h_c) + a_o t^2 V(p_r) + 2(1-t) a_o t C(p_r, h_c) \quad (A5.10)$$

Provided the statistics of the parameters  $p_c, h_c, p_t$  etc are known the variance in X and Y for the four different curves can be obtained from equation A5.3 to A5.10. The standard deviation  $V^{1/2}(Y_i, X_i)$  can then be

calculated. This, when multiplied by the specified test statistic, Z, will provide the required confidence limits.

Values of the parameter variances and cross co-variances as derived from the regression analysis are given in Tables 4.2 and 4.3. Table 4.3 also lists the correlation coefficients for the cross co-variance. Where these are not significantly different from zero at the 1% level the terms may be dropped from equations A5.3 to A5.10 without adversely affecting the calculated variances.

The final confidence limit equations then become,

1) Curve 0:

$$V(X_0) = (1-t)^2 V(p_c) + t^2 V(p_r) + 2.34t(1-t) \quad (A5.11)$$

$$V(Y_0) = (1-t)^2 V(h_c) + a_o t^2 V(p_r) + 0.49t a_o t(1-t) \quad (A5.12)$$

2) Curve 1:

$$V(X_1) = t^2 V(p_c) \quad (A5.13)$$

$$V(Y_1) = t^{2n_1} V(h_c) + (y_1 \log t)^2 V(n_1) \quad (A5.14)$$

3) Curve 2:

$$V(X_2) = t^2 V(p_t) \quad (A5.15)$$

$$V(Y_2) = t^{2n_2} V(h_t) + 0.037 (y_2 \log t)^2 + 0.062 t^{n_2} y_2 \log t \quad (A5.16)$$

4) Curve 3:

$$V(X_3) = (1-t)^2 V(p_t) + \frac{t^2}{a_3} V(h_b) \quad (A5.17)$$

$$\begin{aligned} V(Y_3) = & (1-t^{n_3})^2 V(h_t) + t^{2n_3} V(h_b) + [(y_3-h_t)\log t]^2 V(n_3) \\ & - 0.44t^{n_3} (1-t^{n_3}) + (y_3-h_t) \log t (0.036t^{n_3}-0.014) \end{aligned} \quad (A5.18)$$

